Radiation Effects in Materials

Kurt Sickafus

Professor of Materials Science and Engineering

The University of Tennessee - Knoxville

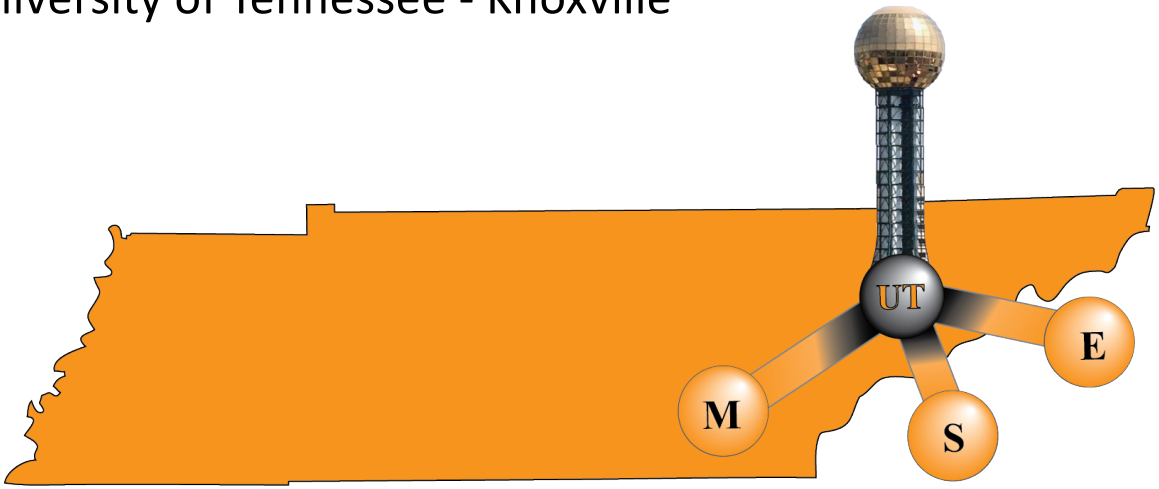

Presentation at the Joint ICTP-IAEA Workshop
Trieste, ITALY
12-16 September 2016

Uranium Fission Yield

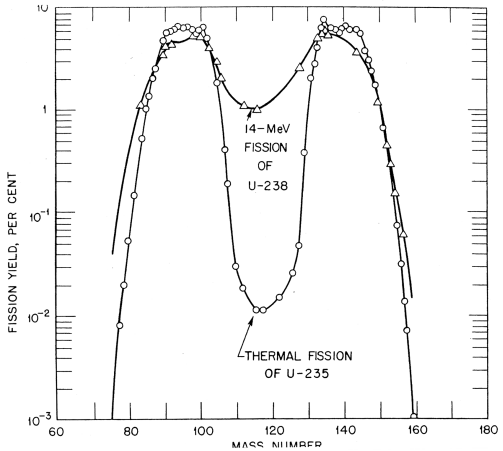

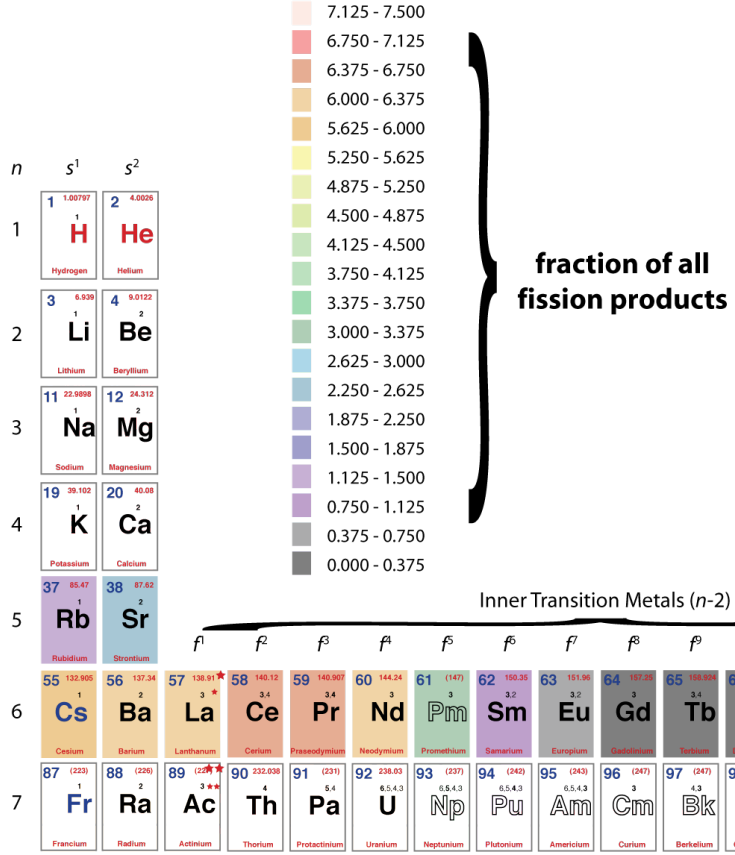

FISSION PRODUCT SPECTRUM (light water reactor)

Volumetric swelling versus fast neutron fluence for two engineering ceramic oxides: α-Al_2O_3 and $MgAl_2O_4$

(also shown in the plot is the displacement damage *dose* in units of displacements per atom (*dpa*))

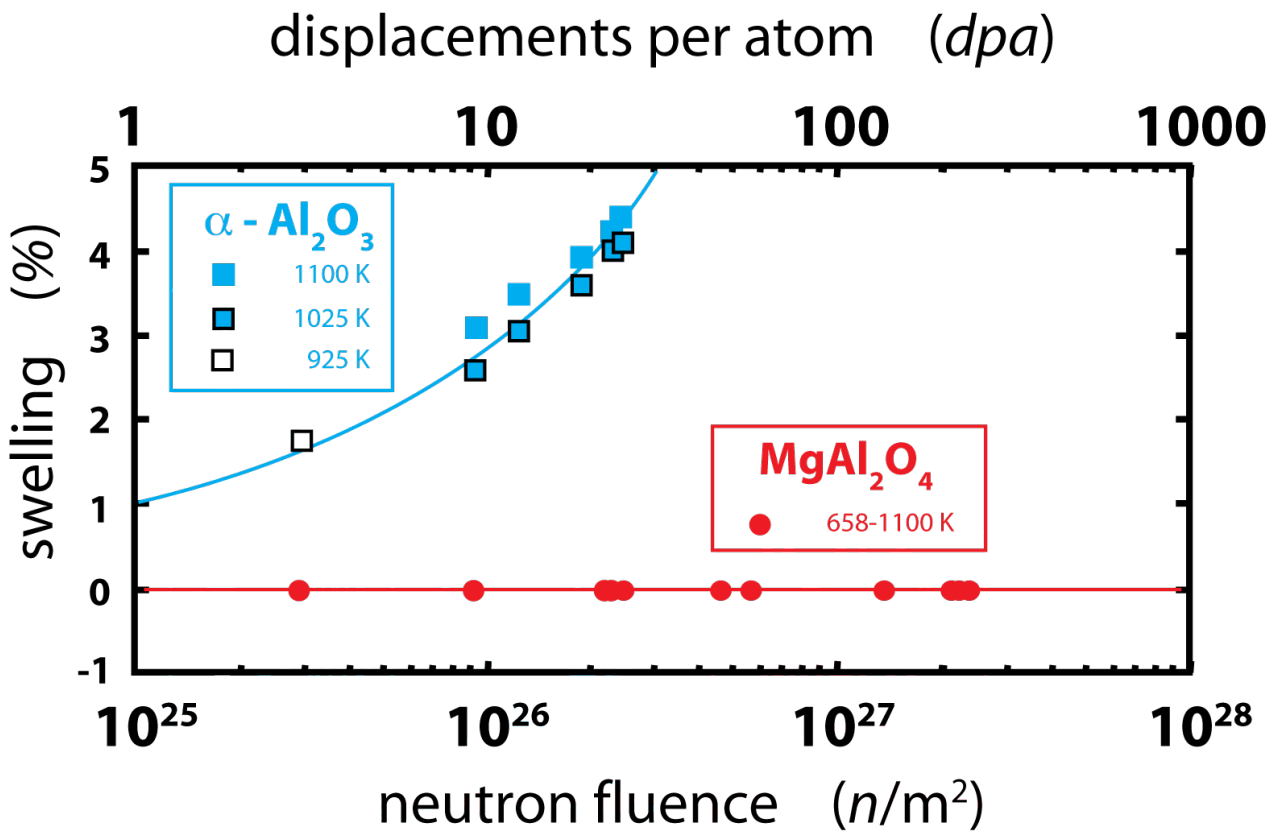

C. Kinoshita and S. J. Zinkle, "Potential and limitations of ceramics in terms of structural and electrical integrity in fusion environments," J. Nucl. Mater. **233-237** (1996) 100-110.

Schematic diagrams showing effects of irradiation on annular cylinders of two engineering ceramic oxides:

(a) α-Al_2O_3 and (b) $MgAl_2O_4$

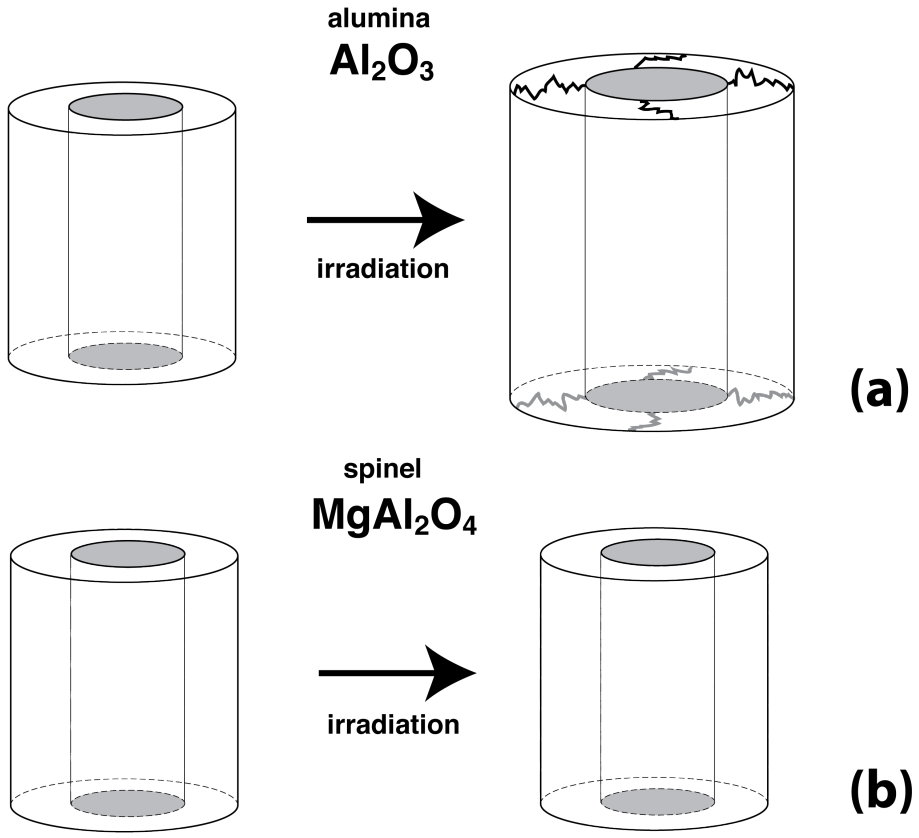

Schematic diagrams showing atomic level effects of energetic particle irradiation on two engineering ceramic oxides:

(a) α-Al_2O_3 and (b) $MgAl_2O_4$

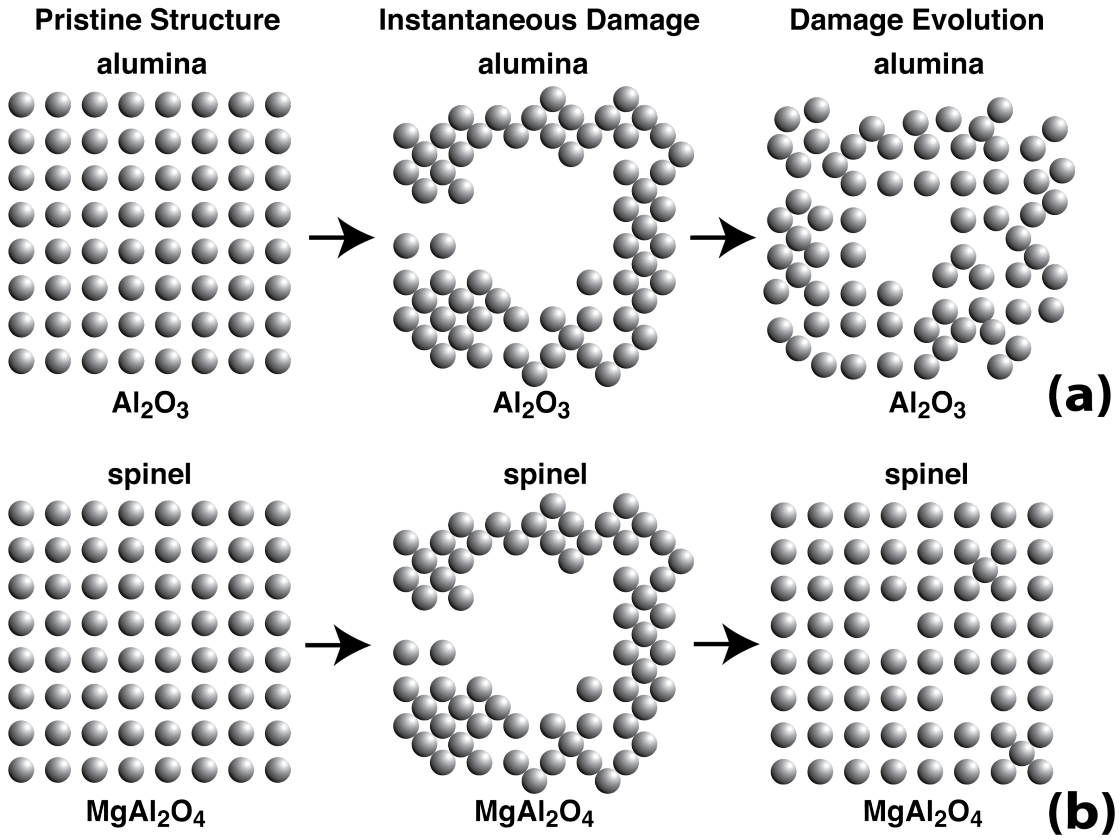

Instantaneous damage **corresponds to approximately a femtosecond (10^{-15} s) after a particle-solid interaction, while** ***damage evolution*** **represents the atomic situation after a few picoseconds (10^{-12} s) of evolved time.**

Radiation-Induced Swelling

Examples of Swelling

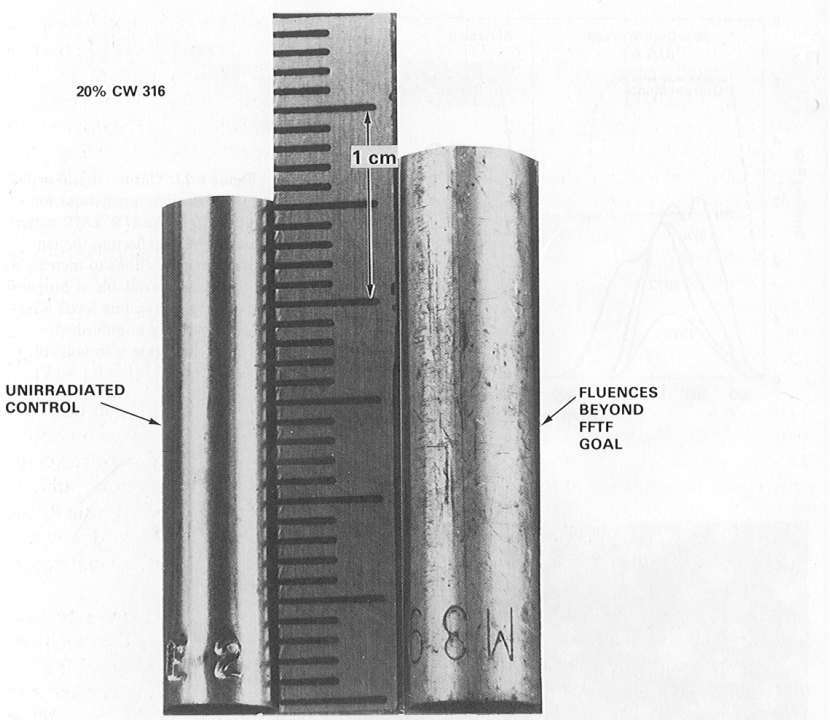

Figure 6-24. Easily observed swelling (≈10% linear, ≈33% volumetric) in unfueled 20% cold worked AISI 316 cladding tube at 1.5×10^{23} n cm^{-2} ($E > 0.1$ MeV) or ≈75 dpa at 510°C in EBR-II (after Straalsund et al., 1982). Note that, in the absence of physical restraints, all relative proportions are preserved during swelling.

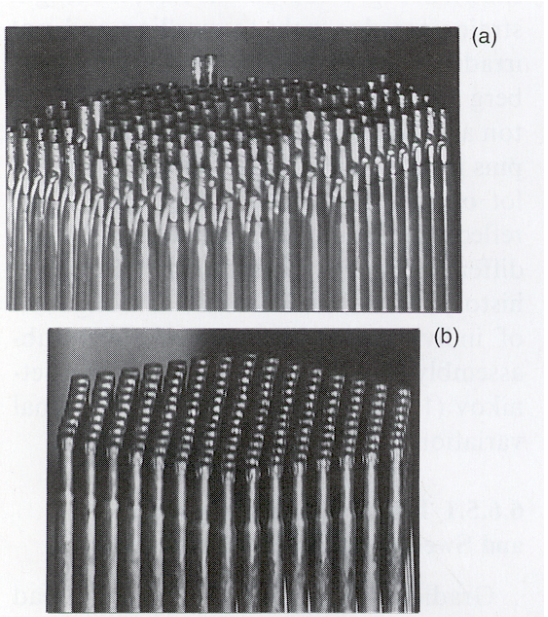

Figure 6-131. (a) Top of a bundle of D9 fuel pins irradiated to a peak fluence of 2.1×10^{23} n cm^{-2} ($E > 0.1$ MeV), showing varying length of pins in response to gradients across the bundle in flux and temperature and also to small variations in pin fabrication history and composition. (b) An undistorted fuel pin assembly with nonswelling HT9 cladding at 1.9×10^{23} n cm^{-2} ($E > 0.1$ MeV) (after Makenas et al., 1990 a).

Ref: Garner, Ch. 6, Irradiation Performance of Cladding and Structural Steels in Liquid Metal Reactors, of "Nuclear materials part 1", Vol 10A, Published by VCH, Germany

Radiation-Induced Swelling

Swelling is one of the most catastrophic consequences of high-dose radiation damage.

Swelling is caused by complicated microstructural changes, especially:

1. Nucleation and growth of *interstitial dislocation loops*

   followed by

2. Nucleation and growth of *voids*

**In certain circumstances where significant transmutation occurs, swelling can be due to the accumulation of bubbles of gas (e.g., He or Xe bubbles).

Radiation-Induced Interstitial Dislocation Loops

Experimental observation of interstitial dislocation loops (electron irradiations)

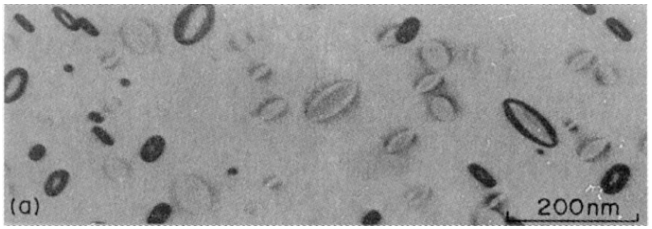

Al

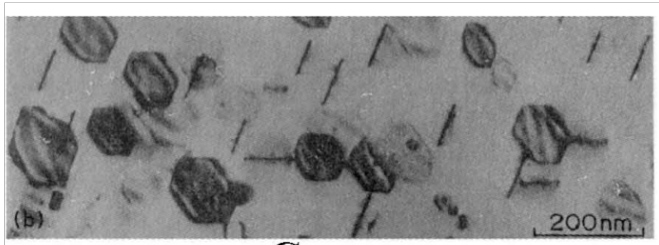

Cu

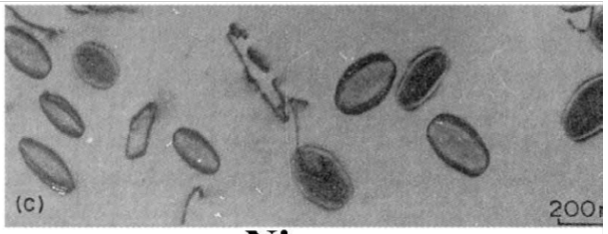

Ni

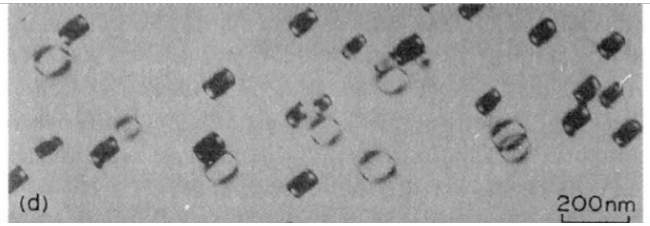

Fe

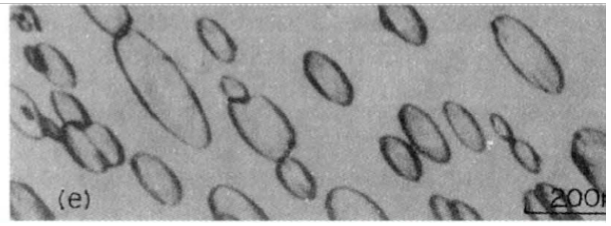

Zn (basal plane)

Radiation-Induced Voids

Bright-field (BF) transmission electron microscopy (TEM) image showing the microstructure of α-Al_2O_3 following fast neutron irradiation at T = 1050 K to a fluence of 310^{25} n/m^2.

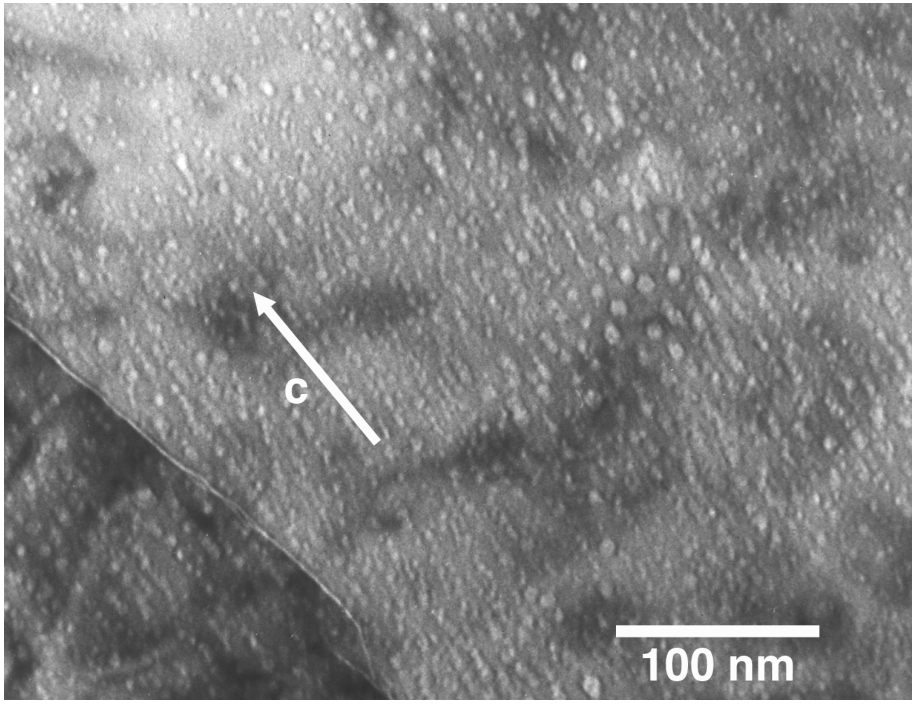

The micrograph reveals a high density of small voids (2-10 nm diameter), arranged in rows along the *c*-axis of the hexagonal unit cell for the α-Al_2O_3.

Micrograph courtesy of F. Clinard, Los Alamos National Laboratory.

Radiation-Induced Bubbles

HFIR irradiation at 400˚C to 51 dpa

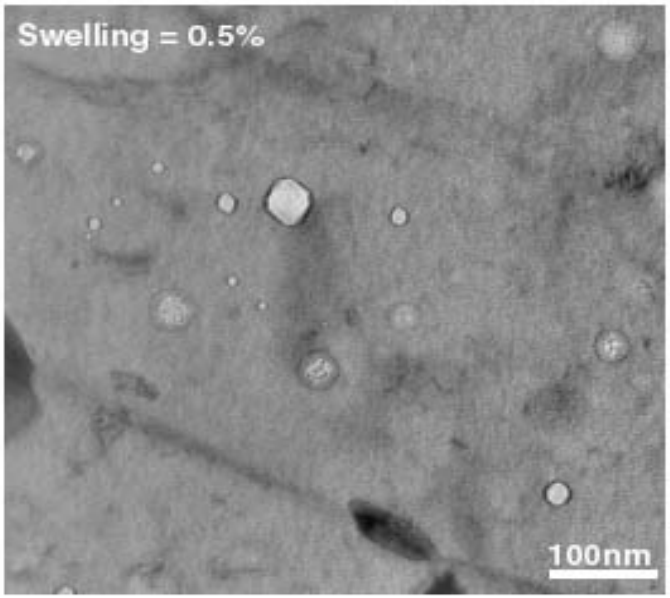

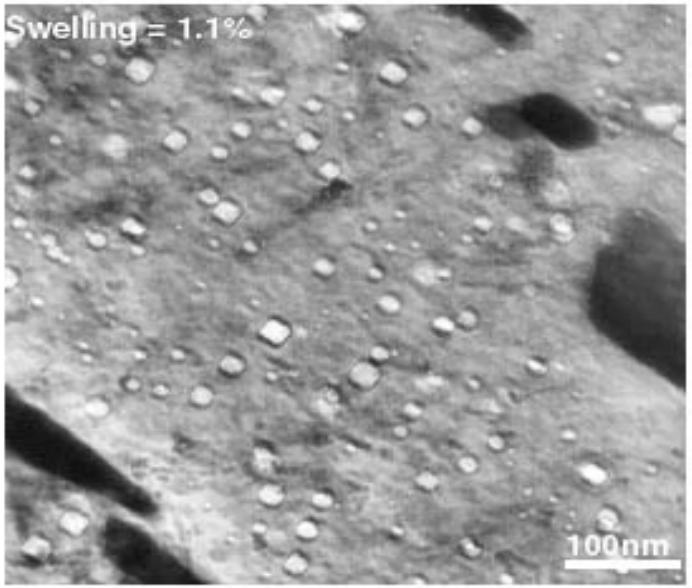

F82H (36 appm He)

^{10}B-doped F82H (330 appm He)

E. Wakai et al. J. Nucl. Mater. 283-287 (2000) 799

$$^{10}_{5}\mathrm{B} + {}^{1}_{0}\mathrm{n} \xrightarrow{3838\ \text{barns}} {}^{7}_{3}\mathrm{Li} + {}^{4}_{2}\mathrm{He}$$

Imagine the radioactive alpha decay of a Pu-239 nucleus sitting in a $(U_{1-x},Pu_x)_1Y_6O_{12}$ actinide waste form

$$^{239}_{94}\mathrm{Pu} \xrightarrow{t_{1/2}=2.410E4\ \text{yrs.}} {}^{235}_{92}\mathrm{U}(88.0119\ \mathrm{keV}) + {}^{4}_{2}\mathrm{He}(5.1683\ \mathrm{MeV})$$

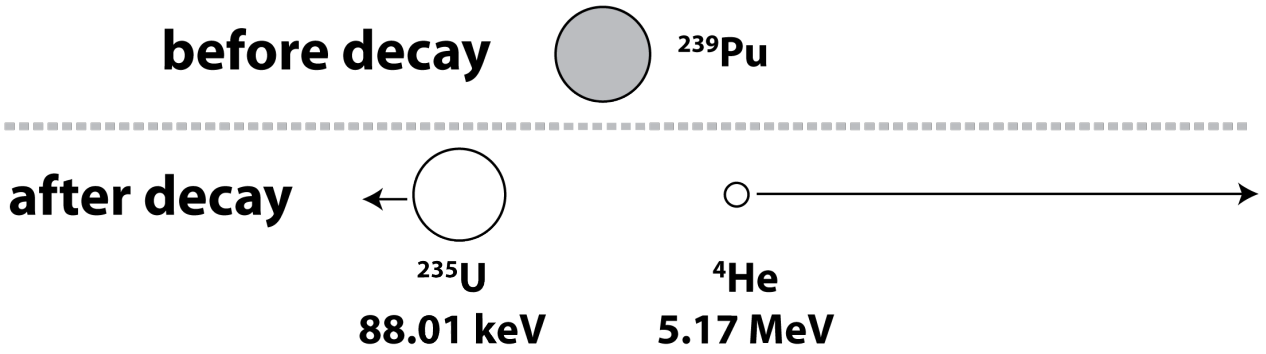

Examples of light-ion and heavy-ion-induced *displacement cascades*

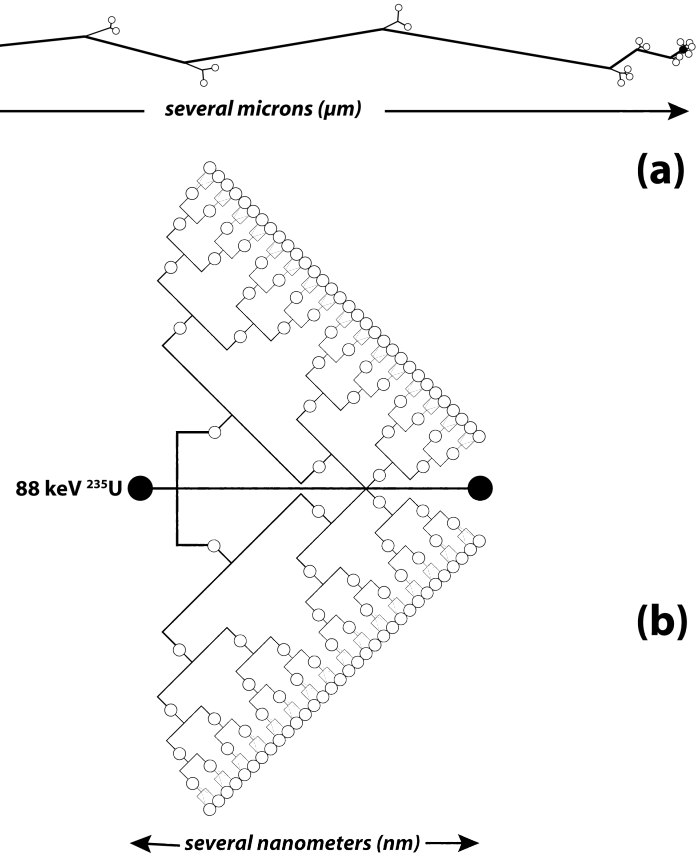

The light ion (a) produces a *dilute* displacement cascade with a characteristic "pearls-on-a-string" geometry. The heavy ion (b) produces a *dense* cascade in which all the atoms in the interior of the cascade are set in motion in a process known as a *displacement spike*.

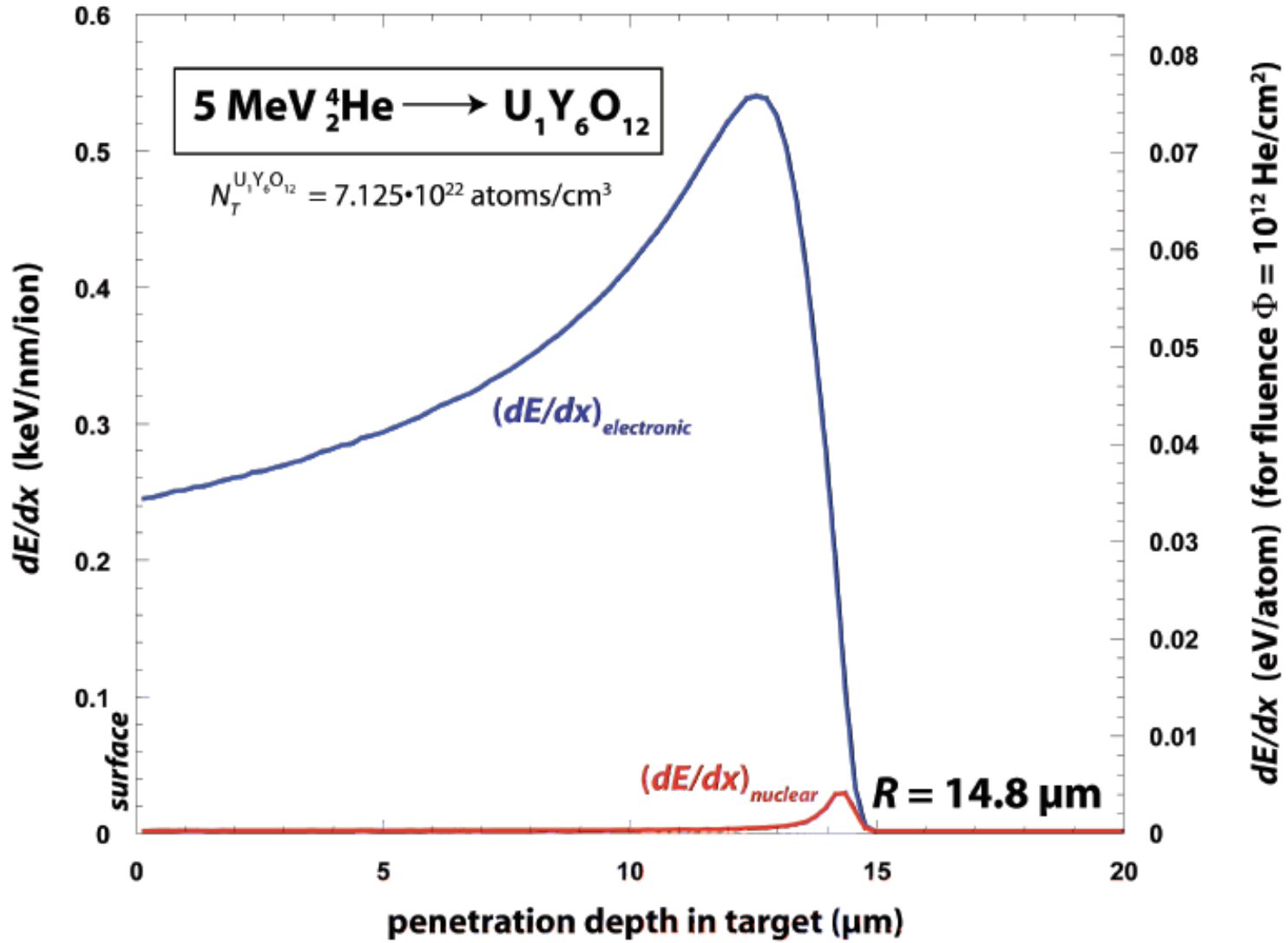
5 MeV $^4_2$He ⟶ $U_1Y_6O_{12}$
$N_T^{U_1Y_6O_{12}}$ = 7.125•10^{22} atoms/cm^3
(dE/dx)$_{electronic}$
(dE/dx)$_{nuclear}$
R = 14.8 µm
surface
dE/dx (keV/nm/ion)
dE/dx (eV/atom) (for fluence Φ = 10^{12} He/cm^2)
penetration depth in target (µm)
0
0.1
0.2
0.3
0.4
0.5
0.6
0.01
0.02
0.03
0.04
0.05
0.06
0.07
0.08
5
10
15
20

Radiolysis

L. W. Hobbs, in *Introduction to Analytical Electron Microscopy*, edited by J. J. Hren, J. I. Goldstein, and D. C. Joy (Plenum Press, New York, 1979), pp. 437-480.

TABLE III

Inorganic solids in which radiolysis is known to occur

alkali halides (LiF, LiCl, LiBr, LiI, NaF, NaCl, NaBr, NaI, KF, KCl, KBr, KI, RbF, RbCl, RbBr, RbI, CsF, CsCl, CsBr, CsI)
alkaline earth halides (CaF_2, SrF_2, BaF_2, MgF_2)
silver halides (AgCl, AgBr, AgI)
cadmium halides (CdI_2)
lanthanum halides (LaF_3)
lead halides (PbI_2)
perovskite halides ($NaMgF_3$, $KMgF_3$)
silicas (quartz, cristobalite, fused silica)
silicates (alkali feldspars, some amphiboles, mica)
ice (H_2O)
alkali hydrides (LiH)
alkali azides (LiN_3, NaN_3, KN_3)
sulfides (MoS_2)
carbonates ($CaCO_3$)
alkali perchlorates (NH_4ClO_3, $NaClO_3$, $KClO_3$)
alkali bromates ($NaBrO_3$)

powellite ($CaMoO_4$)

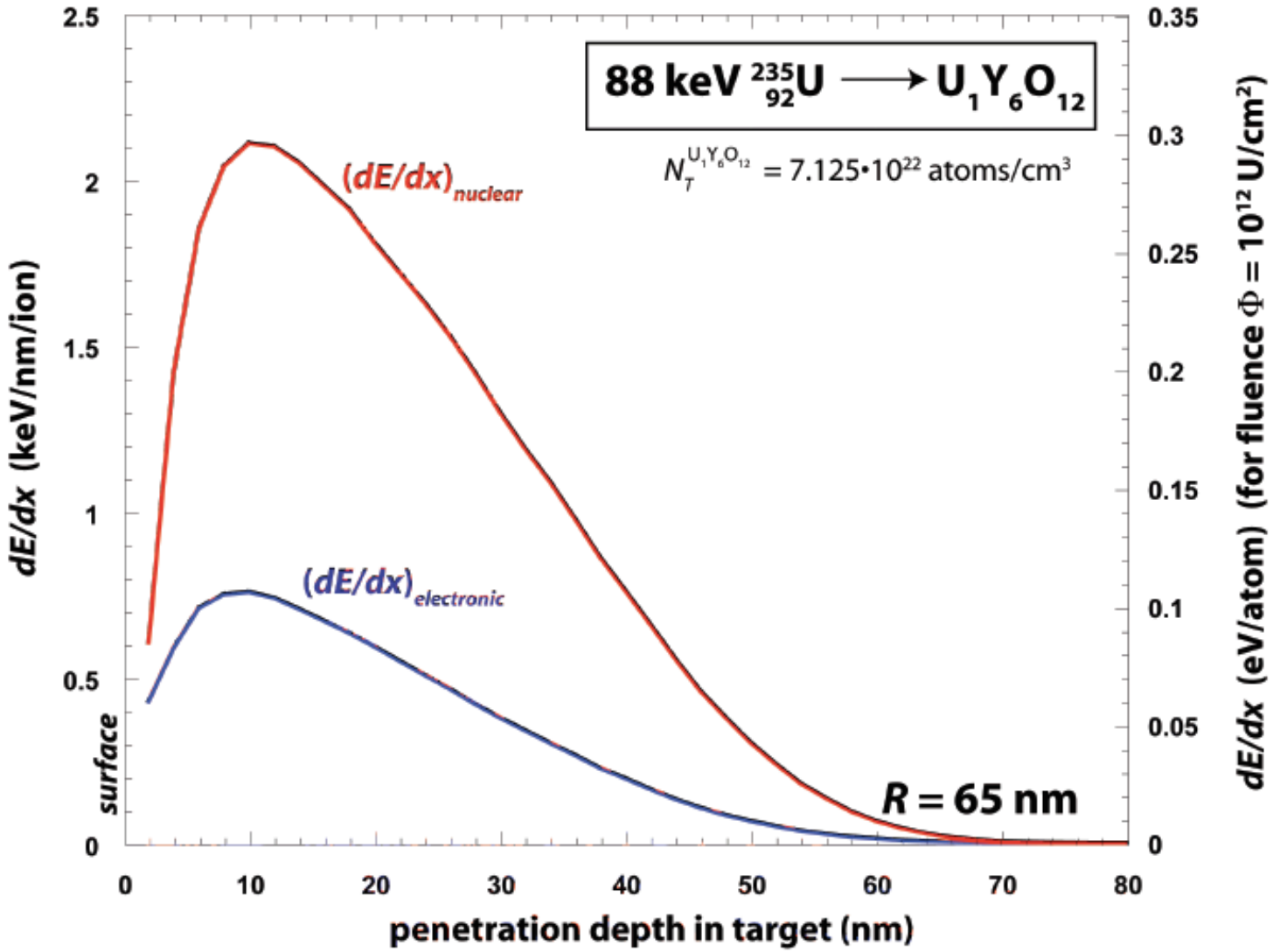
88 keV $^{235}_{92}U \longrightarrow U_1Y_6O_{12}$
$N_T^{U_1Y_6O_{12}}$ = 7.125•10^{22} atoms/cm^3
$(dE/dx)_{nuclear}$
$(dE/dx)_{electronic}$
R = 65 nm
surface
dE/dx (keV/nm/ion)
dE/dx (eV/atom) (for fluence Φ = 10^{12} U/cm^2)
penetration depth in target (nm)
0
0.5
1
1.5
2
2.5
0.05
0.1
0.15
0.2
0.25
0.3
0.35
10
20
30
40
50
60
70
80

Total linear energy loss rate is the sum of nuclear plus electronic energy loss rates

$$\left(\frac{dE}{dx}\right)_{total} = \left(\frac{dE}{dx}\right)_{nuclear} + \left(\frac{dE}{dx}\right)_{electronic}$$

Nuclear vs. Electronic Stopping

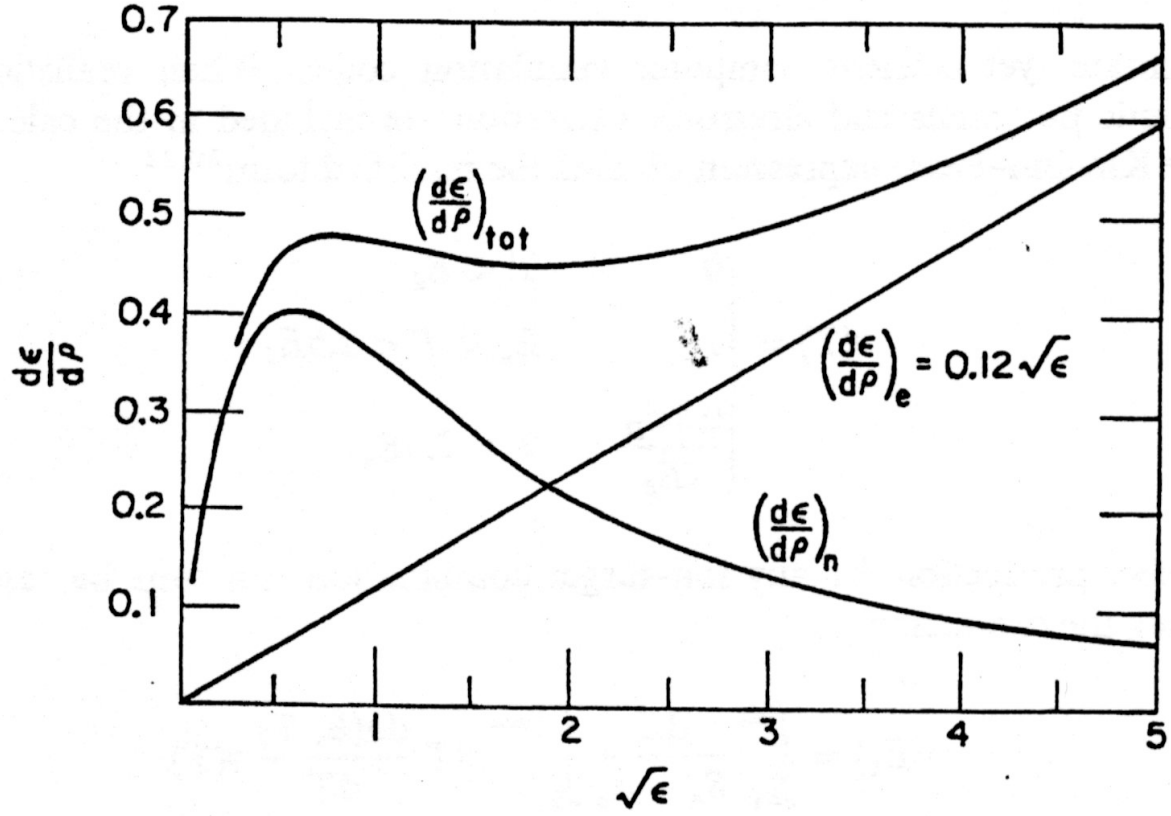

FIG. 4. Nuclear and electronic stopping powers of ions in solids in reduced units.

From R. S. Averback, T. Diaz de la Rubia, "Displacement Damage in Irradiated Metals and Semiconductors," Solid State Physics **51** (1997) 281-402.

Electronic Stopping

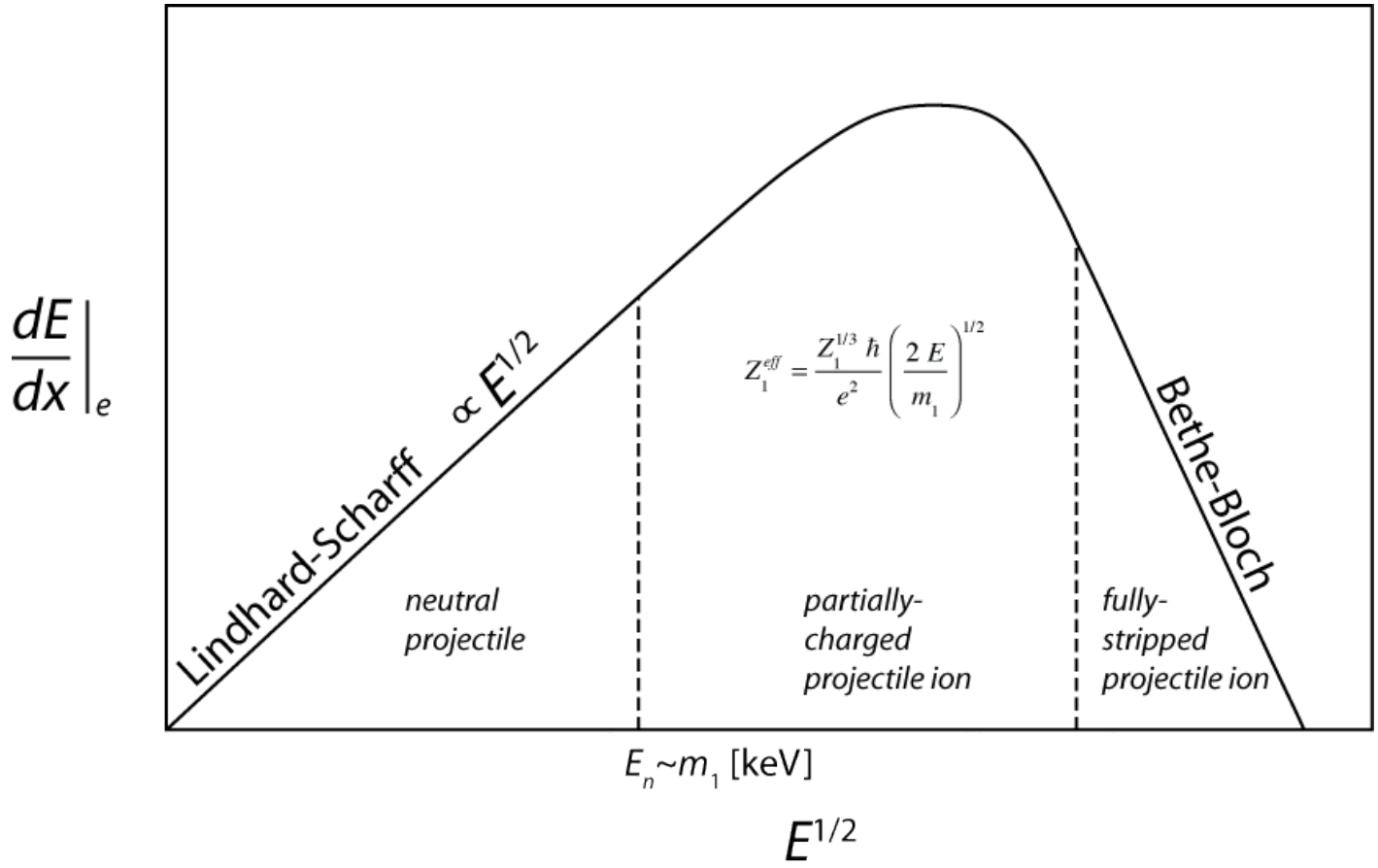

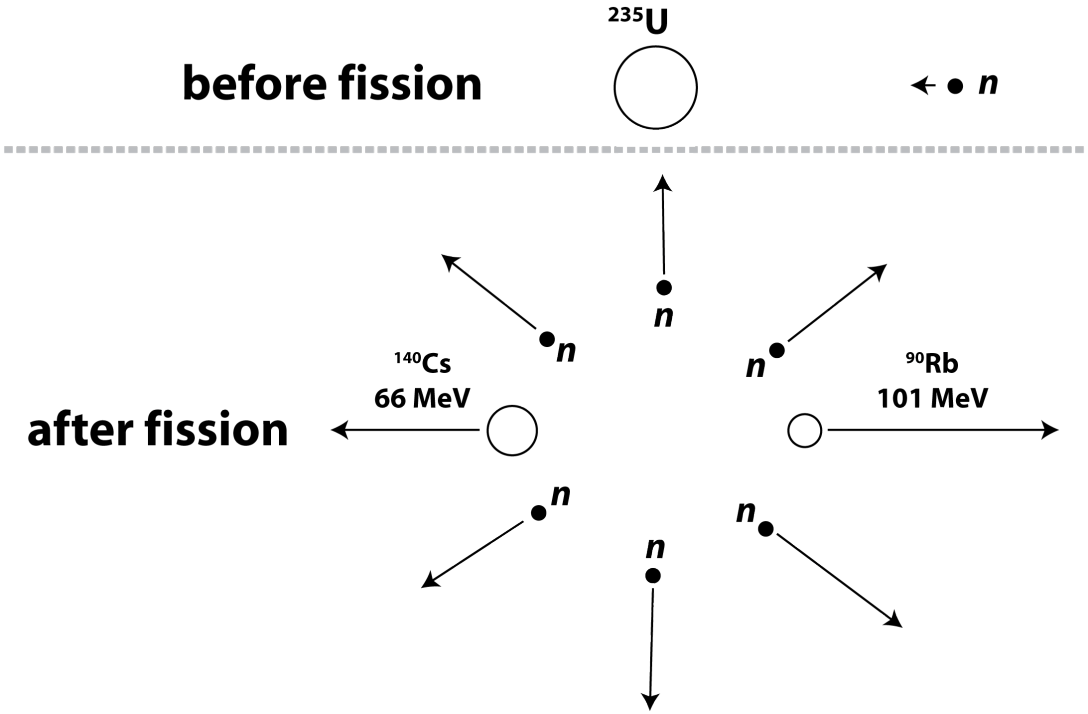

Fissioning of the isotope ^{235}U to form fission products (*FP*s) and neutrons. In the reaction shown, the *FP*s are ^{140}Cs and ^{90}Rb (there are also 6 neutrons produced in this reaction). The arrows are meant to indicate qualitatively relative differences between the product particle velocities.

$$^{235}_{92}\mathrm{U} + {}^{1}_{0}n \longrightarrow {}^{236}_{92}\mathrm{U}^{*} \longrightarrow {}^{140}_{55}\mathrm{Cs}\ \ (66\ \mathrm{MeV}) + {}^{90}_{37}\mathrm{Rb}\ \ (101\ \mathrm{MeV}) + 6\ {}^{1}_{0}n$$

Electronic Energy Loss and Nuclear Energy Loss Partitioning for 66 MeV Cs vs. 101 MeV Rb

(SRIM simulation results)

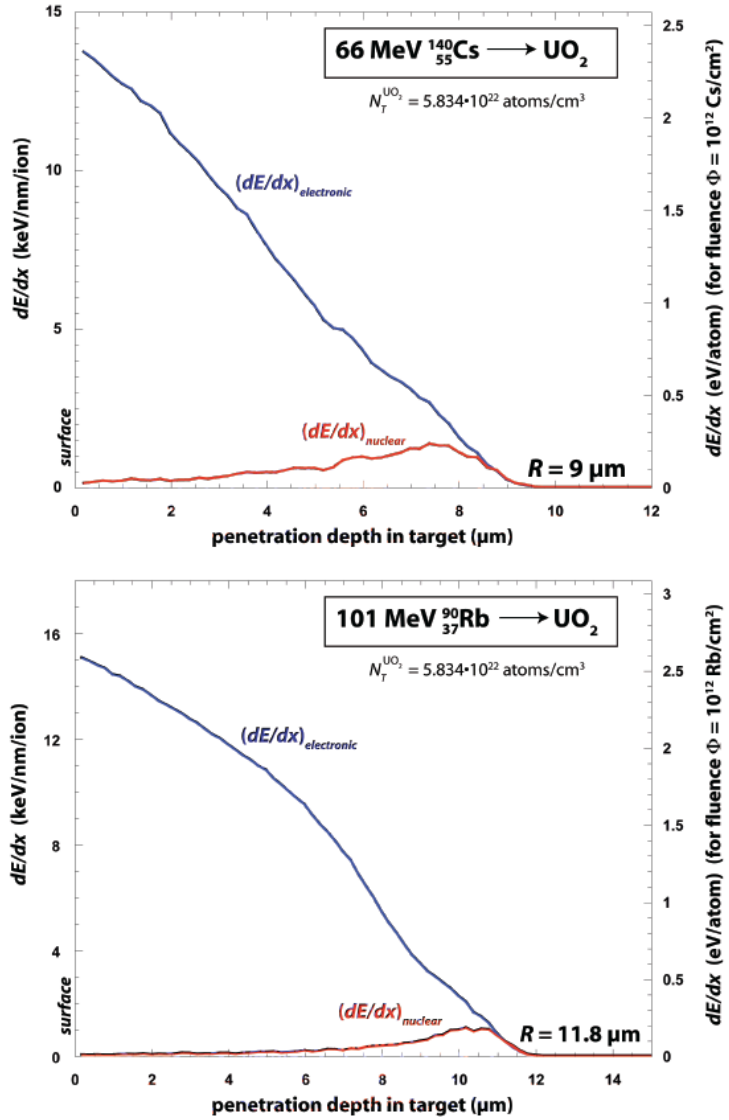

Fission track or swift heavy ion track damage

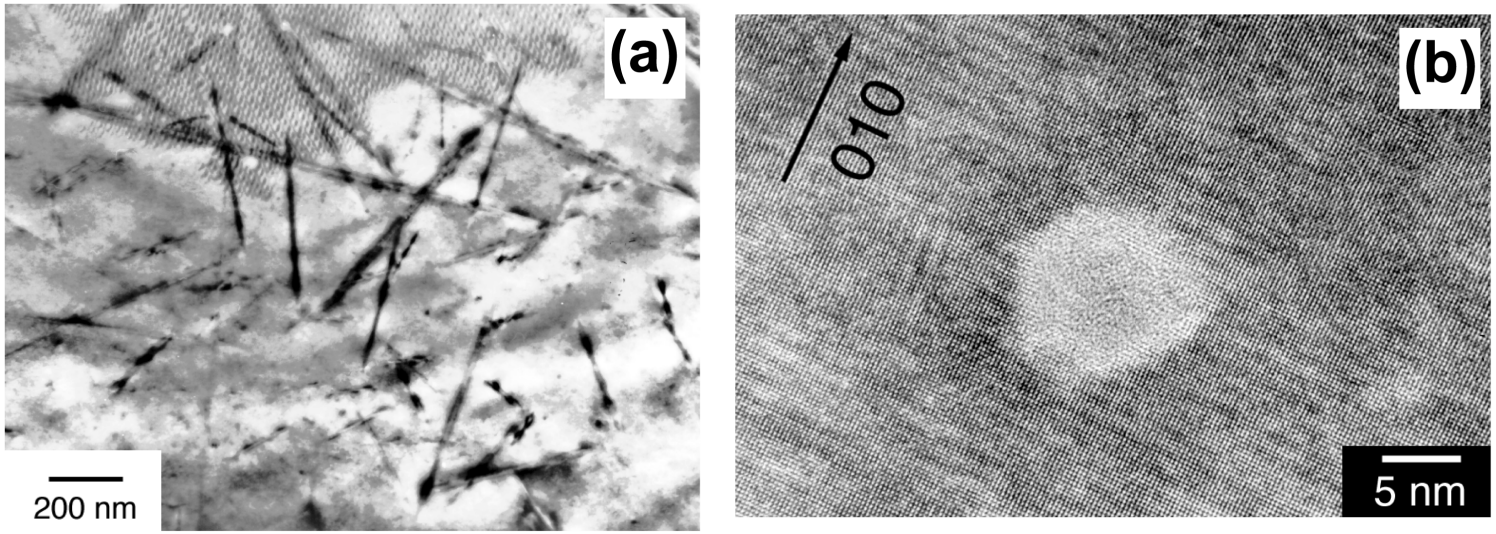

TEM micrographs showing ion tracks produced by 800 MeV H^+ fission events originating on Bi atoms in the oxide superconductor, Bi-2212. Samples irradiated in the LANL-WNR proton irradiation facility. **(a)** Side view of ion tracks; **(b)** End-on view of a single ion track. This image, obtained using atomic resolution TEM, shows that the core of the ion track is amorphous, not crystalline. The surrounding matrix material is crystalline. Micrographs courtesy of K. Sickafus & D. Phillips, Los Alamos National Laboratory.

Electronic stopping gone bonkers!

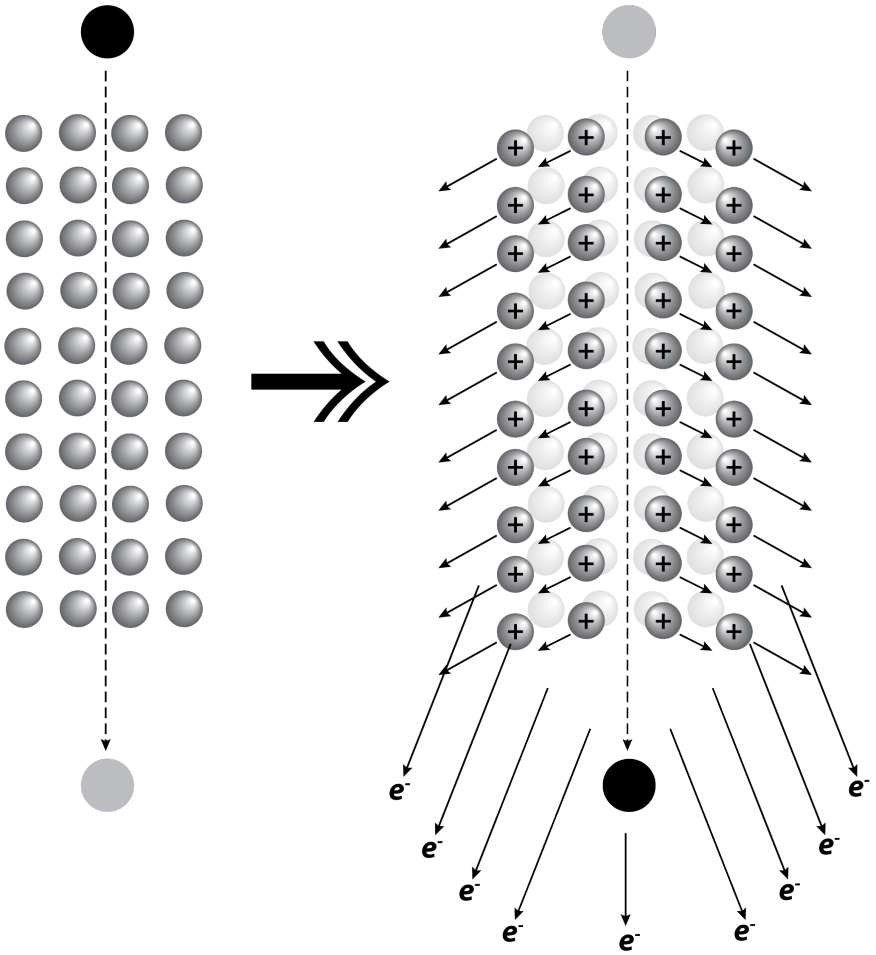

Schematic drawing of a crystalline material before (left) and after (right) irradiation with a swift heavy ion such as a fission fragment. The fission fragment ionizes the target atoms causing these positively-charged atoms to repel one another. This process is known as *Coulomb Explosion*.

Consider an ion of energy E traversing a solid and losing energy by successive nuclear and electronic scattering events. When all is said and done, this ion will come to rest in the solid, having dissipated all of its kinetic energy, E. For a given energy, E, the *linear rate* at which the ion loses energy, dE/dx, is known as the *stopping power* of the solid. The total stopping power of the target is the sum of the nuclear and electronic stopping powers:

$$\left(\frac{dE}{dx}\right)_{total} = \left(\frac{dE}{dx}\right)_{nuclear} + \left(\frac{dE}{dx}\right)_{electronic}$$

where $(dE/dx)_{nuclear}$ and $(dE/dx)_{electronic}$ are the nuclear and electronic stopping powers, respectively. Using Eqn. (4.1), we can write an expression for the range, R, of an ion in a solid. The *ion range*, R, is simply the reciprocal of the stopping power, integrated from the position of the ion at birth to its position when it comes to rest:

$$R = \int_{E=E_0}^{E=0} \frac{dE}{\left(dE/dx\right)_{total}} = \int_{E=E_0}^{E=0} \frac{dE}{\left(dE/dx\right)_{nuclear} + \left(dE/dx\right)_{electronic}}$$

where $E = E_0$ is the ion energy upon birth and $E = 0$ is the ion kinetic energy when it comes to rest at the *end-of-range*.

Range of 1 MeV energetic particles in lead (Pb)

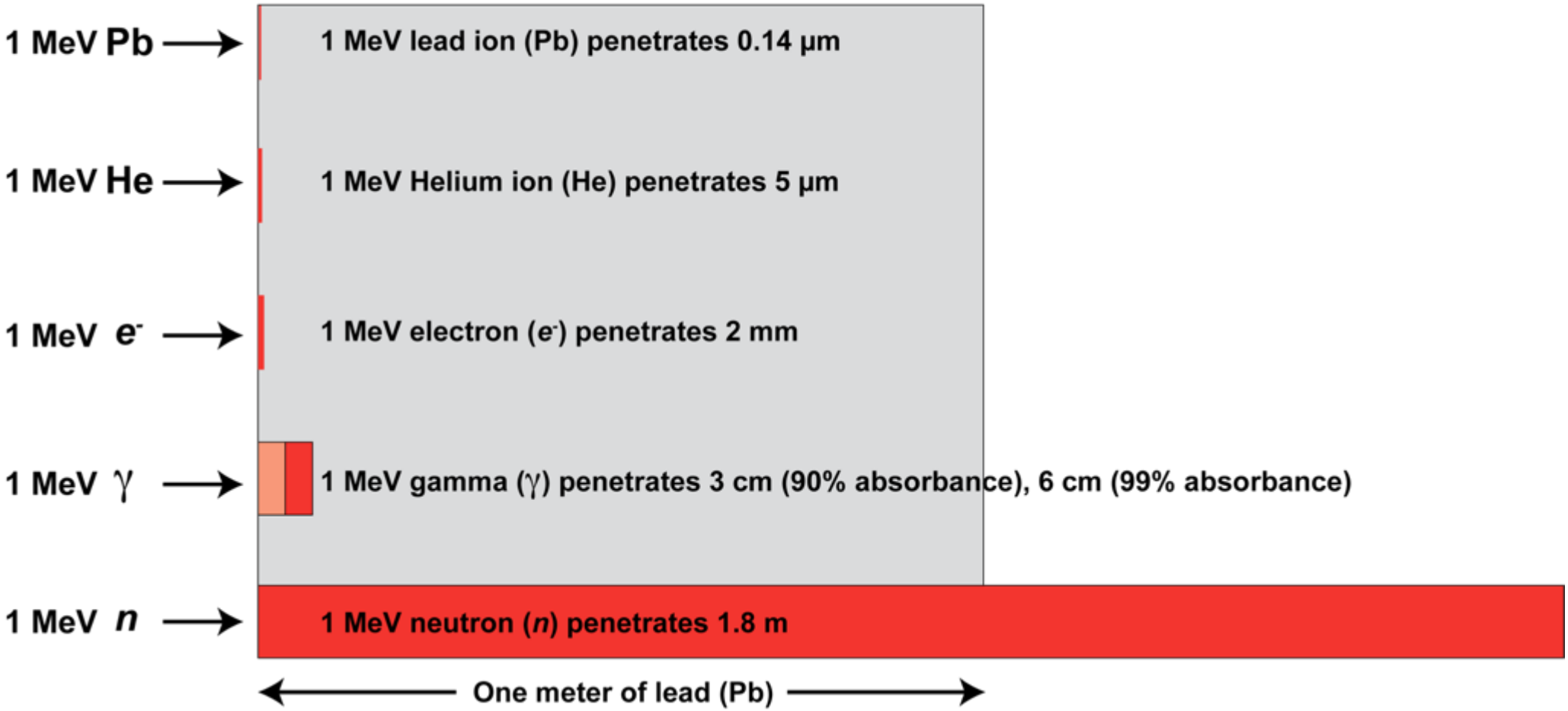

Displacement Damage

We will try to quantify damage production rates in solids under irradiation (by damage we will mean stable interstitial-vacancy (*i*-*v*) pairs)

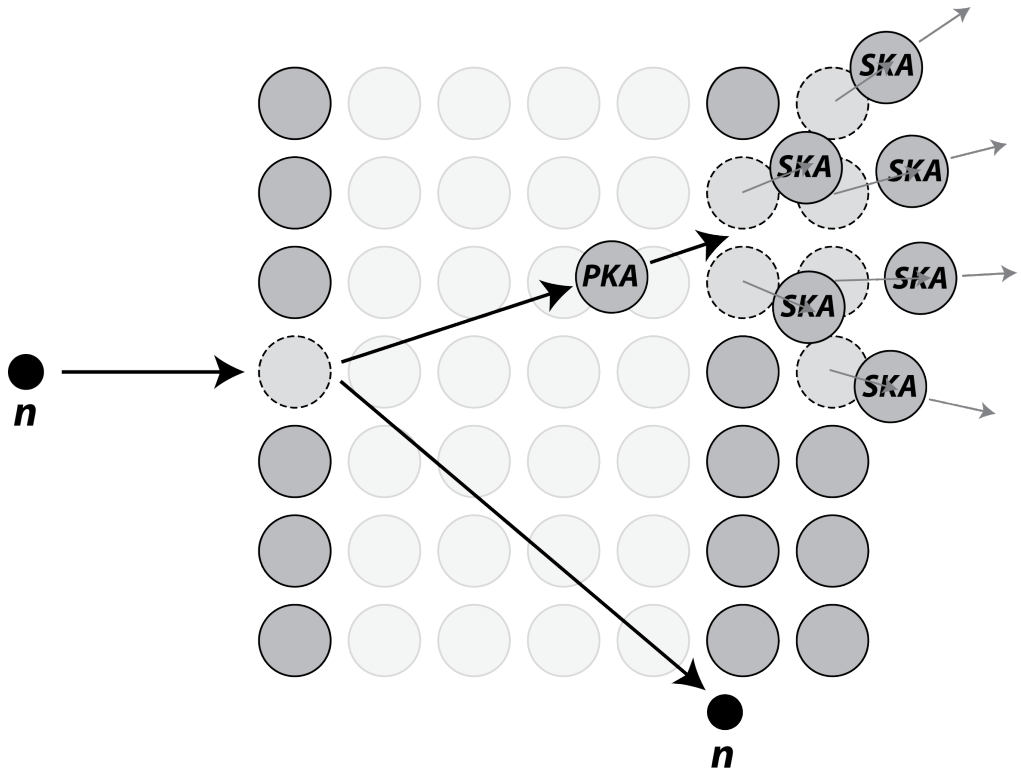

Kinetic energy deposition in a crystalline solid by a fast neutron (*n*). The neutron imparts kinetic energy to a lattice atom and displaces the atom from its lattice site. This atom is called a primary knock-on atom (*PKA*). The *PKA* displaces additional lattice atoms which become secondary knock-on atoms (*SKA*s). The ensemble of displaced atoms is known as a *displacement cascade*.

Frenkel Pair (*i-v* pair) Formation Under Irradiation

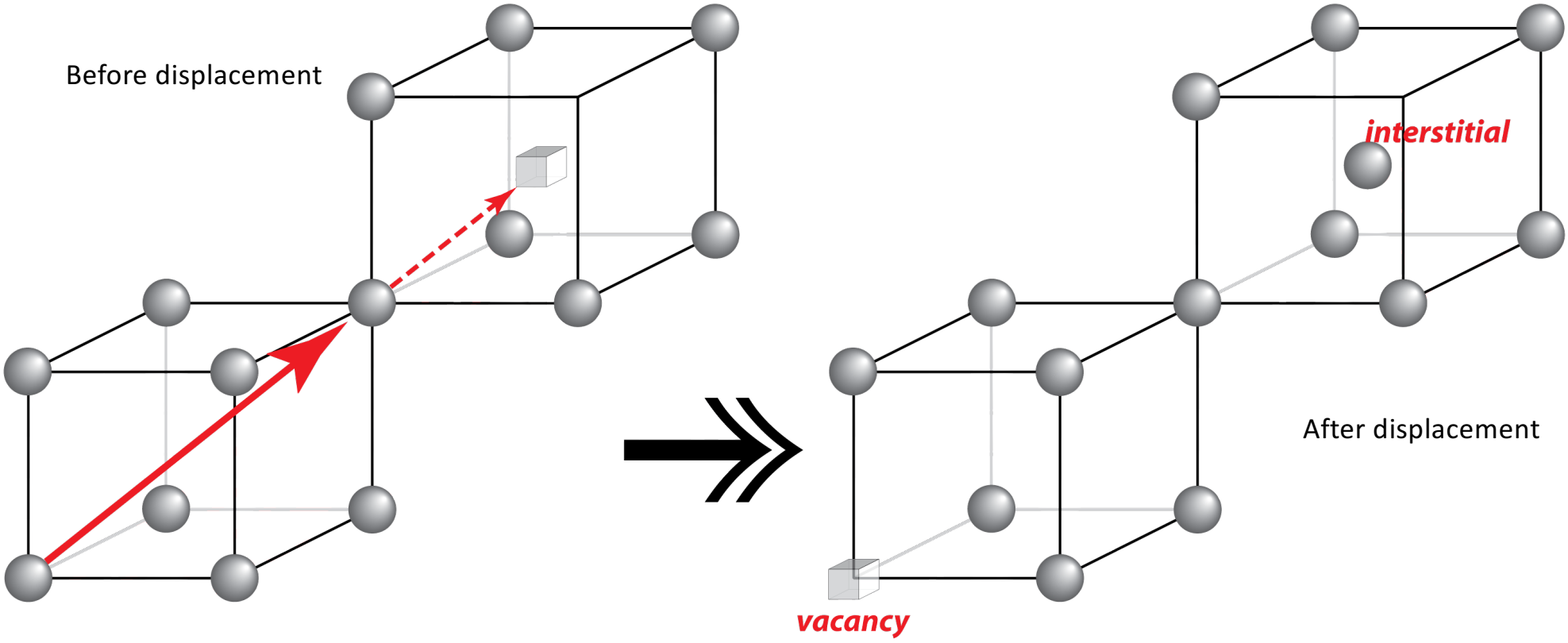

It is interesting that the process of making one point defect in a solid actually makes two point defects!

The process of producing a point defect begins with knocking one atom off of its lattice site into an *interstice* in the lattice. This produces an interstitial (*i*) atom.

However, at the same time, a vacancy (*v*) is produced, because the knock-on atom leaves behind an empty lattice site.

In some instances, the energy of the projectile ion that initiates the knock-on event is sufficiently low that it comes to rest following its knock-on collision. It then spontaneously fills the vacated site and only one *net* defect is produced (the interstitial). This is known as a ***replacement collision***.

Kinchin-Pease (*KP*) Formula

$$N_d = \begin{cases} 0 & ; \quad 0 < E \leq E_d \\ 1 & ; \quad E_d < E \leq 2\,E_d \\ \dfrac{E}{2\,E_d} & ; \quad E > 2\,E_d \end{cases}$$

Total number of *i-v* pairs produced per primary knock-on atom (*PKA*)

G. H. Kinchin, R. S. Pease, "The Displacement of Atoms in Solids by Radiation," Reports on Progress in Physics **18** (1955) 1-51.

Kinchin-Pease Eqn.

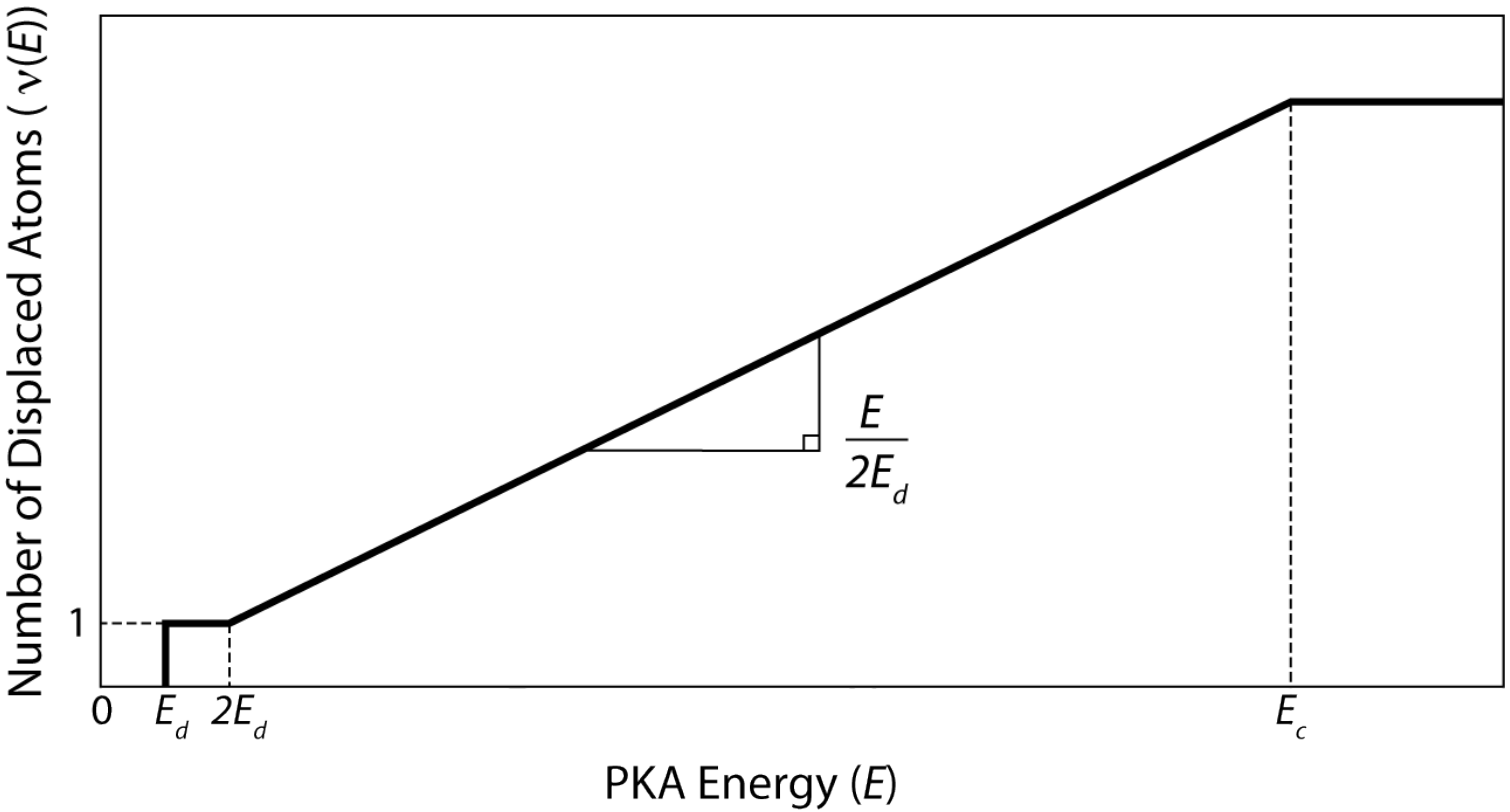

The critical (or cutoff) energy, E_c

In a metal, a reasonable estimate for E_c is given by (see, e.g., Olander [Ch. 17]):

$$E_c\left[\text{keV}\right] \cong M_T\left[\text{amu}\right]$$

where M_T is the target atom mass in atomic mass units. Thus, for copper (M_{Cu} = 63 amu), E_c = 63 keV, such that for ion energies above E = 63 keV, we assume only electronic stopping occurs.

Kinchin-Pease Eqn.

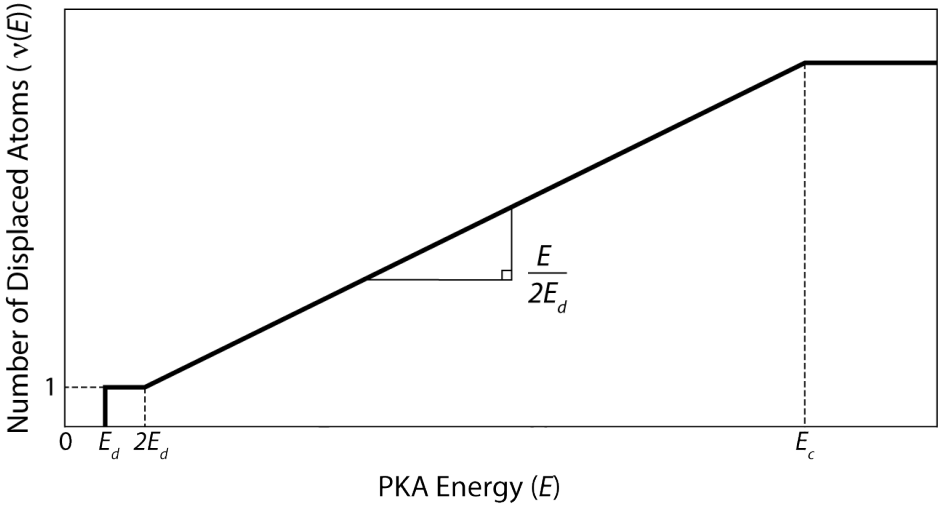

$$\nu(E) = \begin{cases} 0 & (0 < E < E_d) \\ 1 & (E_d < E < 2E_d) \\ \dfrac{E}{2E_d} & (2E_d < E < E_c) \\ \dfrac{E_c}{2E_d} & (E > E_c) \end{cases}$$

Estimating *Frenkel Pair* (*i-v* pair) Formation Under Irradiation Using the Kinchin-Pease Formula

* Frenkel pair formation is equal to the number of displacements produced per projectile ion, N_d

$$N_d = \begin{cases} 0 & ; \quad 0 < E \leq E_d \\ 1 & ; \quad E_d < E \leq 2\,E_d \\ \dfrac{0.8\;\xi(E)}{2\,E_d} & ; \quad E > 2\,E_d \end{cases}$$

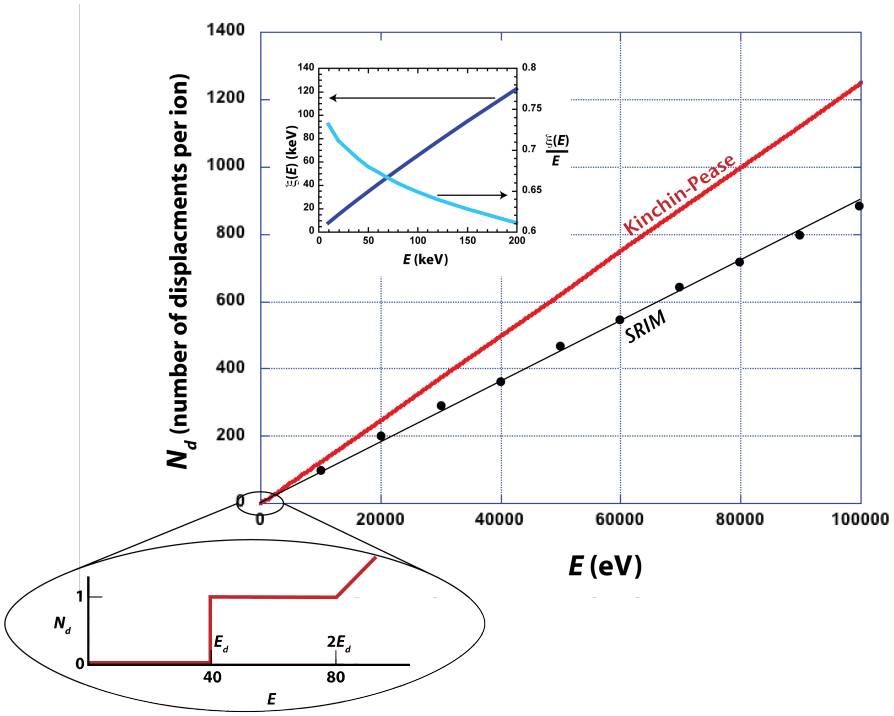

The black curve, with calculated points displayed as solid circles, shows N_d vs. E for ^{235}U irradiations of the actinide-host oxide, $U_1Y_6O_{12}$, based on *SRIM* simulations and assuming E_d = 40 eV for all target atoms.

i-v pair production and *dpa*

One *dpa* represents the dose at which every target atom has been *knocked* from its lattice site, on average, one time. The conversion from units of (*i-v pairs*)*/nm/ion* to *displacements per atom* (*dpa*) is given by:

$$\left[\frac{i\text{-}v \text{ pairs}}{\text{nm}\cdot\text{ion}}\right] \Rightarrow \left[\frac{i\text{-}v \text{ pairs}}{\text{nm}\cdot\text{ion}}\right] \frac{1}{[10^{-7} \text{ cm}/\text{nm}]} \frac{\Phi\ [\text{ions}/\text{cm}^2]}{\rho_a\ [\text{atoms}/\text{cm}^3]}$$

Get from SRIM "vacancy.txt" file

$$= \left[\frac{i\text{-}v \text{ pairs}}{\text{atom}}\right] \equiv \left[\frac{\text{displacements}}{\text{atom}}\right] \equiv [dpa]$$

In ion irradiations, the depth distributions of displacements are generally referred to as *damage profiles*. Each damage profile exhibits a maximum at some depth prior to the end-of-range of the ion. The dose at this maximum is termed the *peak dpa*.

SRIM simulation of *i-v* pair production for He ions in UY_6O_{12}

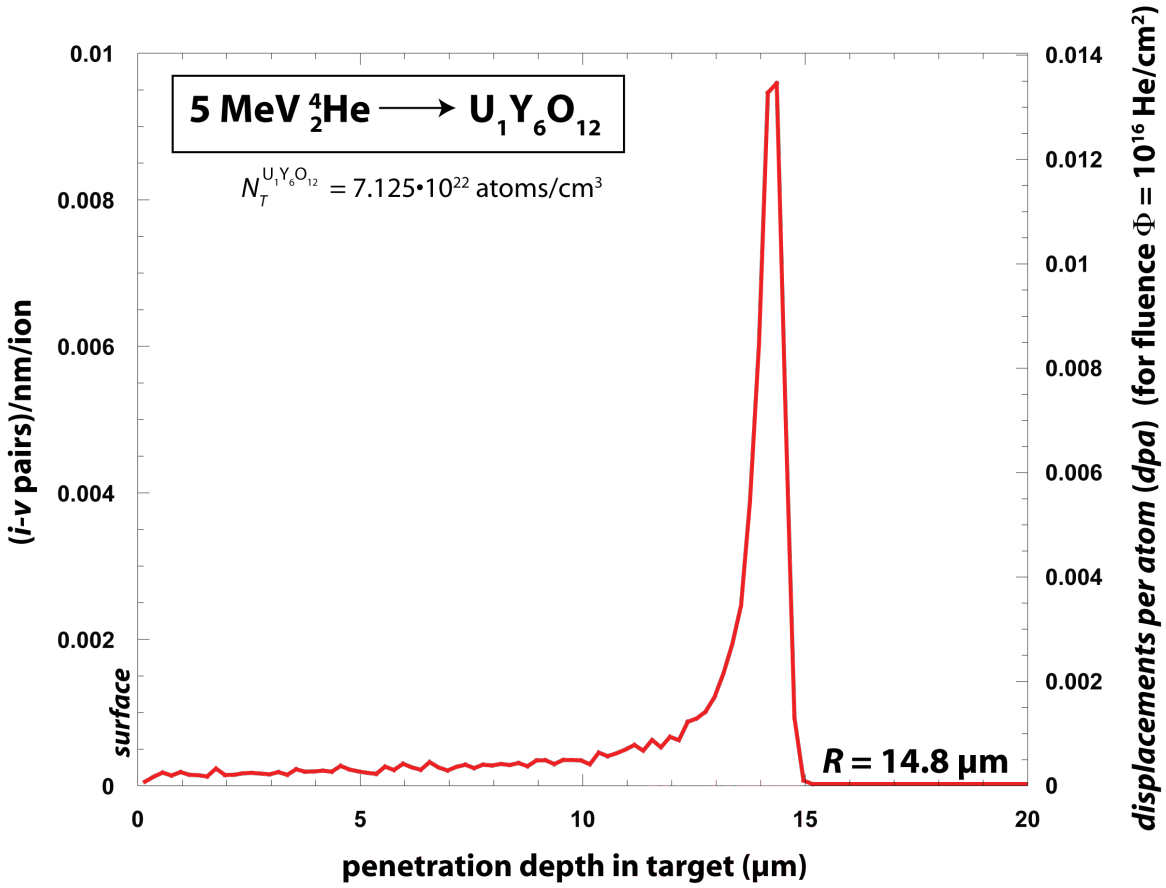

SRIM simulation of *i-v* pair production for U ions in UY_6O_{12}

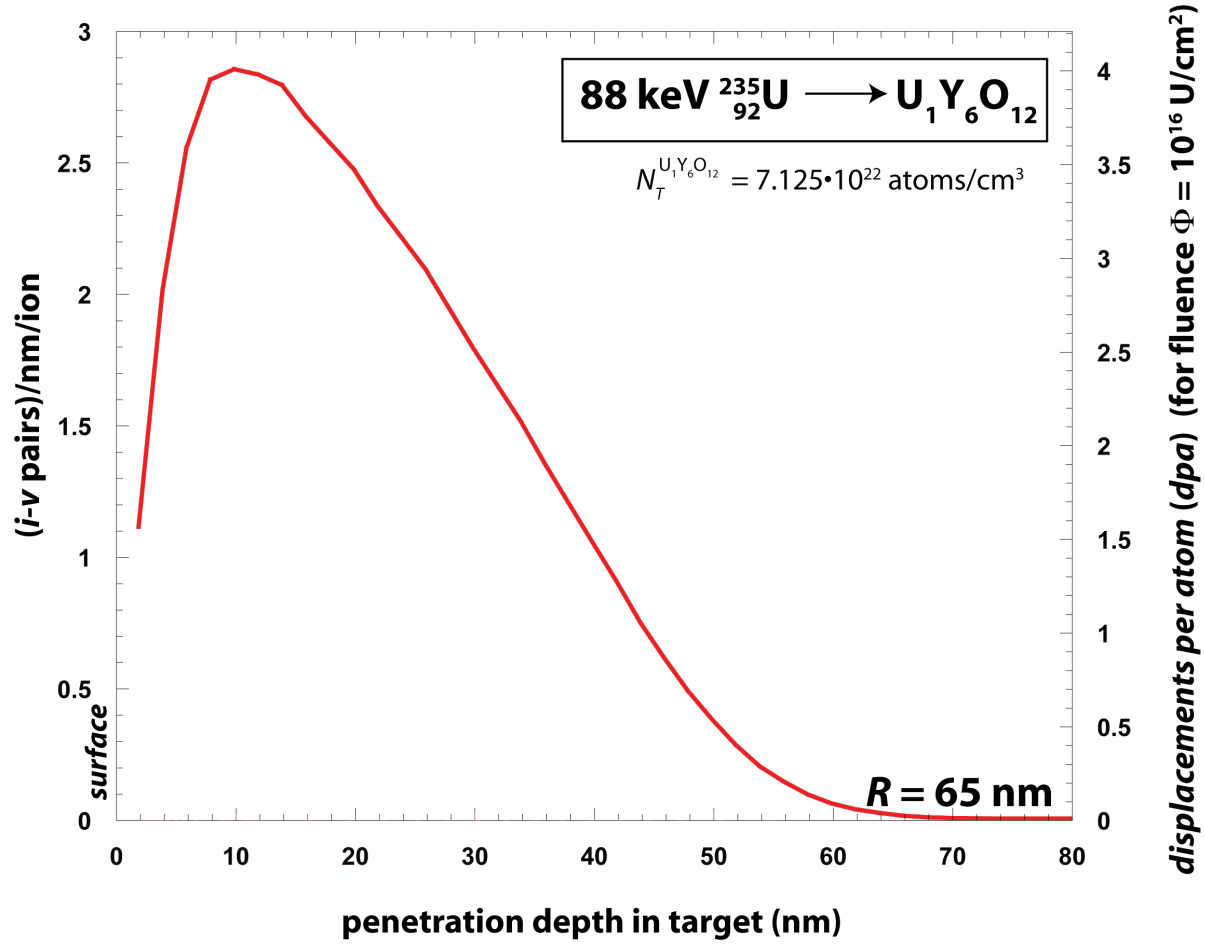

Perfect Lattice

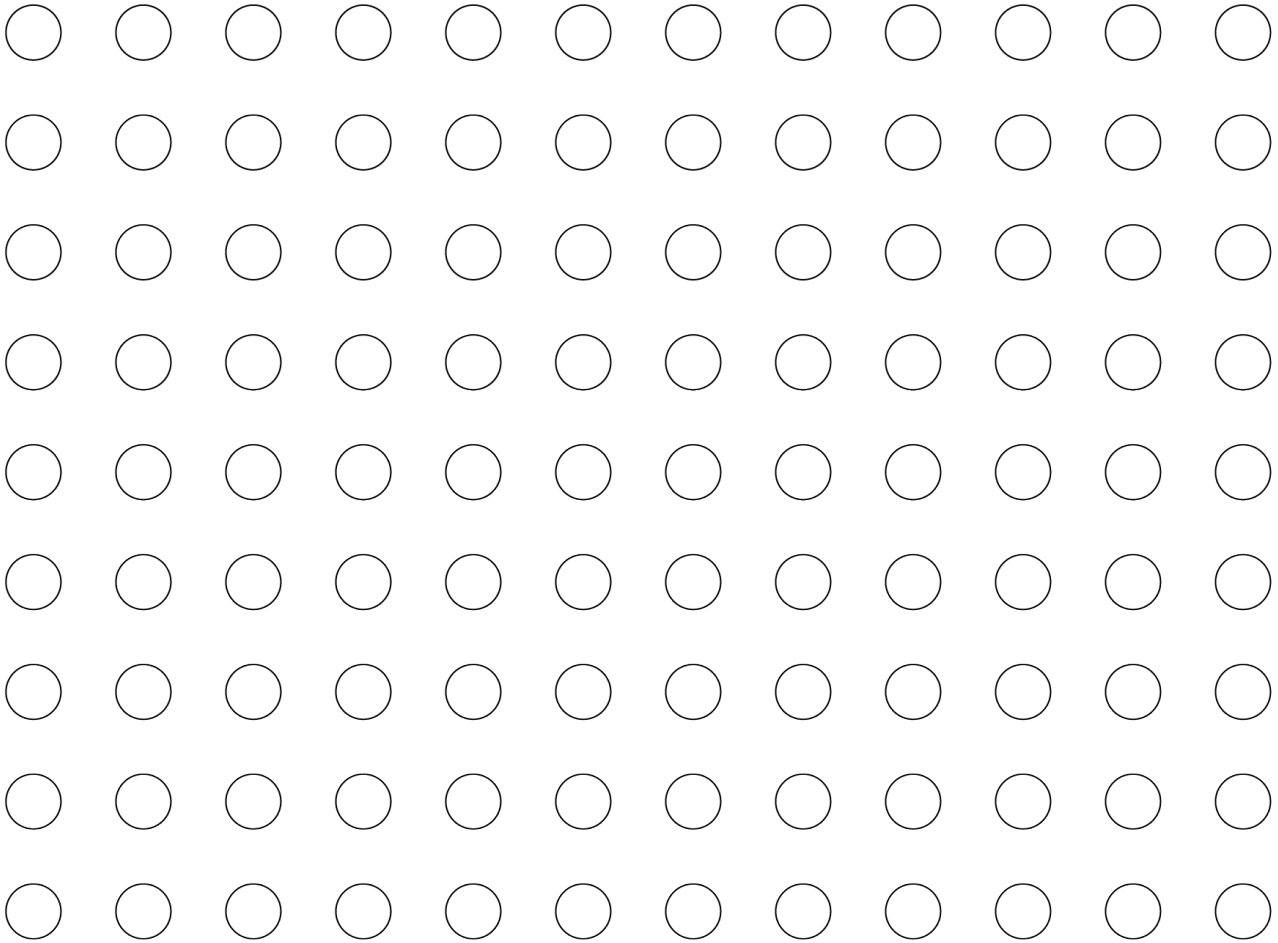

Perfect Lattice + Interstitial Point Defect

In a monoatomic solid, this would be called a self-interstitial atom

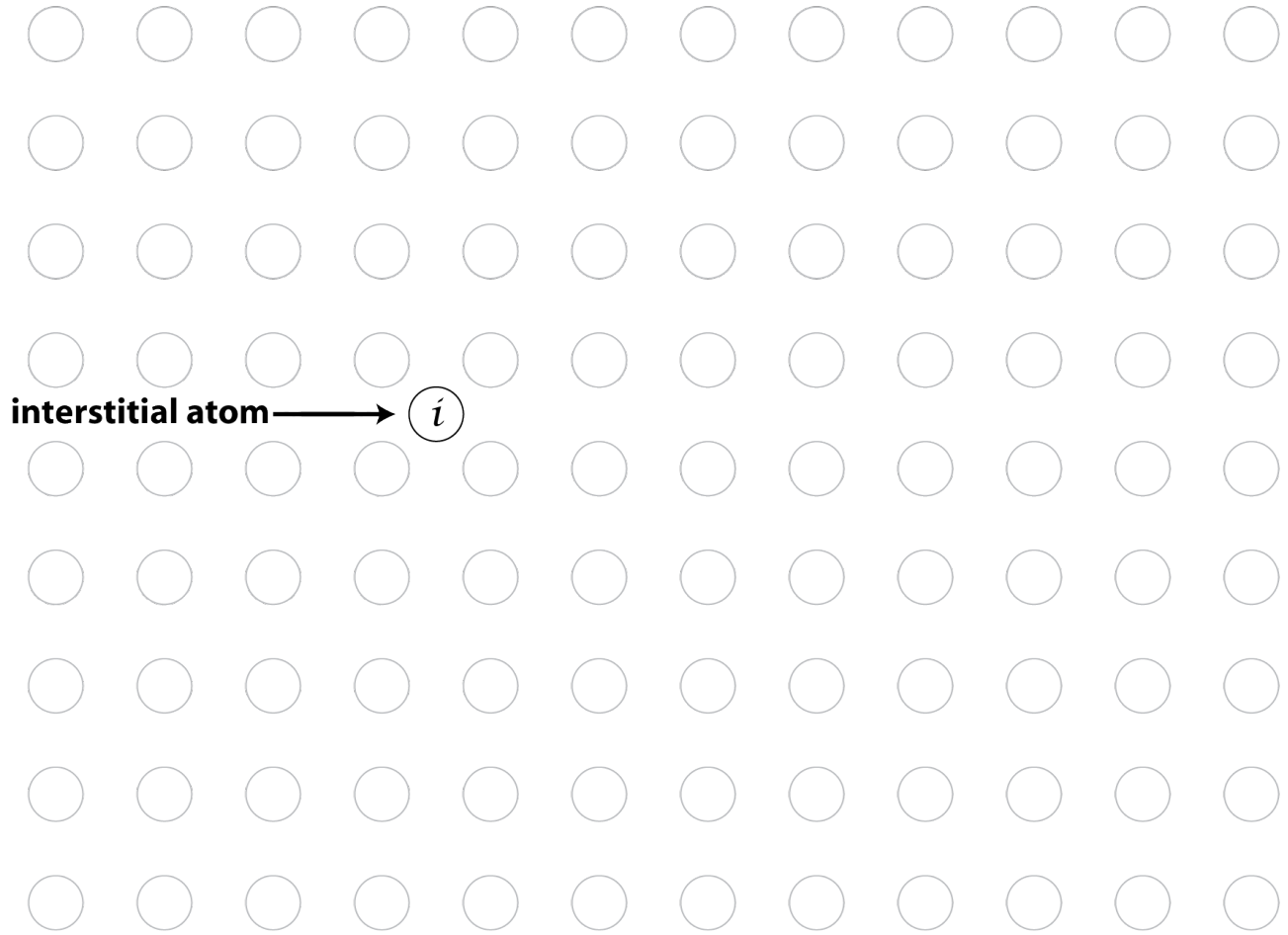

Perfect Lattice + *Freely-Migrating* Self-Interstitial Atom (*SIA*)

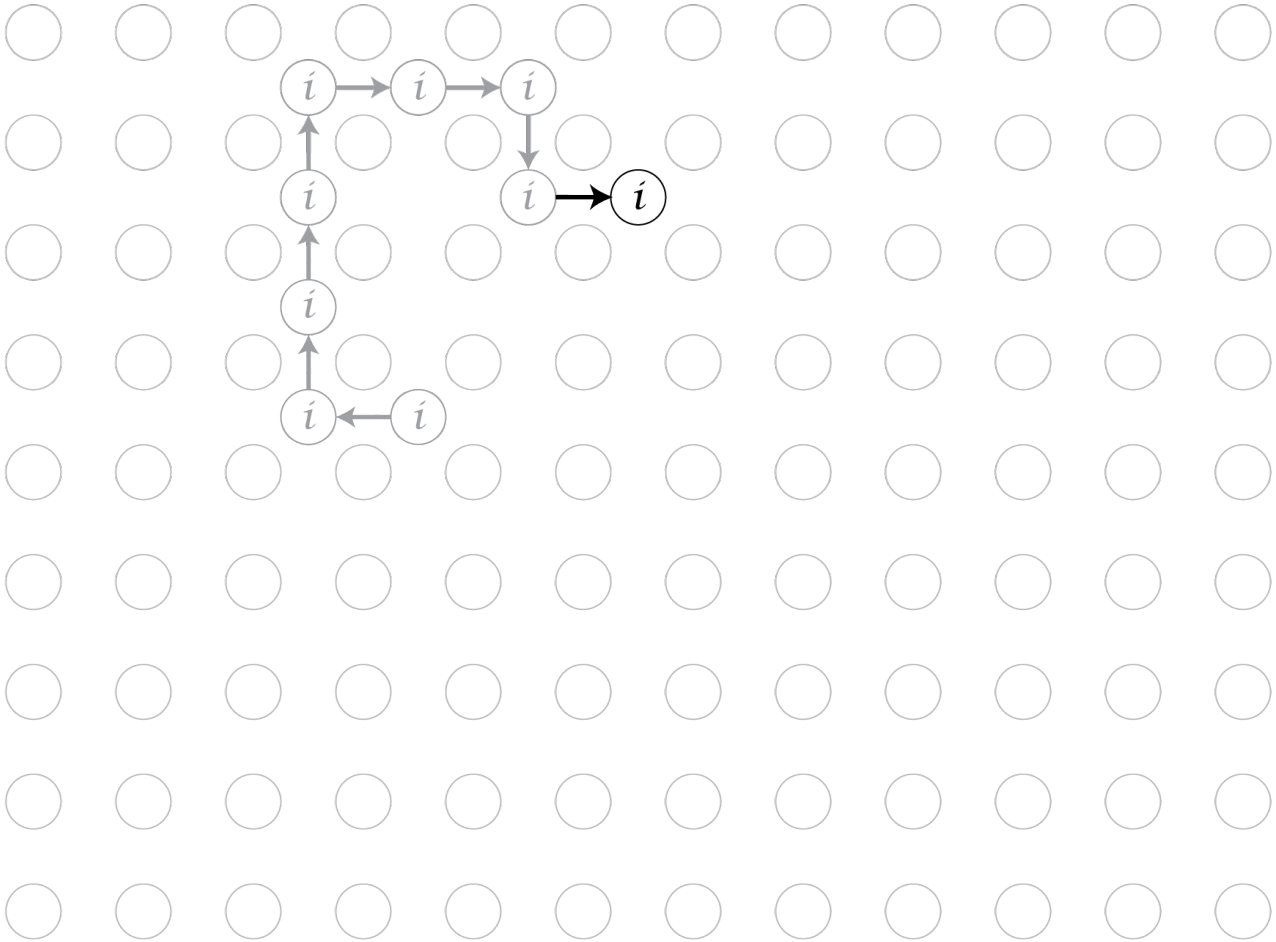

Perfect Lattice + *Freely-Migrating SIA* #1

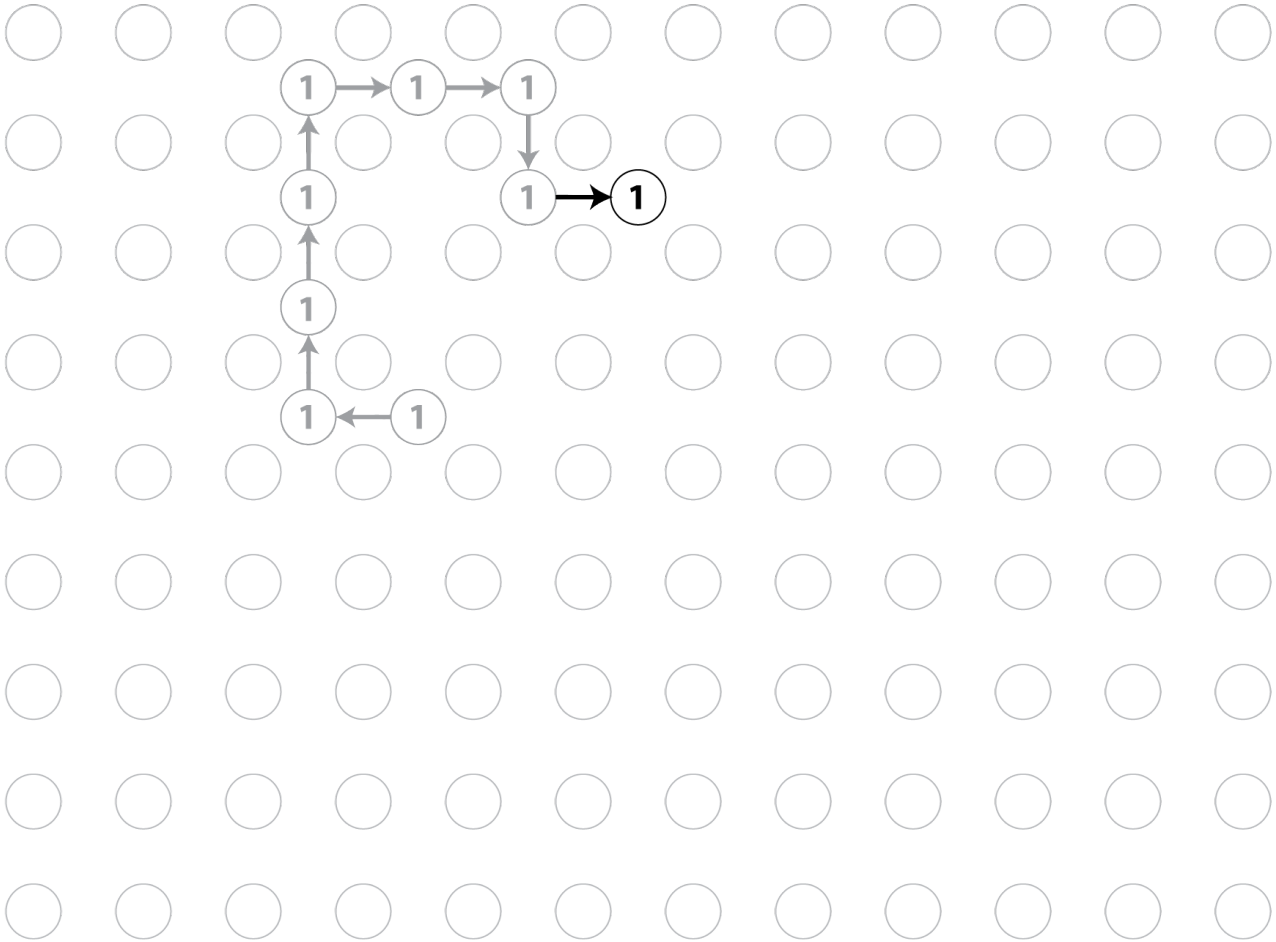

Perfect Lattice + *Freely-Migrating SIA #2*

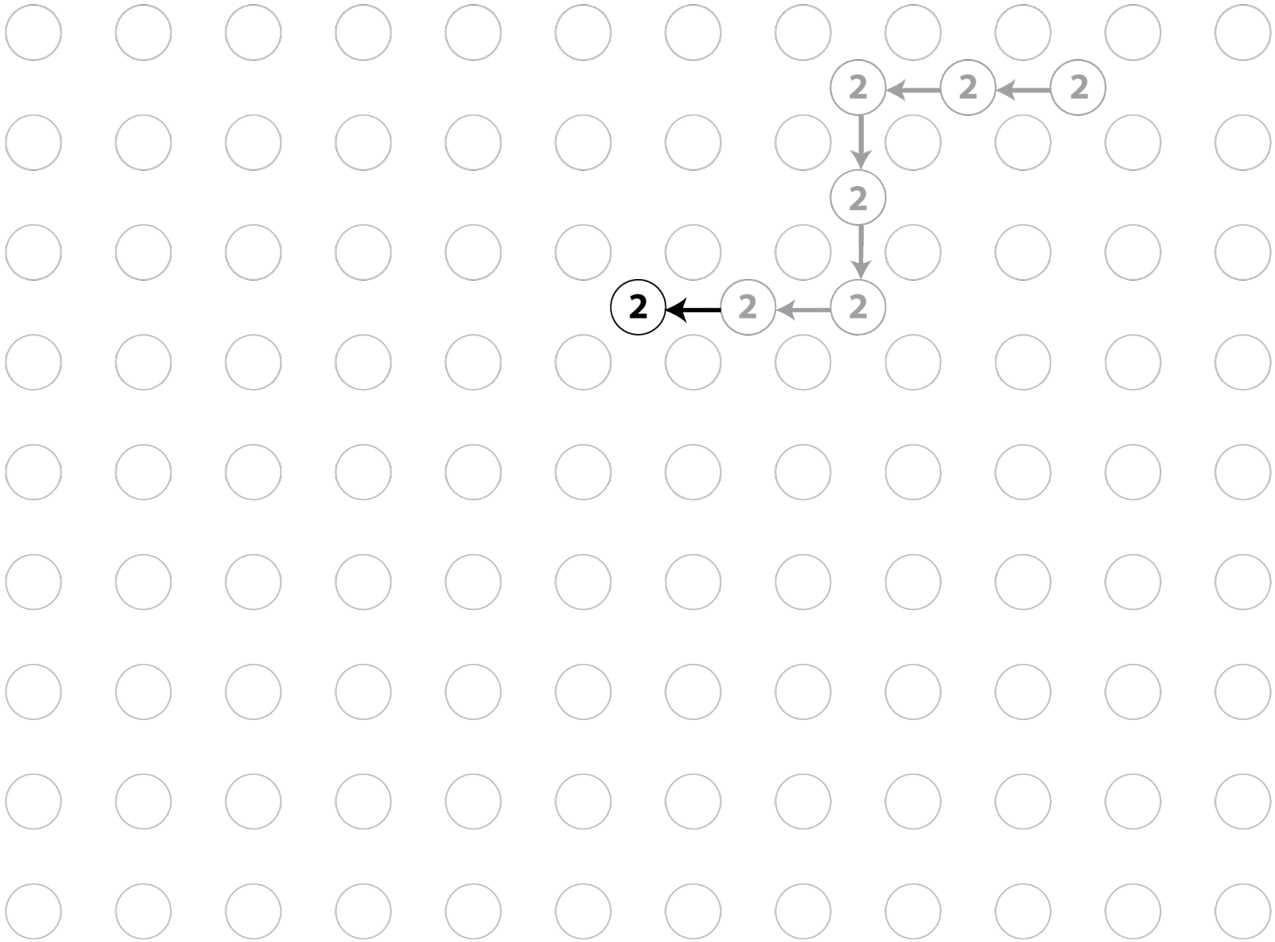

Perfect Lattice + *Freely-Migrating SIA #3*

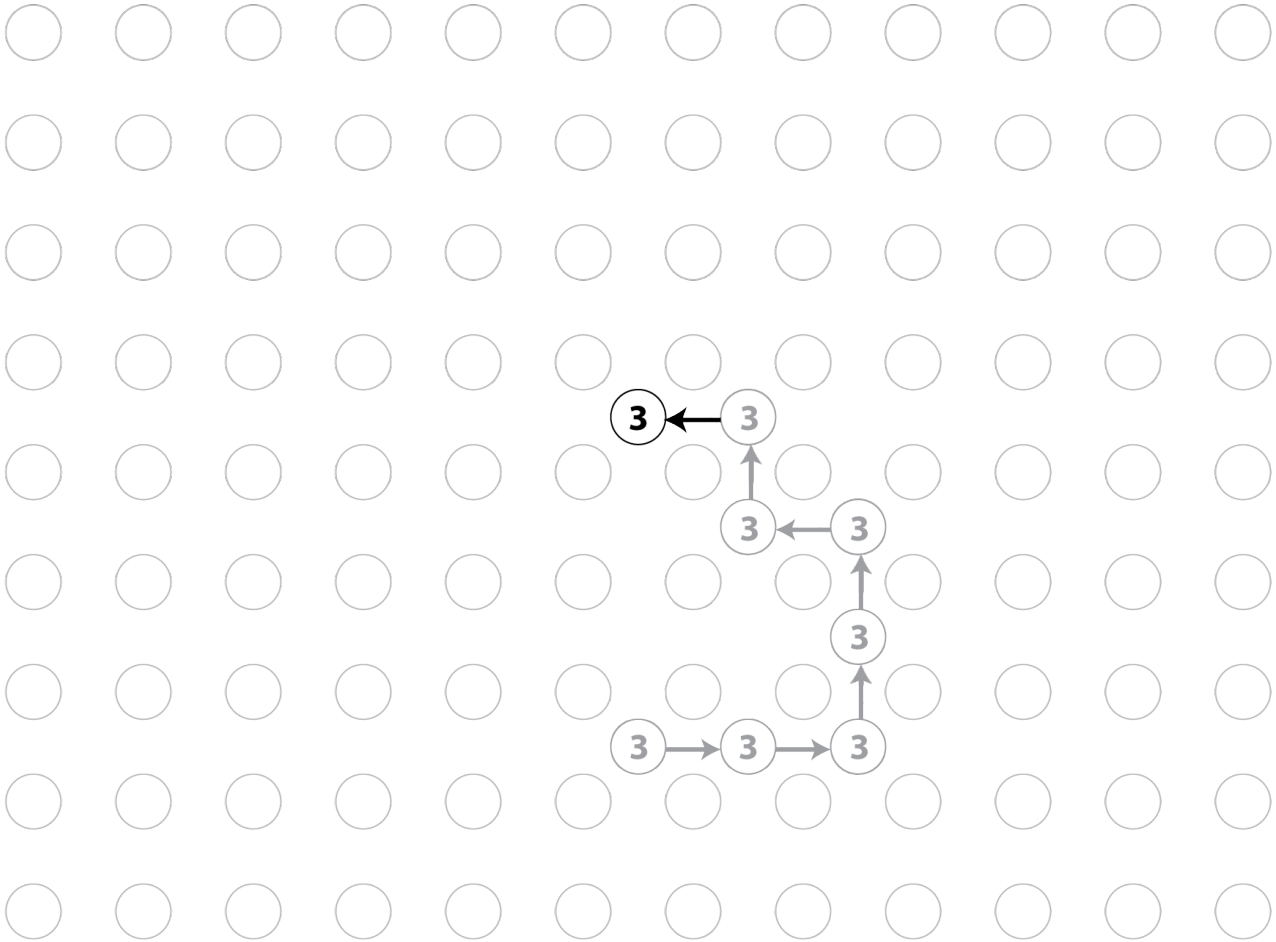

Perfect Lattice + *Freely-Migrating SIA #4*

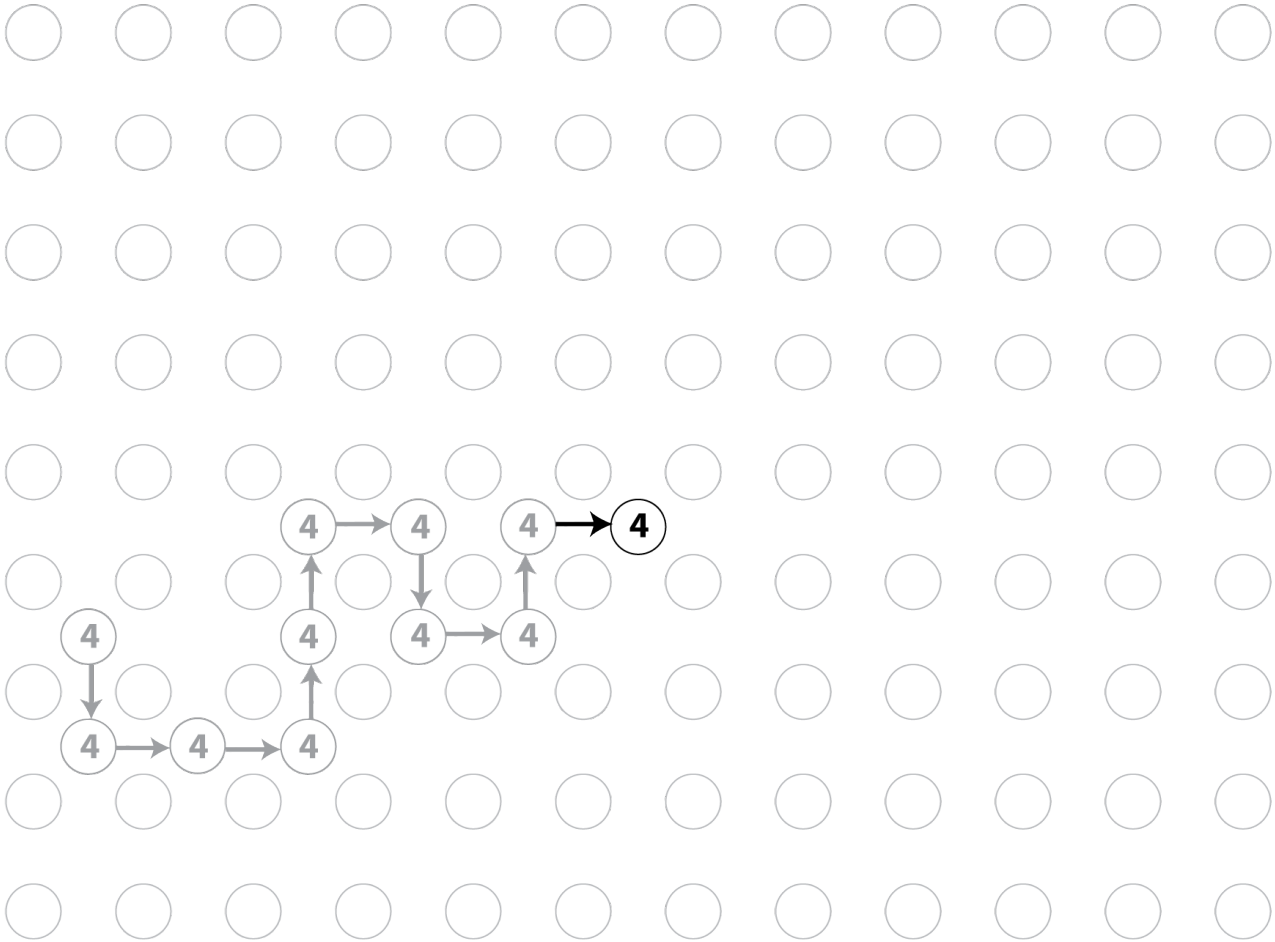

Perfect Lattice + Several *Freely-Migrating SIAs*

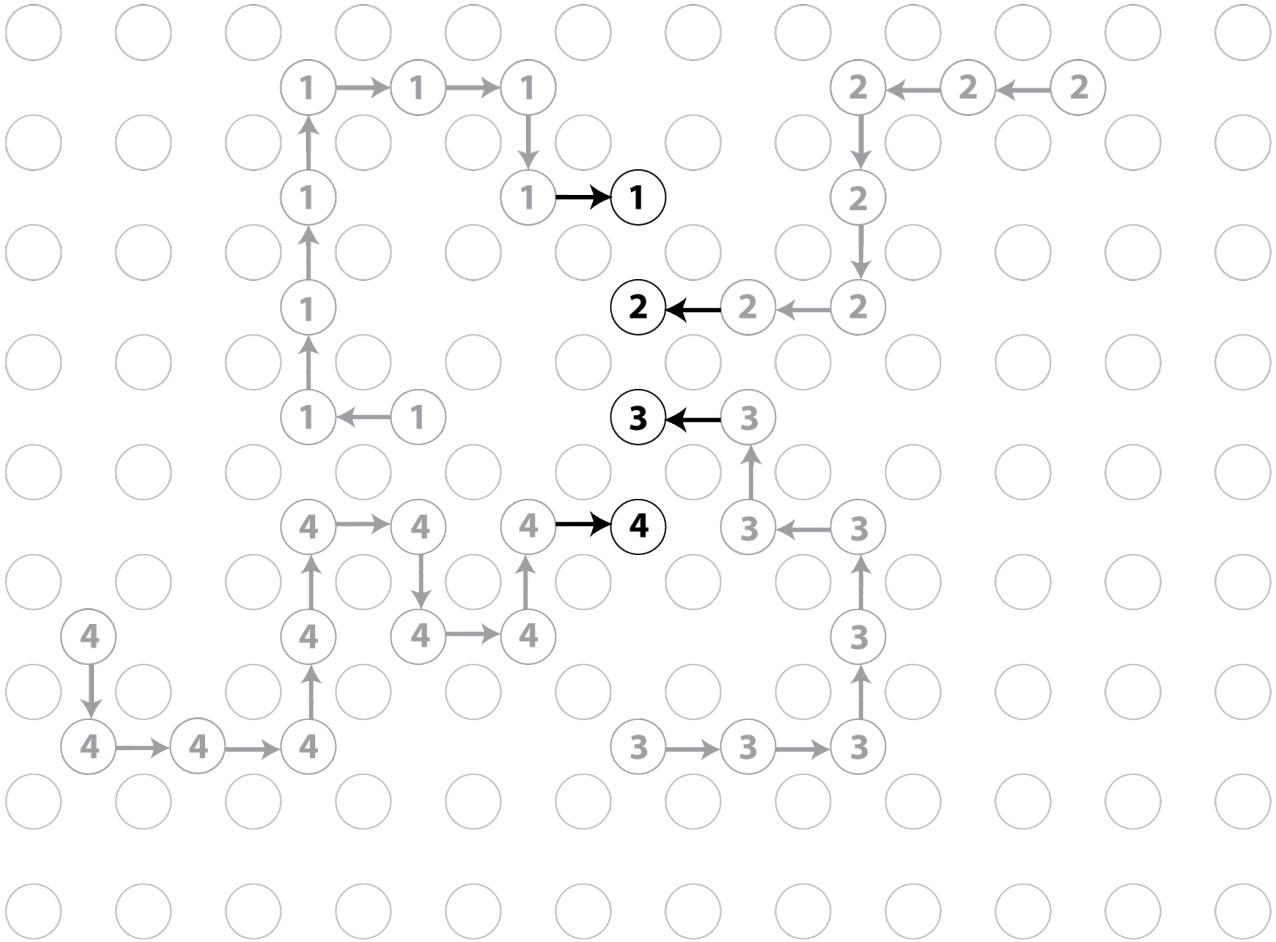

Perfect Lattice + *Interstitial Loop*

Loop condensed from freely-migrating *SIA*s

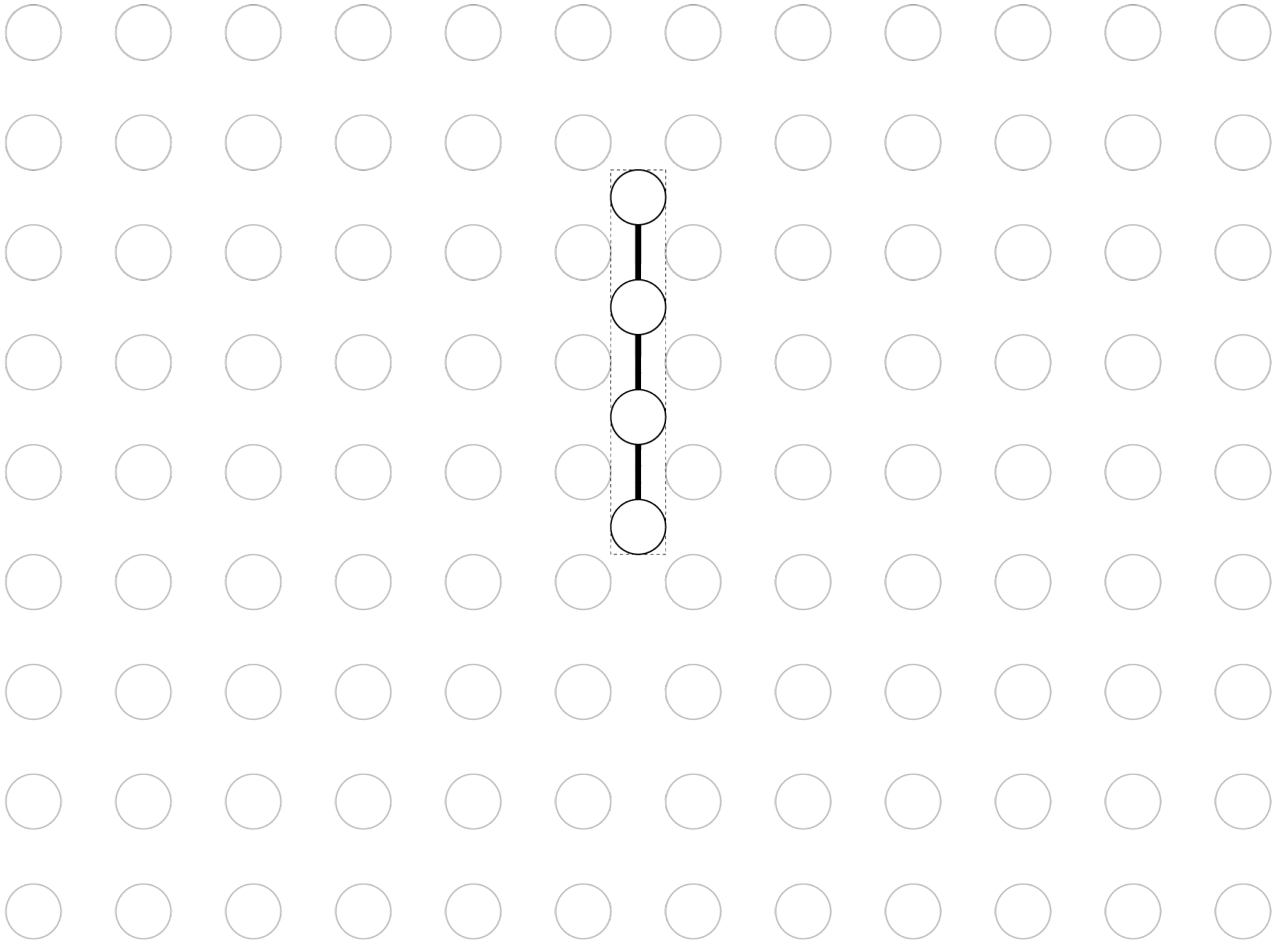

Perfect Lattice + Vacancy Point Defect

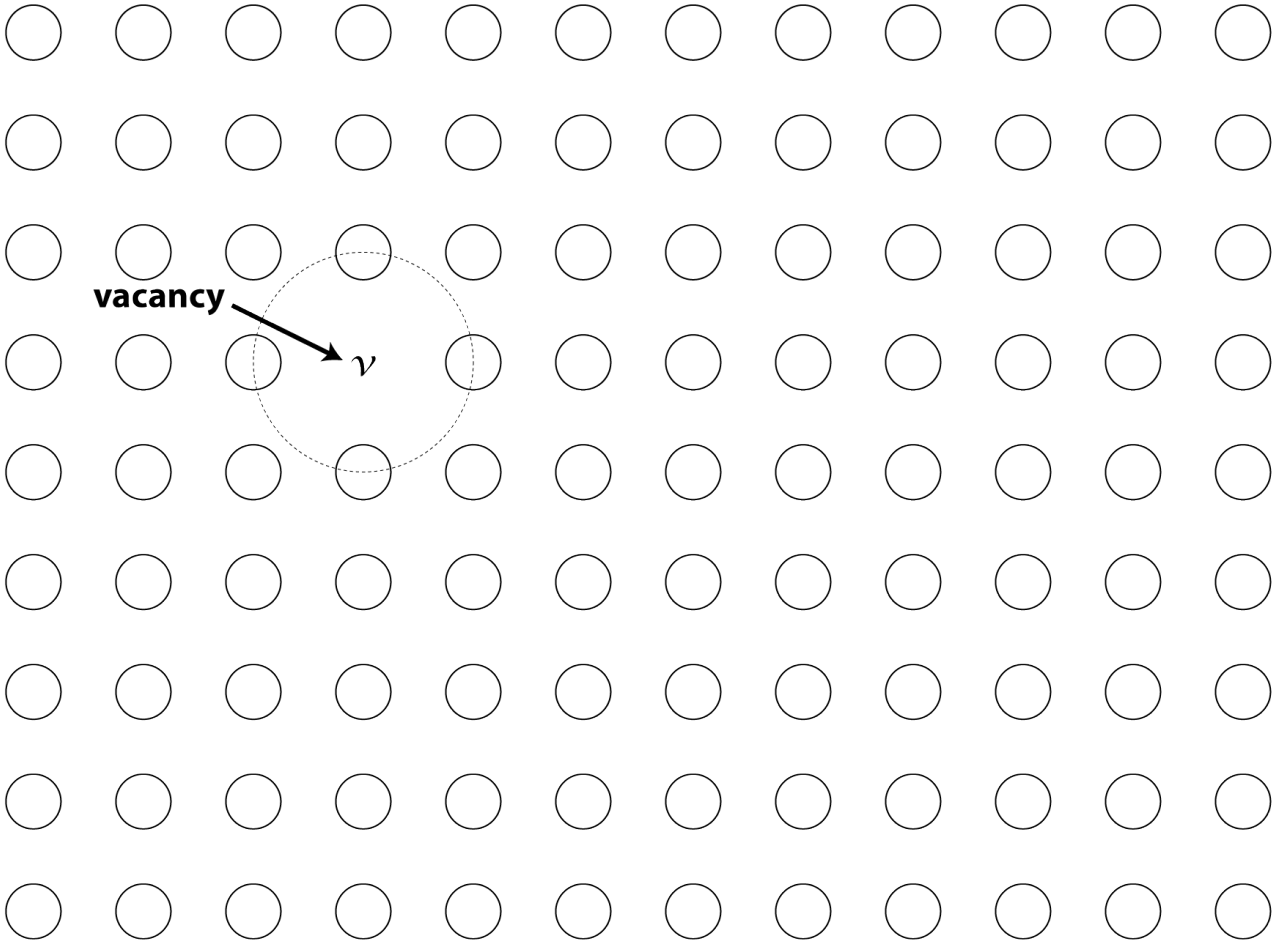

Perfect Lattice + Vacancy Point Defect

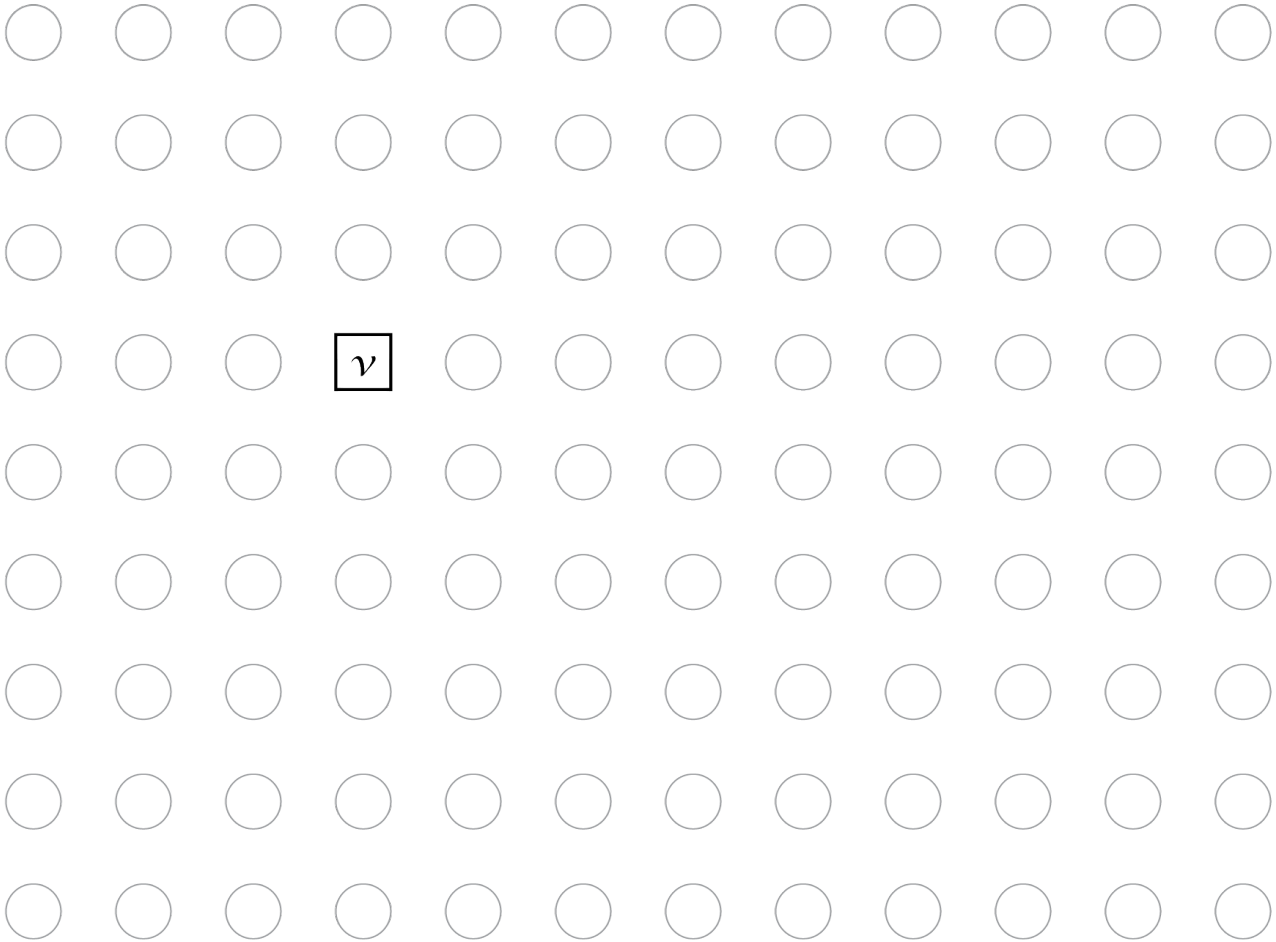

Vacancy Before Migration

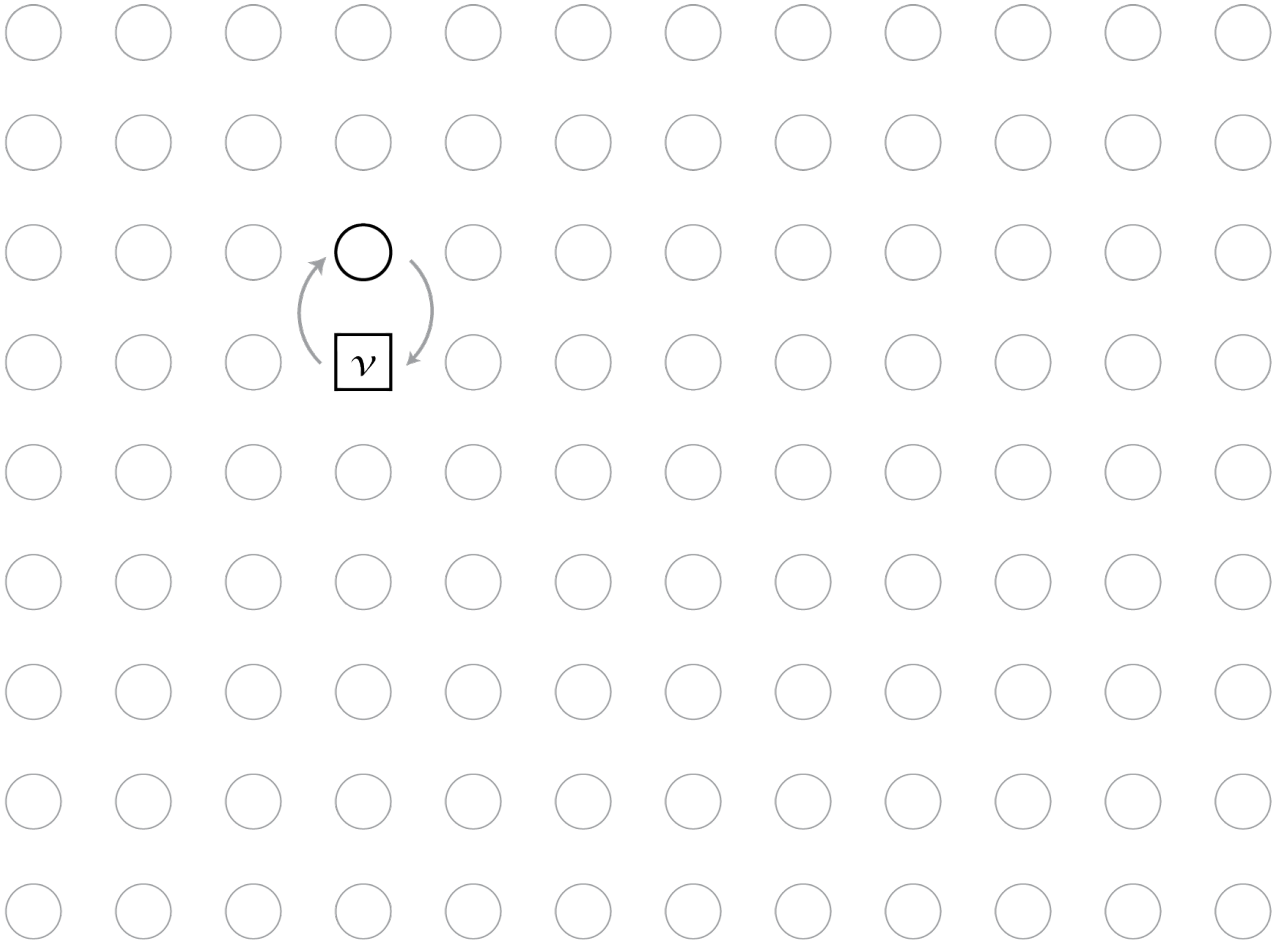

Vacancy After Migration

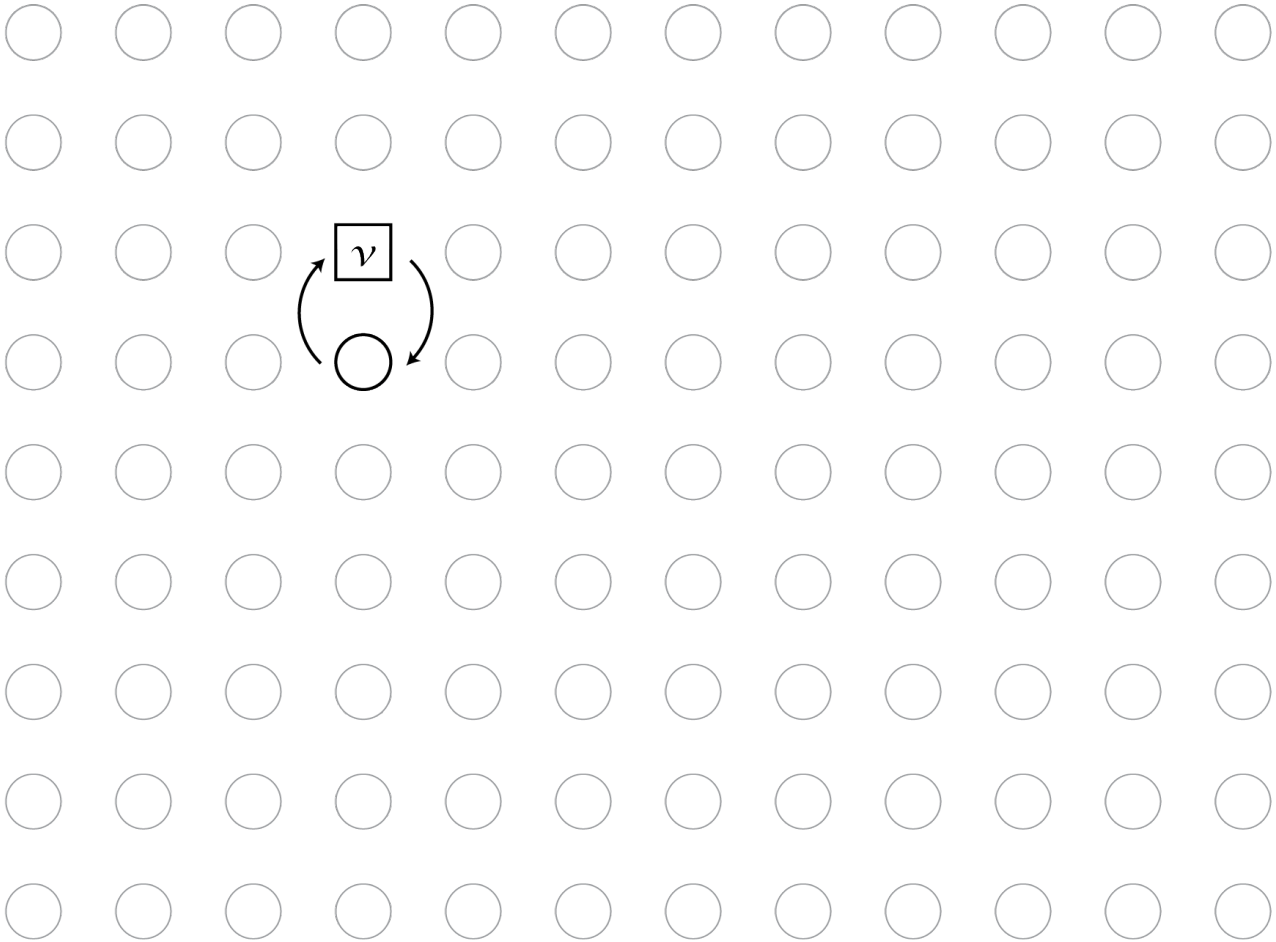

Perfect Lattice + *Freely-Migrating* Vacancy

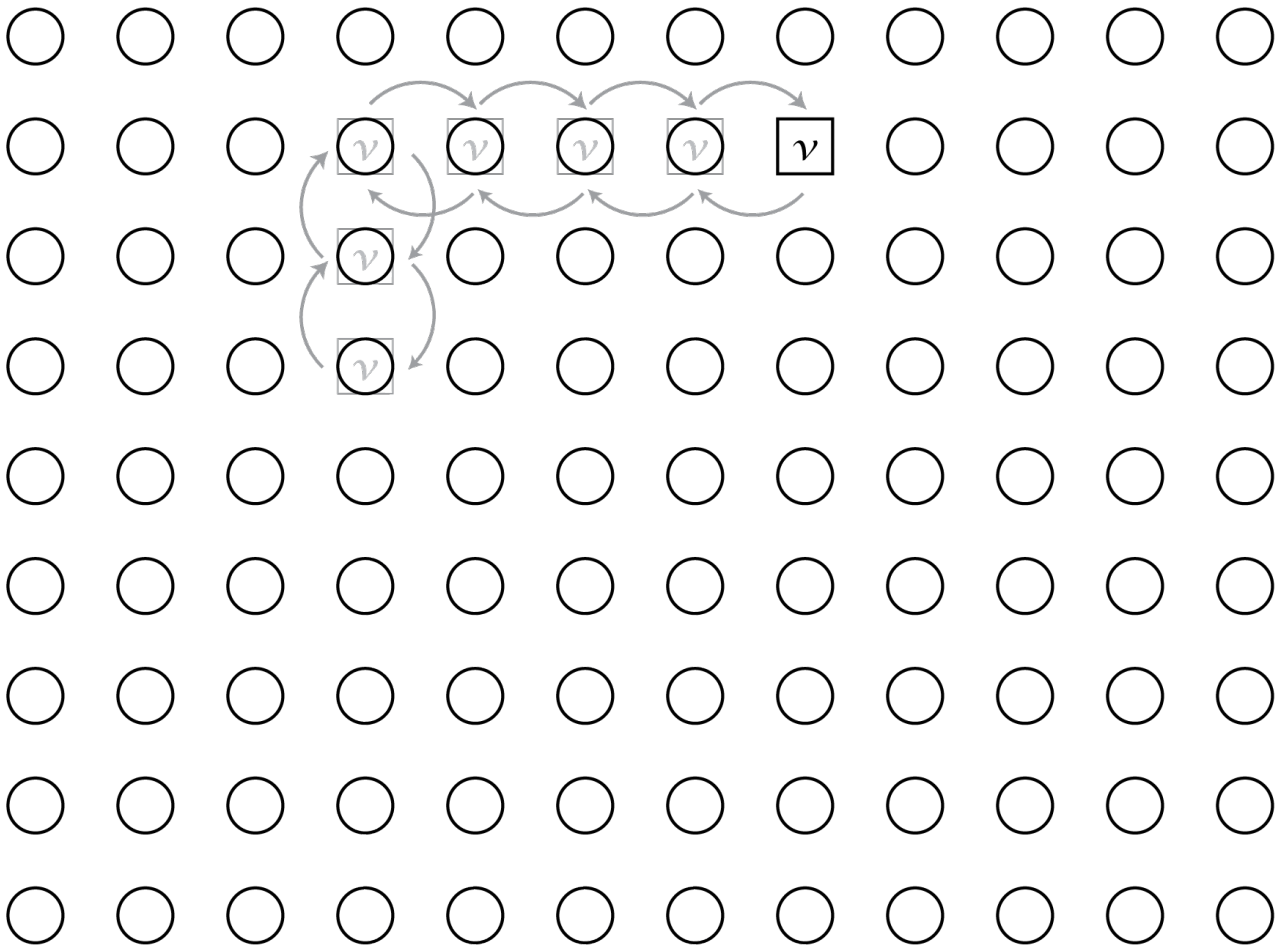

Perfect Lattice + *Freely-Migrating Vacancy* #1

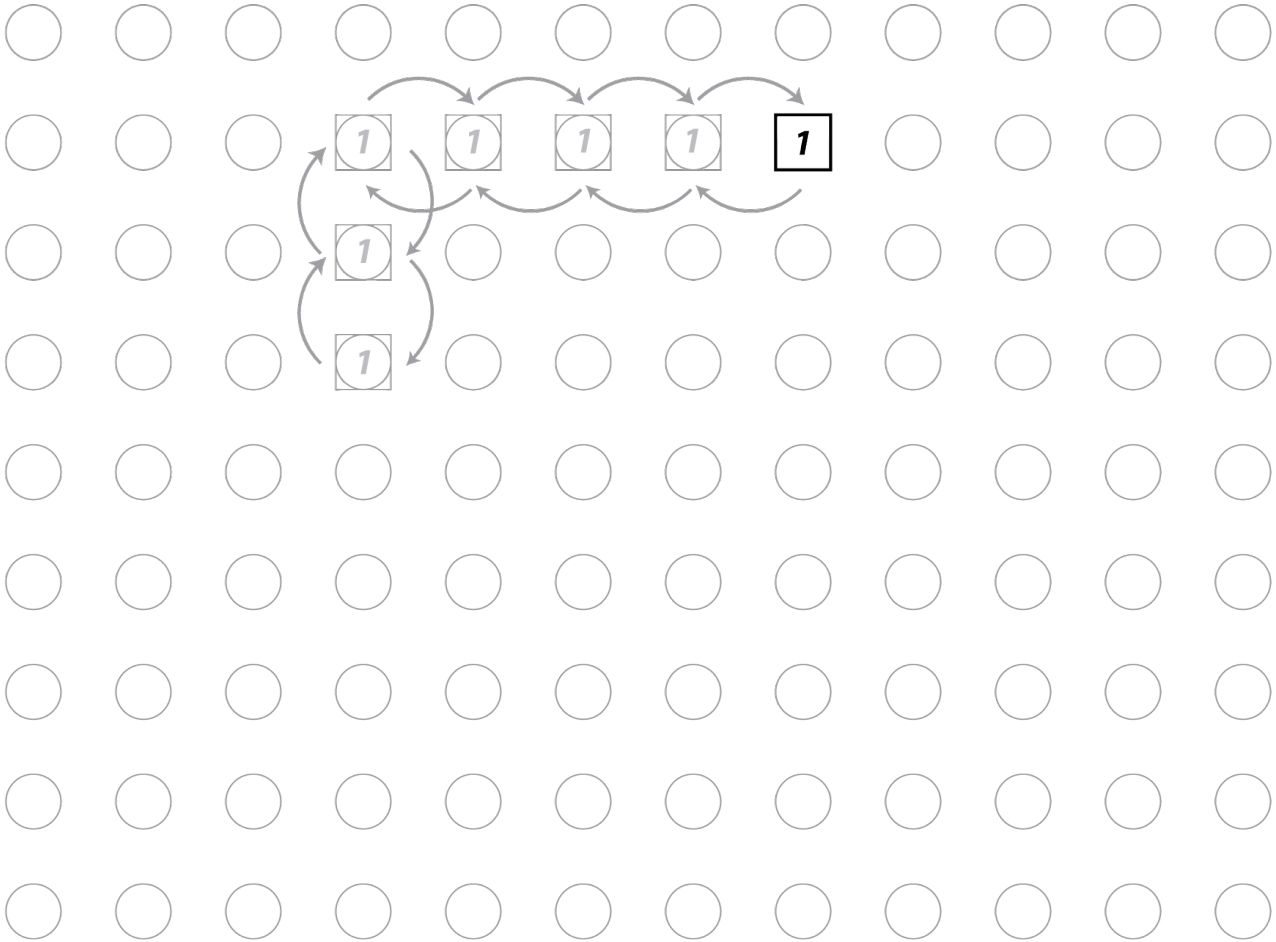

Perfect Lattice + *Freely-Migrating Vacancy #2*

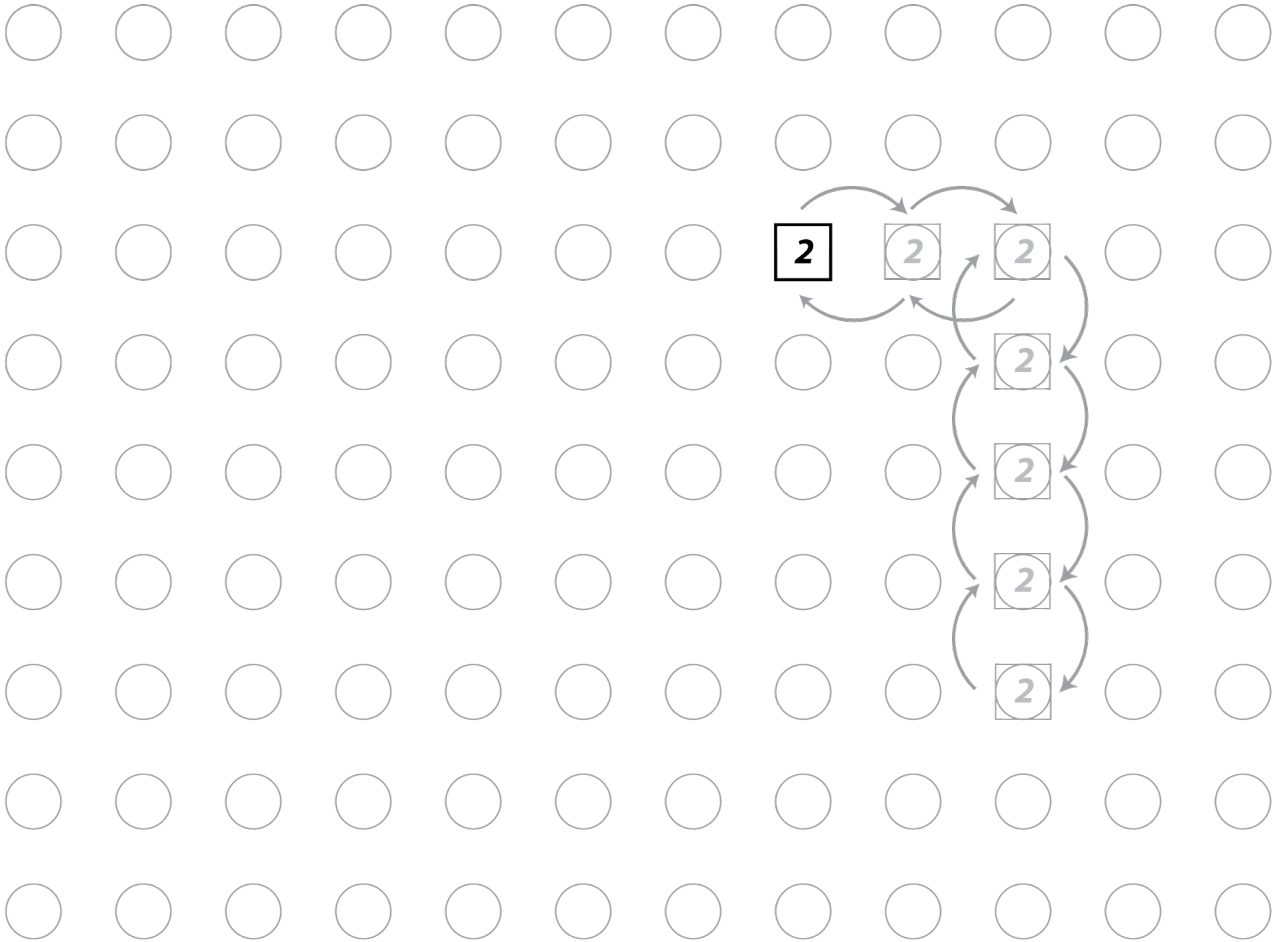

Perfect Lattice + *Freely-Migrating Vacancy #3*

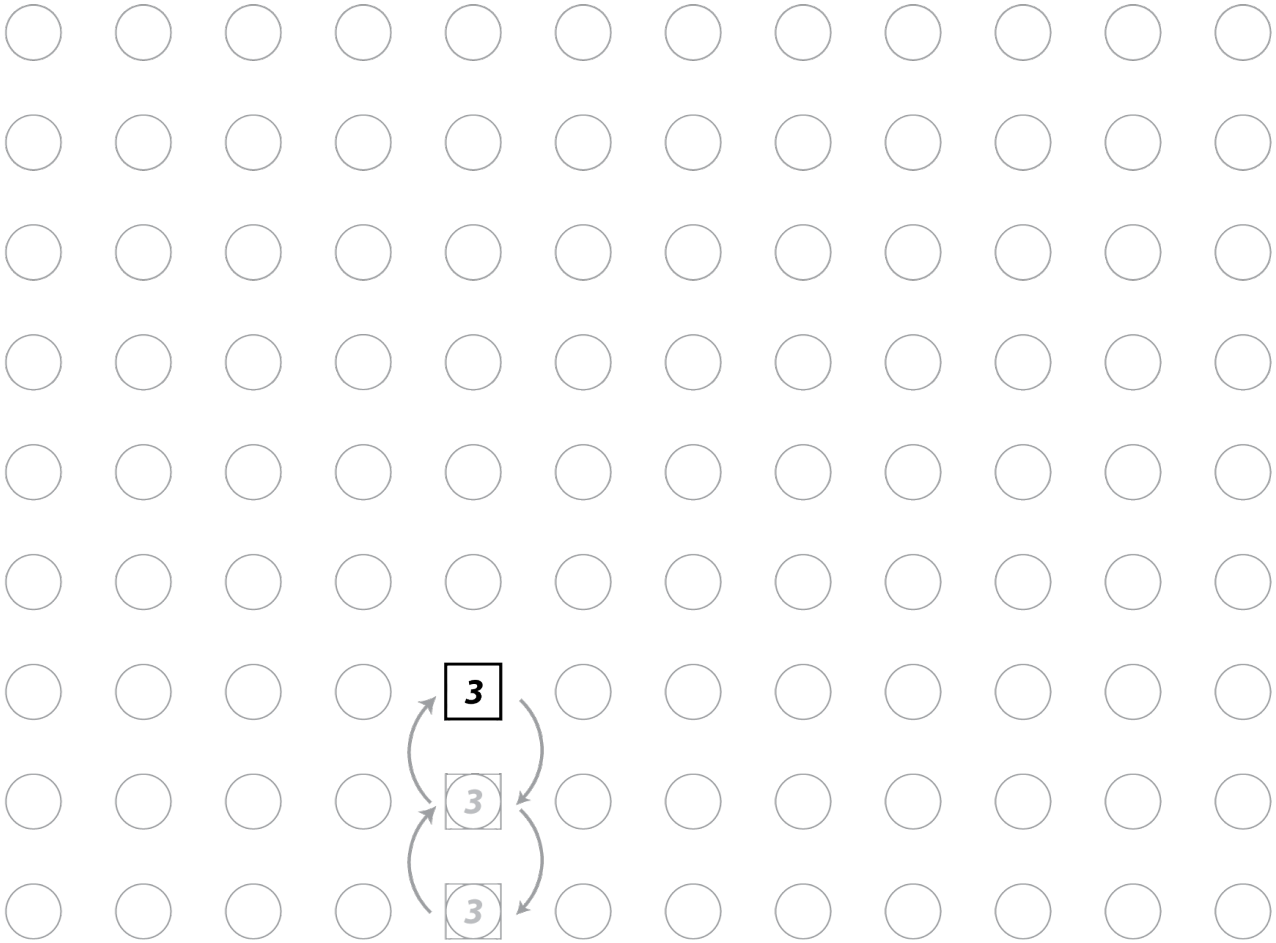

Perfect Lattice + *Freely-Migrating Vacancy #4*

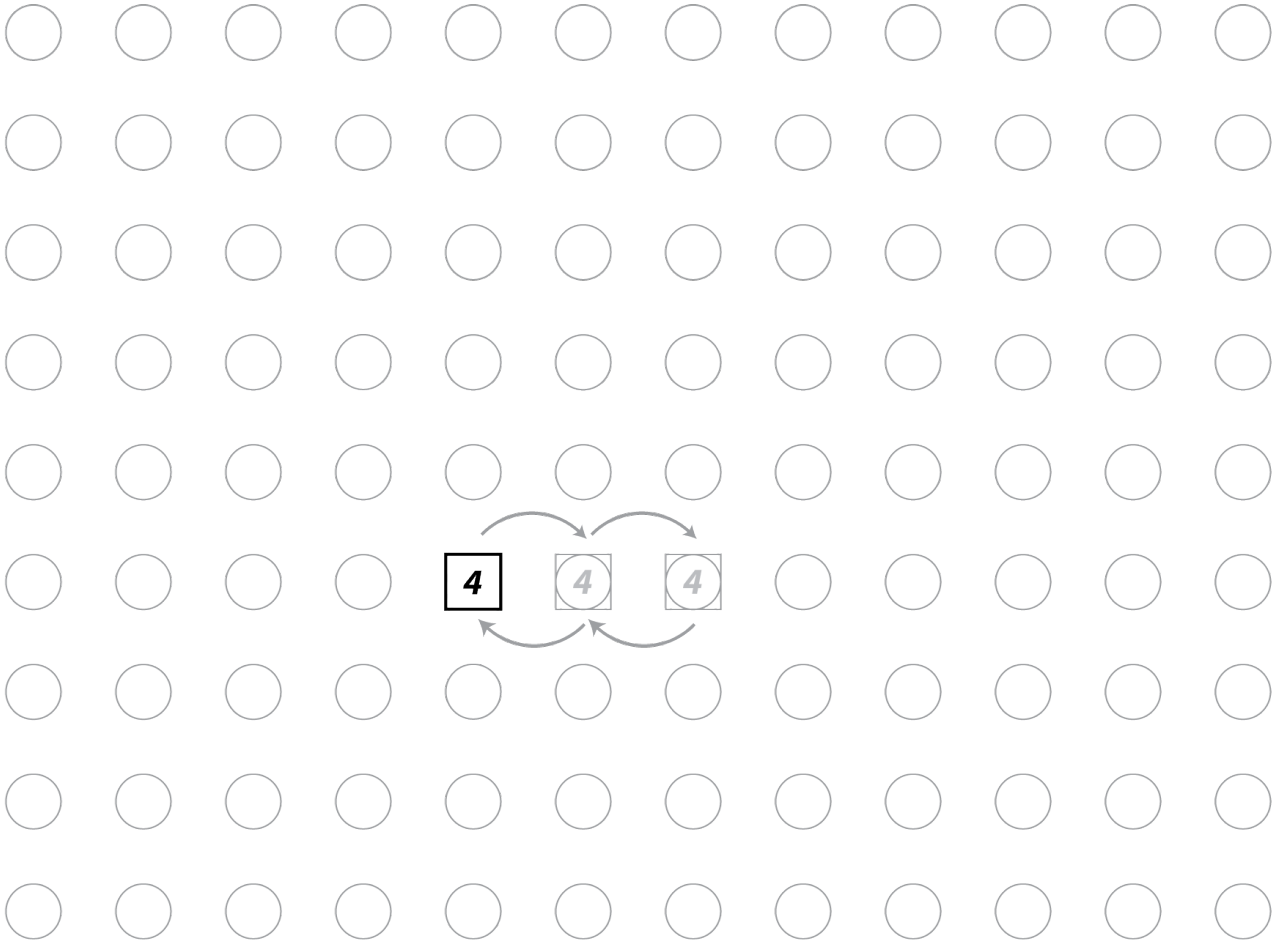

Di - Vacancy Formation

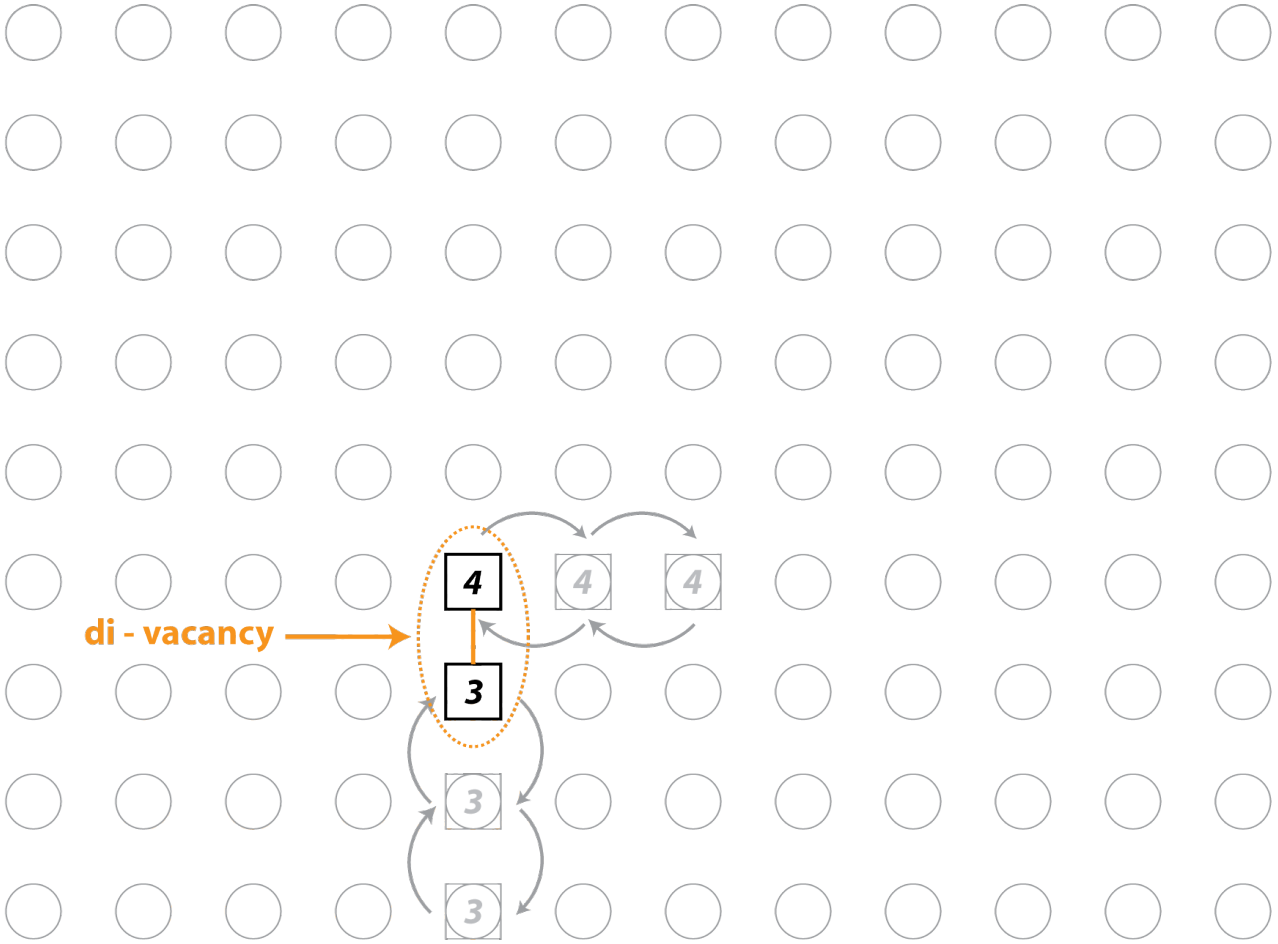

Di - Vacancy Formation

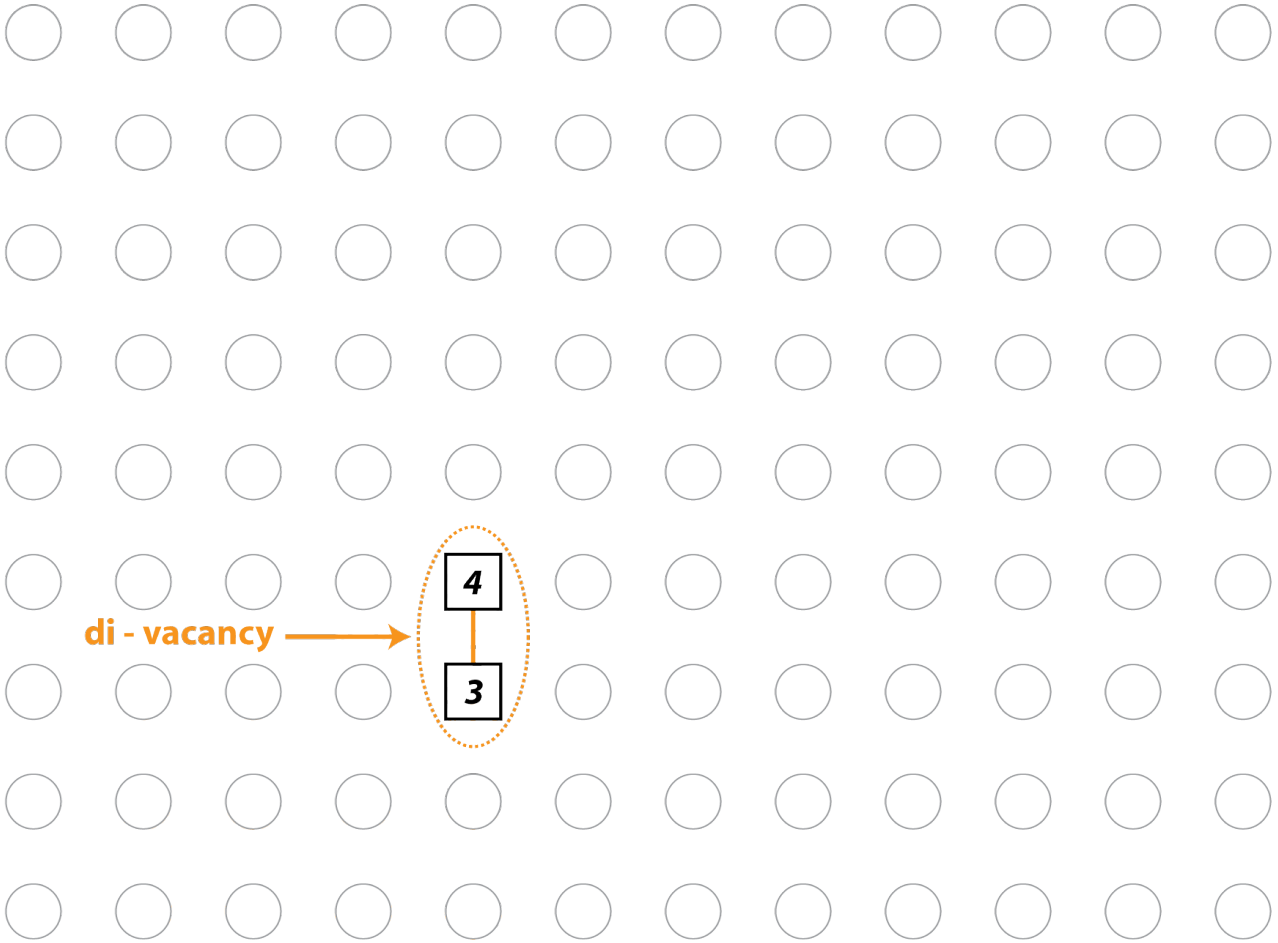

Di - Vacancy Migration

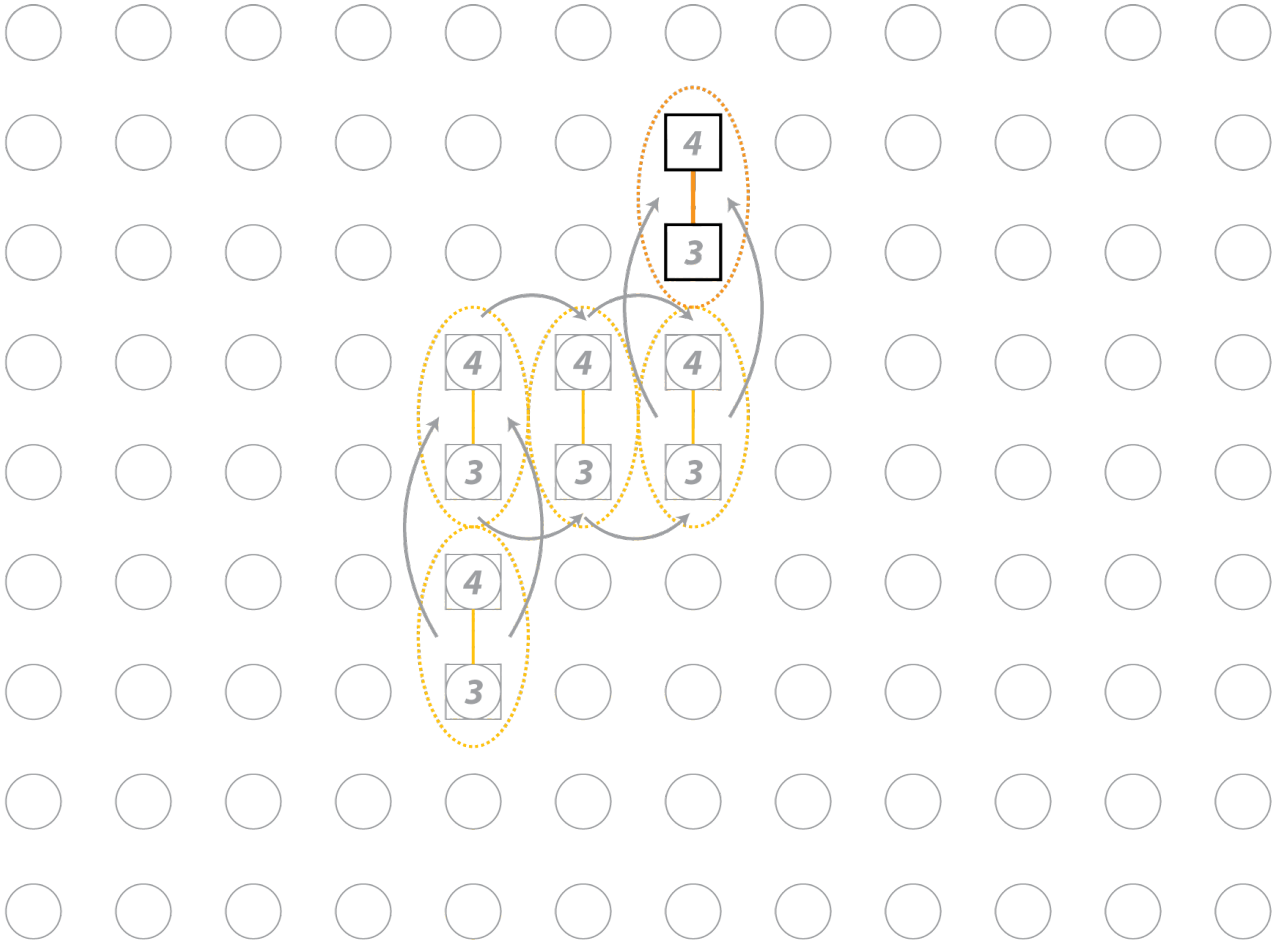

Freely-Migrating Vacancy Point Defects - Void Nucleation

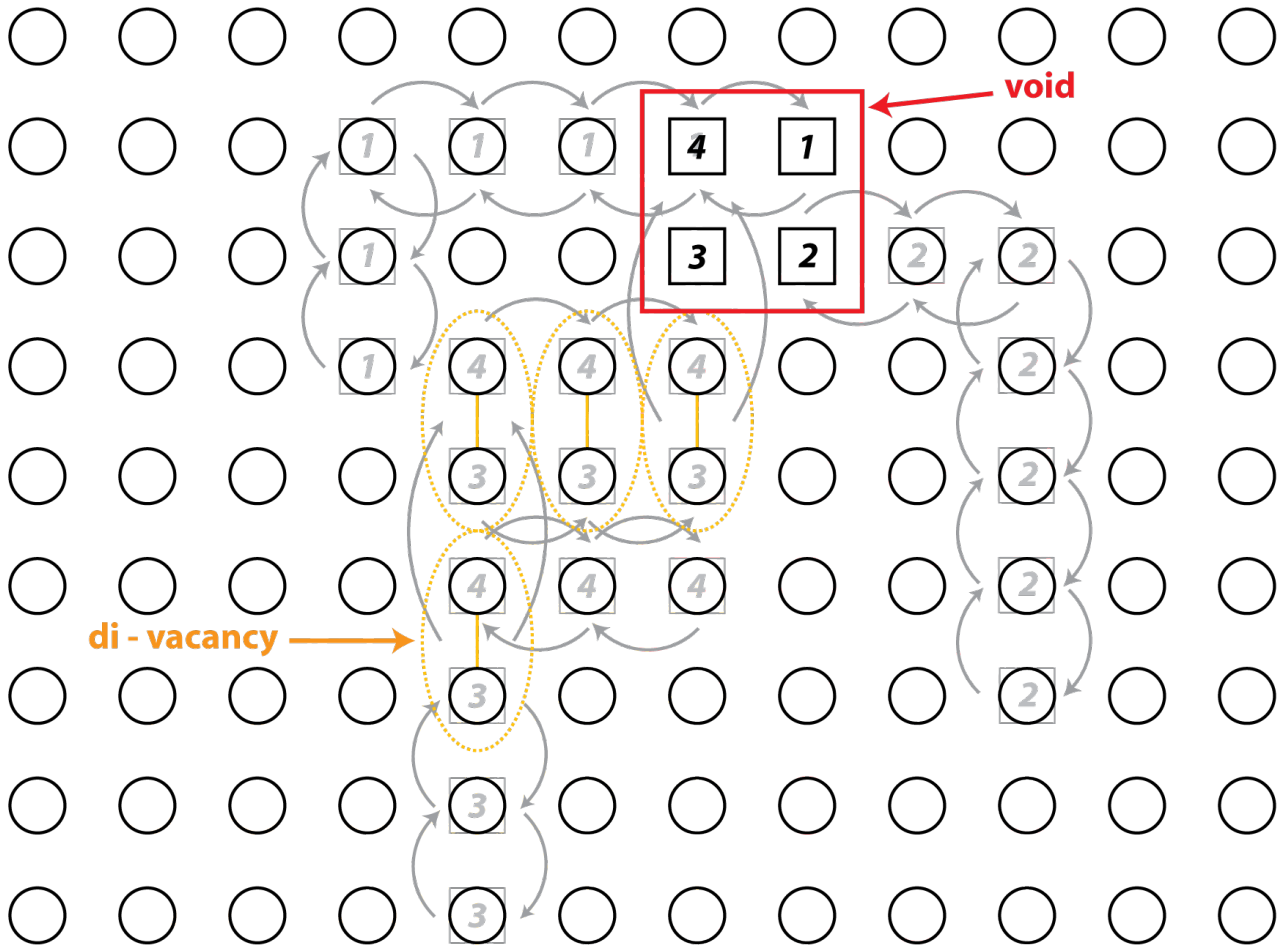

Freely-Migrating Vacancy Point Defects - Void Formation

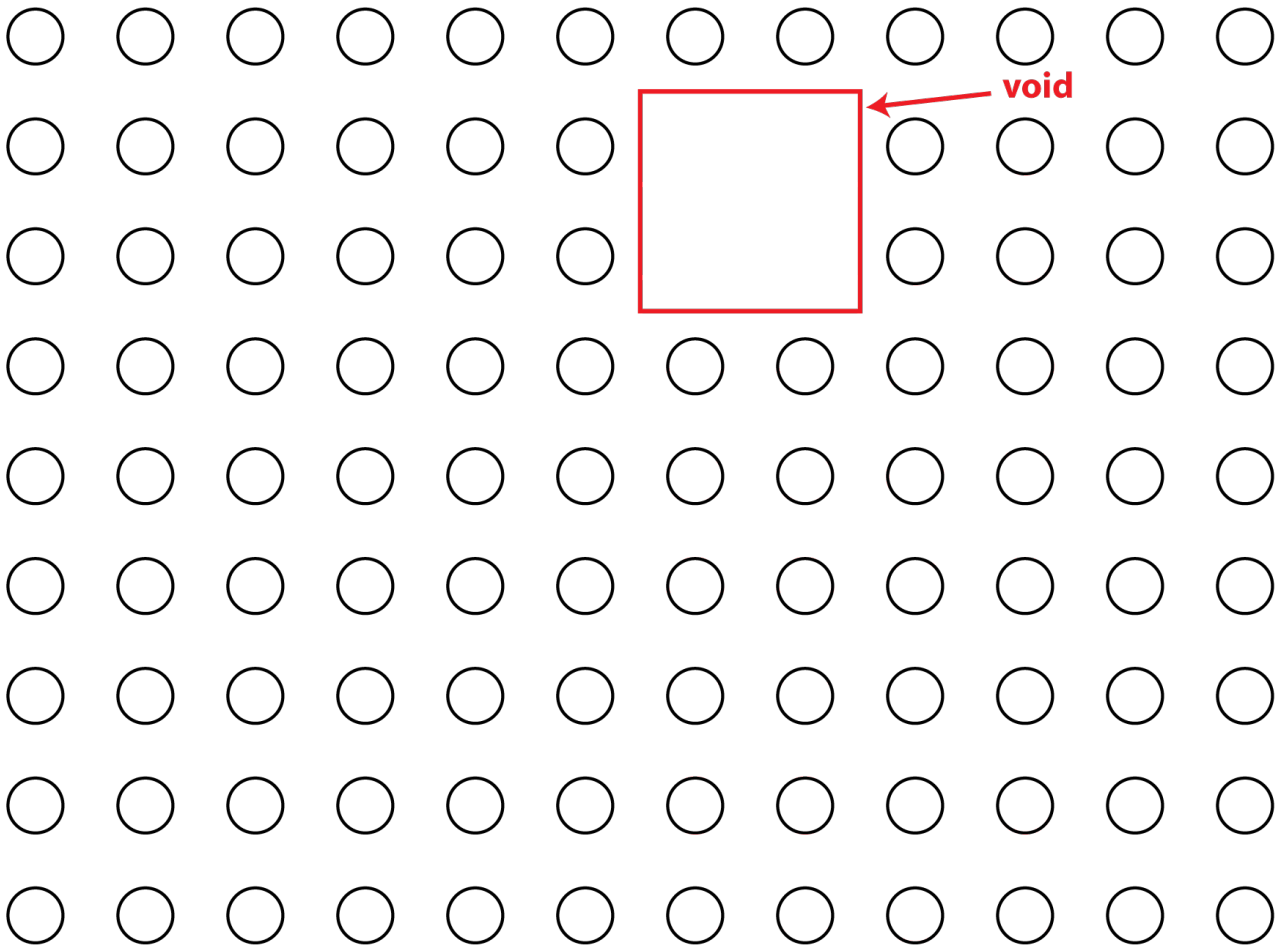

Interstitial (i) - Vacancy (v) Migration

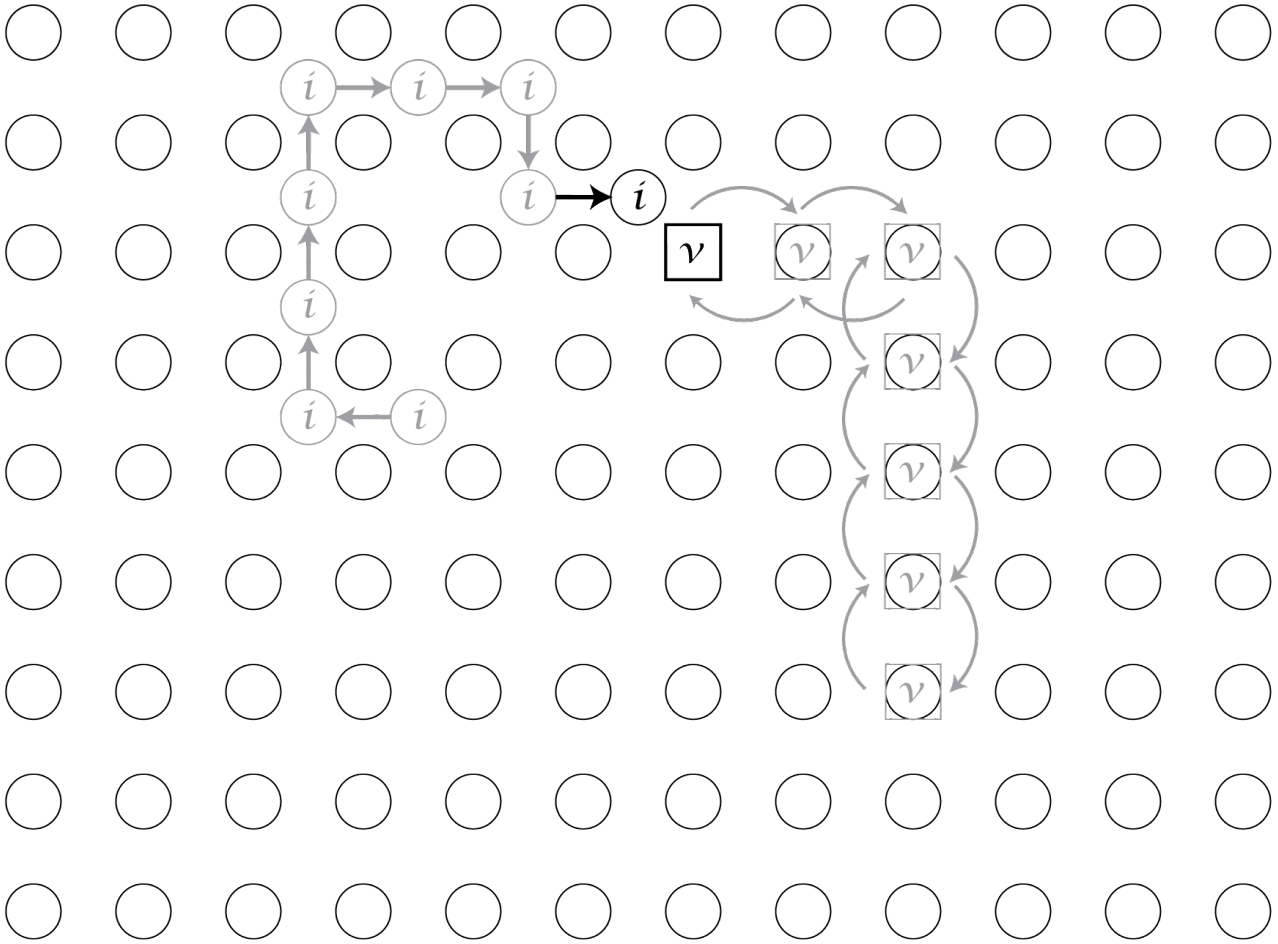

i - v Recombination - just prior to recombination

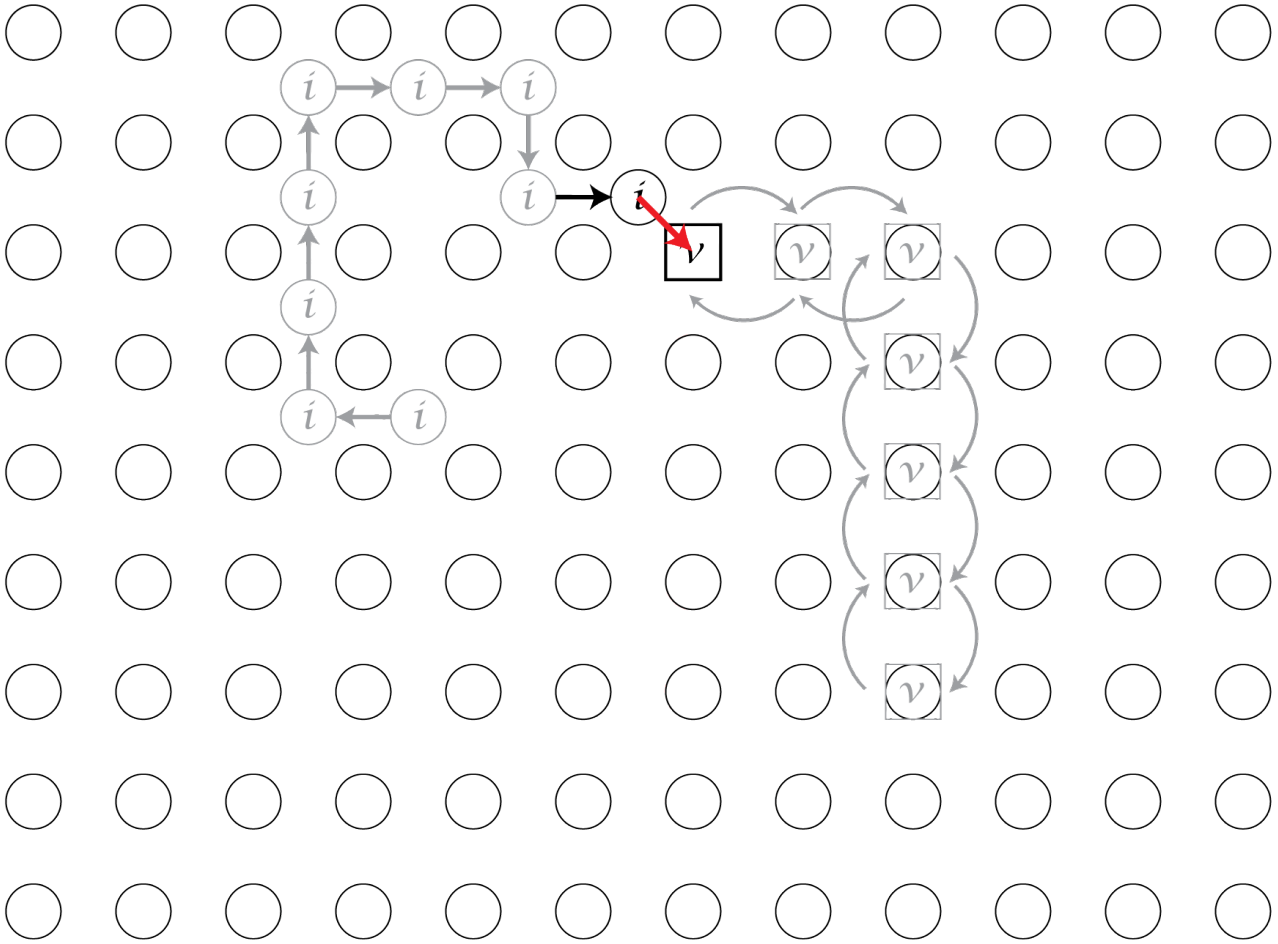

i - v Recombination - after recombination

Note that both *i* and *v* point defects are annihilated by this process

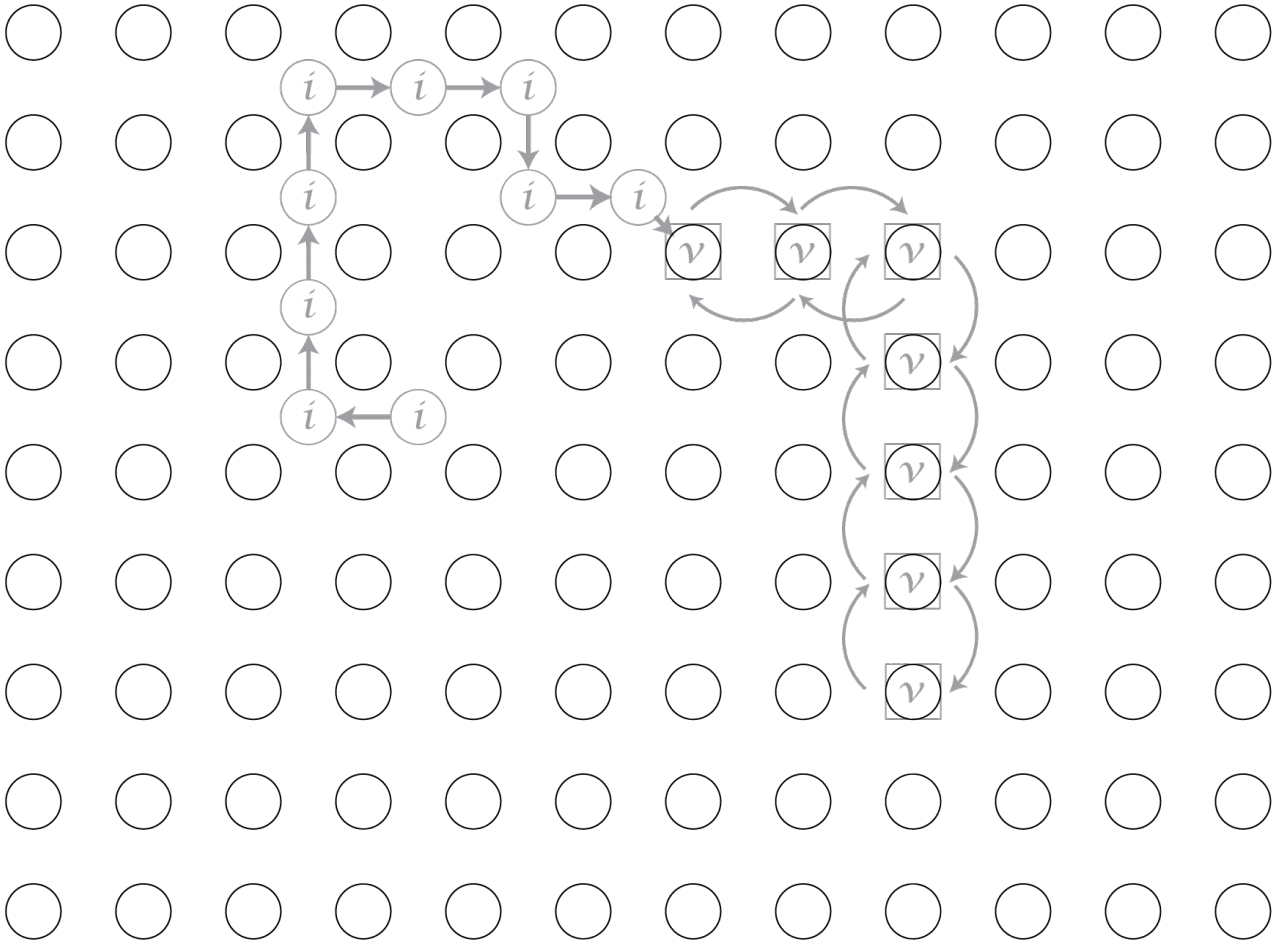

Perfect Lattice is Restored Following *i* - *v* Recombination

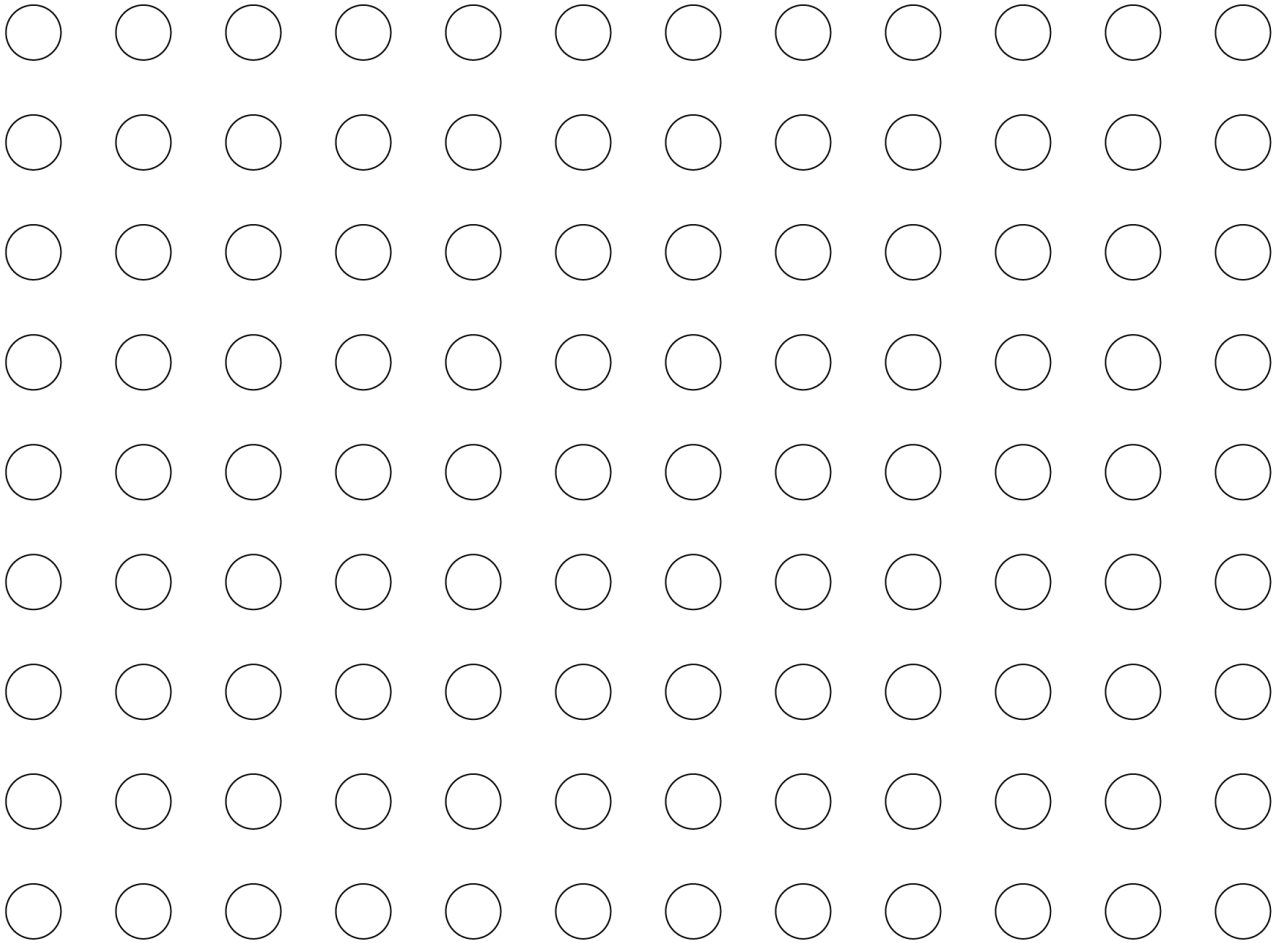

So What Have We Learned?

1. Freely-migrating point defects (interstitials and vacancies) aggregate in crystal lattices to form extended defects (dislocation loops and voids).
2. Extended defects (dislocation loops and voids) are bad because they produce macroscopic property alterations such as embrittlement and swelling.
3. The best way to achieve radiation resistance in a material exposed to irradiation is to enhance the mechanism of interstitial-vacancy (*i*-*v*) recombination. This is a *harmless* radiation damage mechanism because it serves to restore the perfect crystal lattice.

Radiation Damage Evolution

Radiation damage is a competition between the harmless annihilation of irradiation-induced point defects by *i-v* recombination and the harmful condensation of point defects to form extended lattice defects such as dislocation loops and voids.

These harmless and harmful damage mechanisms are at *crossed* purposes: one works to restore the perfect crystal lattice, while the other works to disrupt the lattice by introducing detrimental lattice imperfections.

Much of the field of radiation damage research is devoted to developing an understanding of the interplay between these radiation damage mechanisms (e.g., *chemical rate theory*).

Fate of Irradiation-Induced Interstitials (Chemical Rate Theory)

$$\frac{dC_i}{dt} = P_i \quad \left(A_A \longrightarrow A_i + V_A\right)$$ *Frenkel pair* production rate

$$-R_{i-v}\left(A_i + V_A \longrightarrow A_A\right)$$ } *i-v* recombination rate — Harmless

$-N$ (nucleation rate for interstitial loops)

$-G$ (growth rate for interstitial loops)

} BAD!

So how many freely-migrating point defects are produced under irradiation conditions?

This is the starting point for assessing radiation damage effects.

The rate of creation of freely-migrating point defects produced during irradiation is called the ***production rate***.

The production rate of point defects depends specifically on the amount of energy transferred to lattice atoms by the irradiating species (for instance, energetic ions in an ion beam irradiation experiment).

Qualitatively, it is always true that the higher the energy of the projectile particle impinging on a solid target, the greater the number of point defects generated in the target.

To illustrate this point, we show next computer simulation results comparing and contrasting point defect formation in an oxide compound known as spinel, $MgAl_2O_4$, for two projectiles with very different kinetic energies:

1. 400 eV Magnesium (Mg) ion irradiation of $MgAl_2O_4$
2. 10 keV Magnesium (Mg) ion irradiation of $MgAl_2O_4$

Each simulation shows a "cascade" of displaced target atoms produced by a single incident projectile ion.

400 eV Mg^{+} ion-induced "*cascade*" in $MgAl_2O_4$

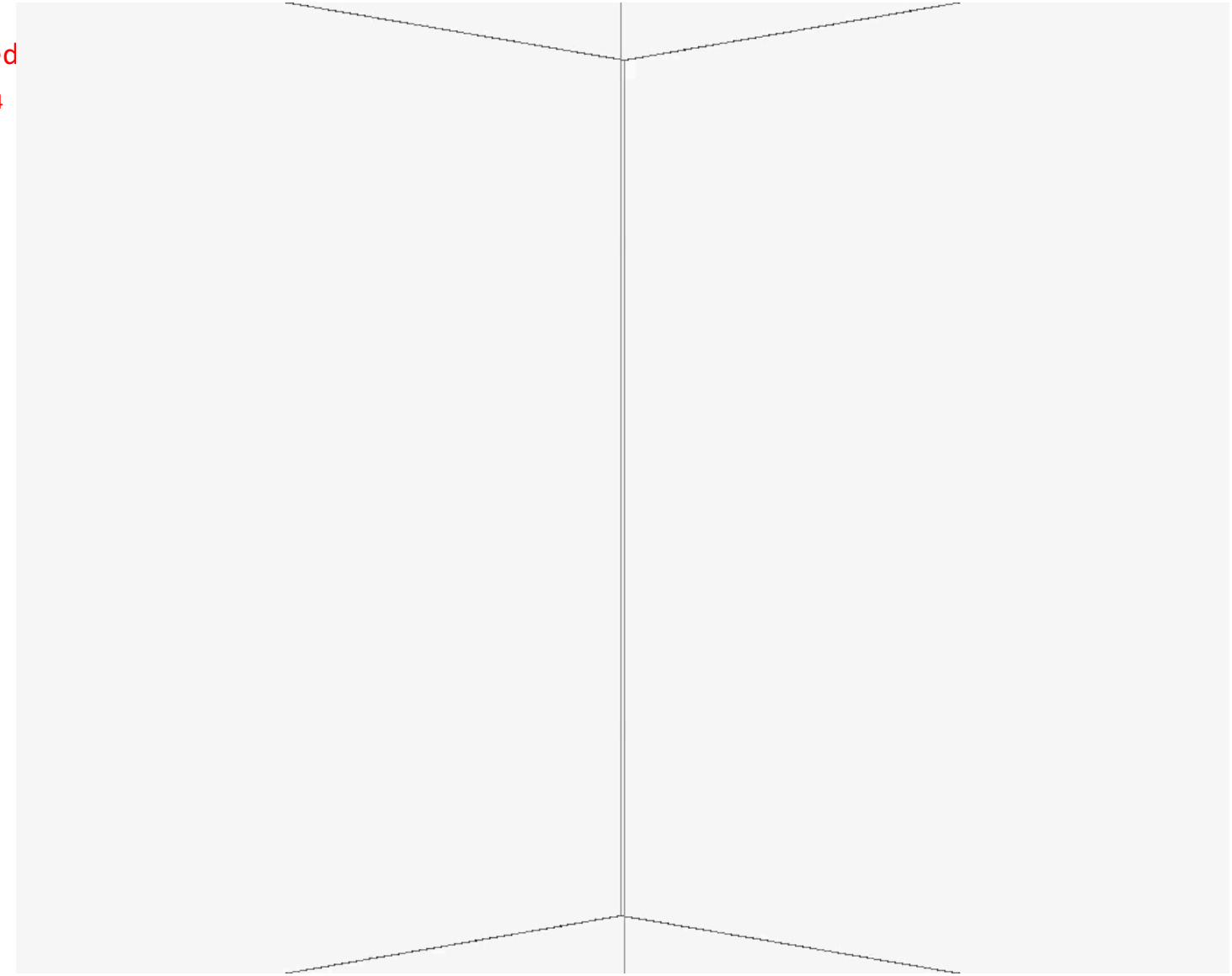

10 keV Mg^{+} ion-induced "*cascade*" in $MgAl_2O_4$

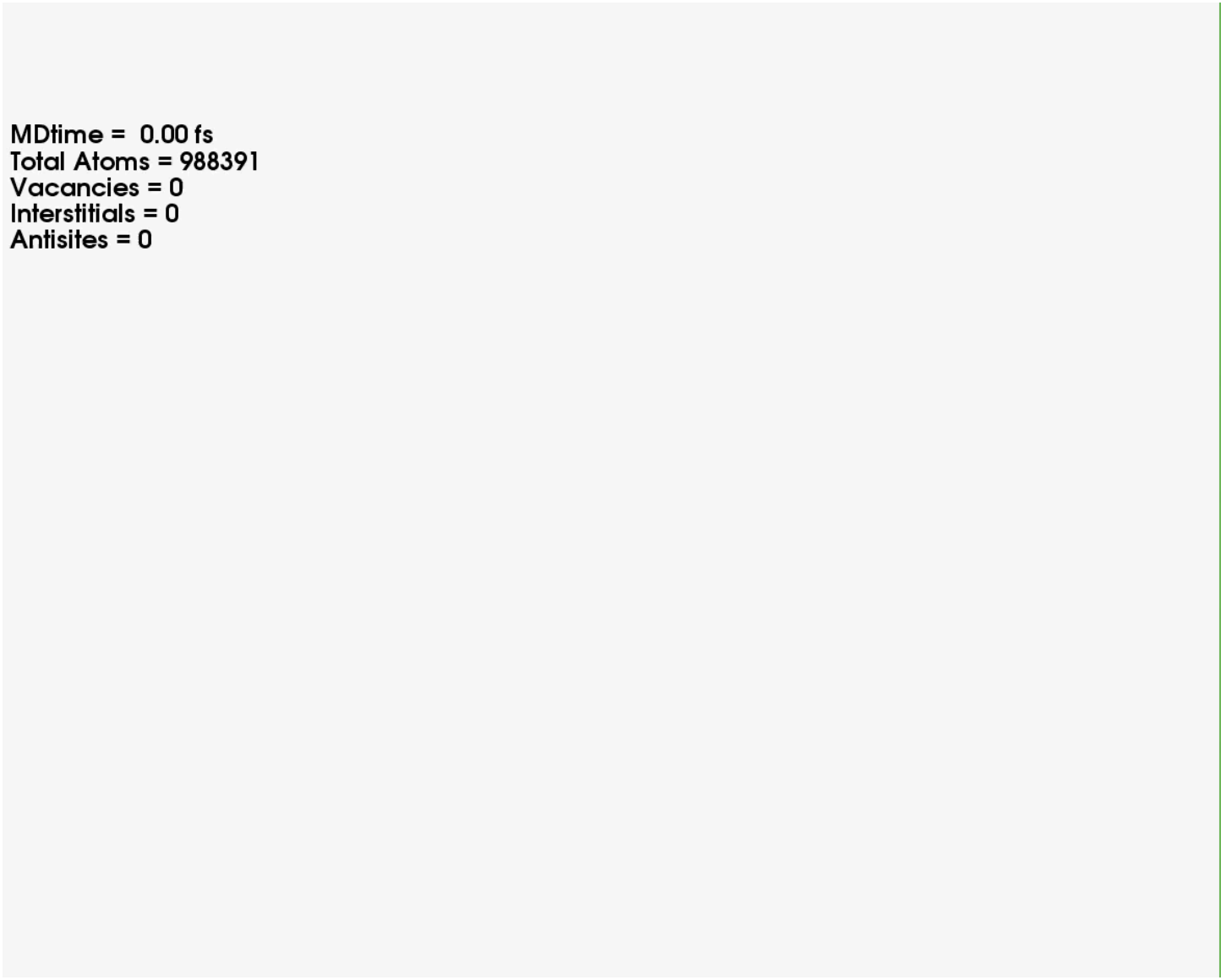

Ion cascade at a
Cu-Nb interface

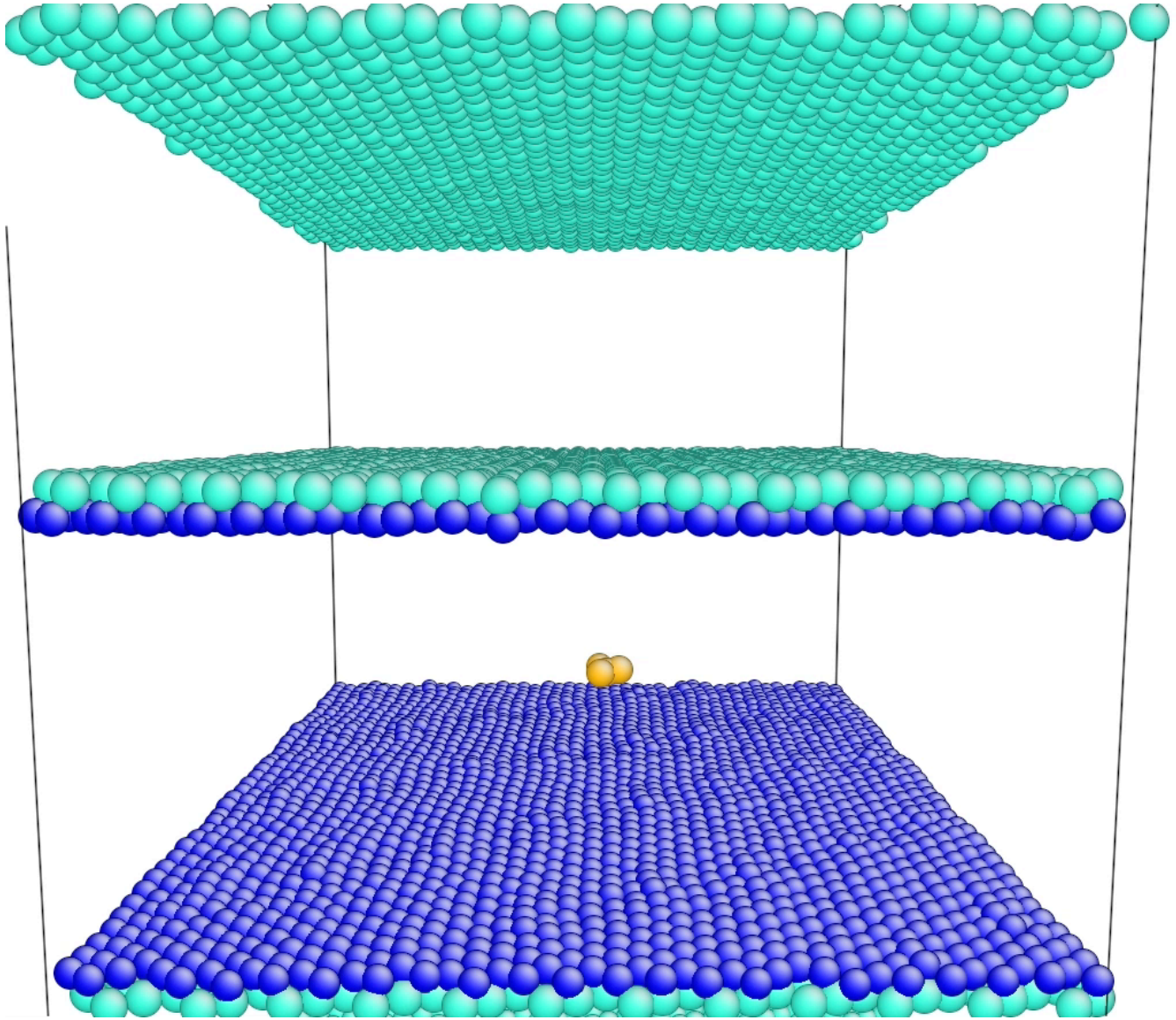

Introduction to Ion-Solid Interactions

(the *two-body collision*)

So, how much energy can be transferred from a projectile particle, such as an ion, to a lattice atom in a target solid?

To solve this problem, it is useful to consider details of the so-called ***Two-Body Interaction or Two-Body Collision***.

This problem was made famous by astronomers when they worked out details concerning the orbital motion of the planets about the Sun.

Two-Body Collision

Calculation of the energy transferred
during the scattering interaction

Two-Body Collision
(Coulombic Repulsive Interaction Force)

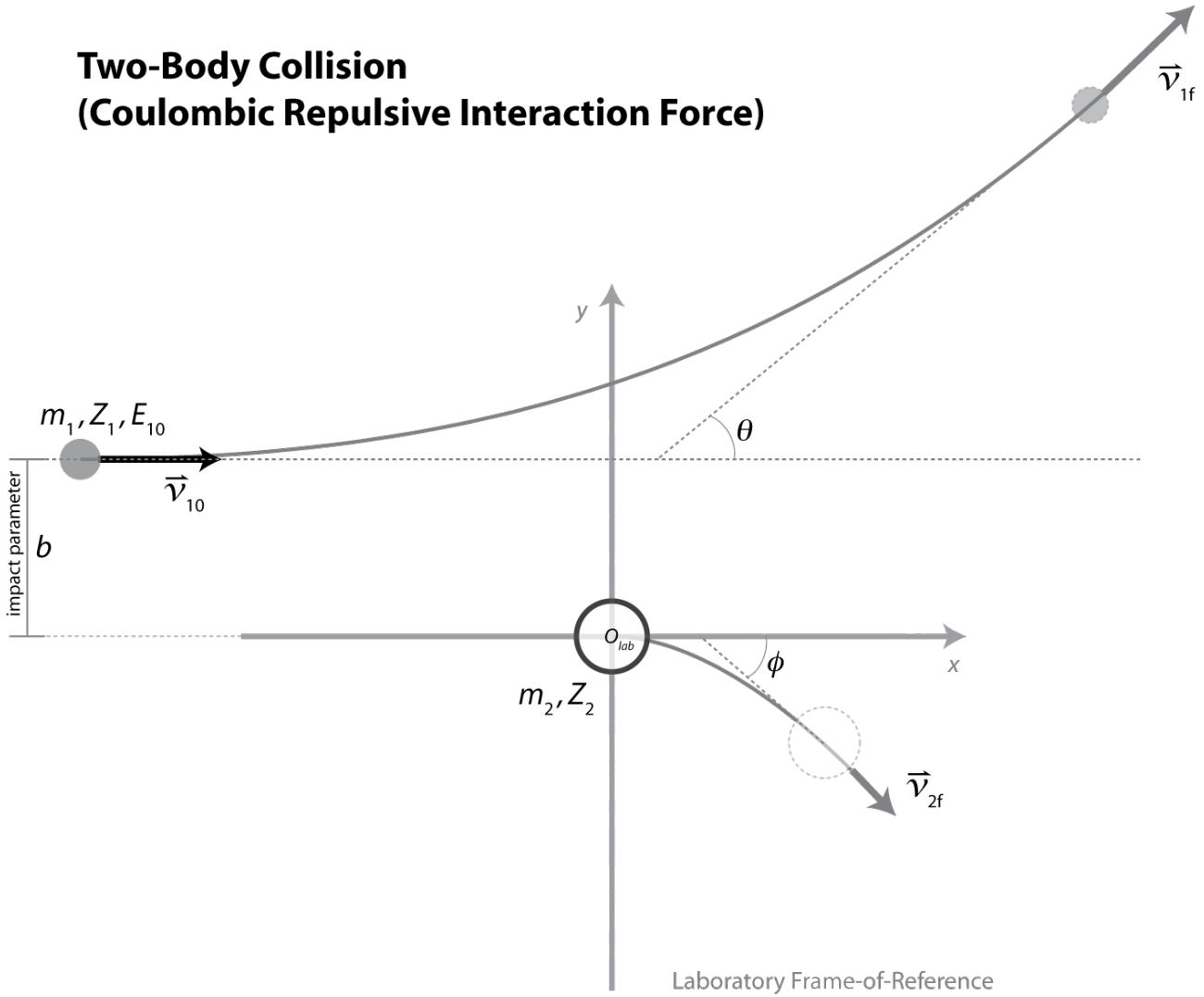

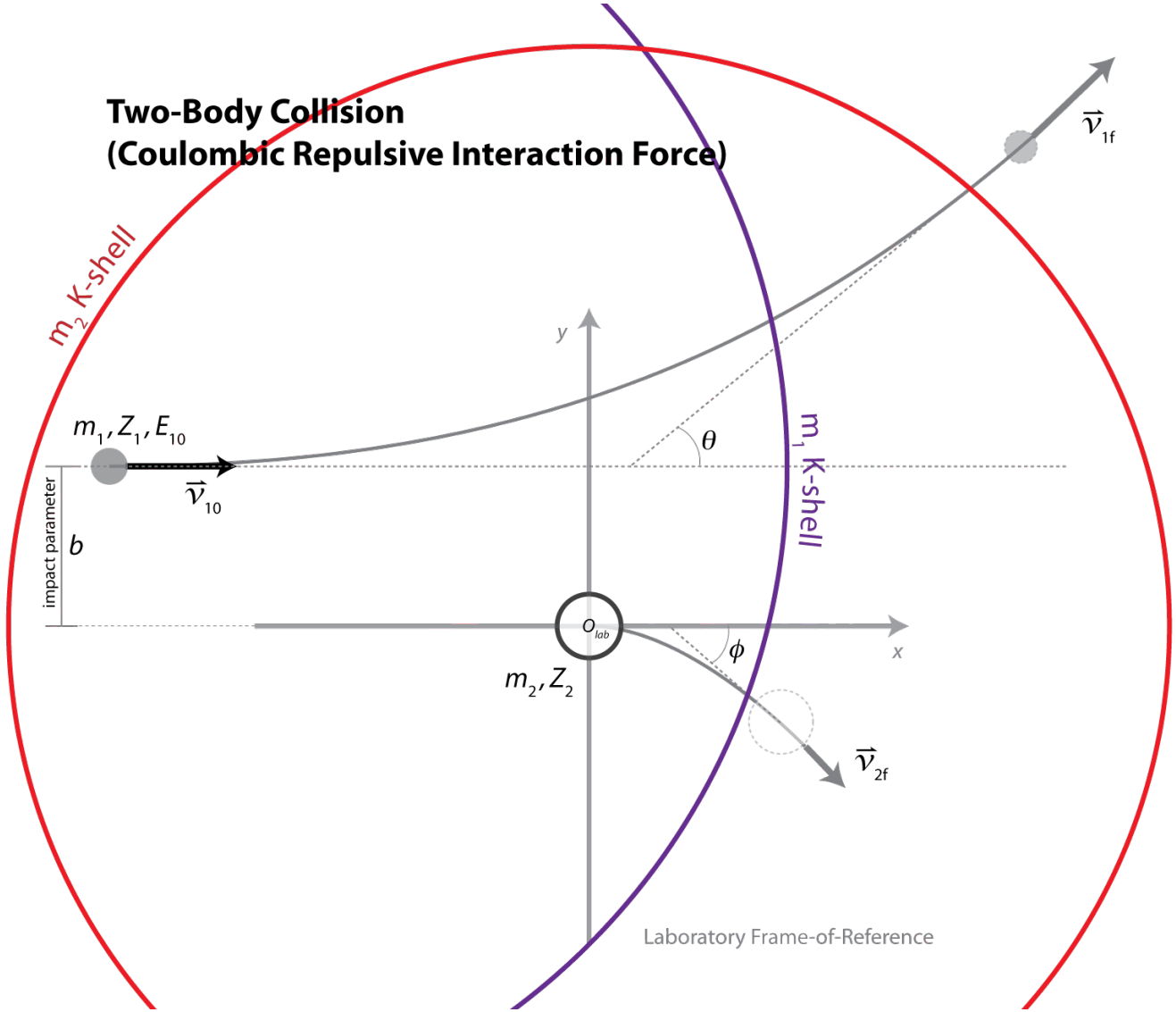
Two-Body Collision
(Coulombic Repulsive Interaction Force)
m_2 K-shell
m_1 K-shell
$\vec{v}_{1f}$
m_1, Z_1, E_{10}
$\vec{v}_{10}$
impact parameter
b
θ
y
x
O_{lab}
ϕ
m_2, Z_2
$\vec{v}_{2f}$
Laboratory Frame-of-Reference

What is the Rutherford (Coulomb) potential of interaction?

$$V(r) = ?$$

What is the Rutherford (Coulomb) potential of interaction?

$$V(r) = \frac{K}{r}$$

$$K = (Z_1\ e)(Z_2\ e)$$

$$= Z_1\ Z_2\ e^2$$

What is the value of the constant, e^2?

$$e^2 = ?$$

What is the value of the constant, e^2?

$$e^2 = 14.4\ eV \cdot \mathring{A}$$

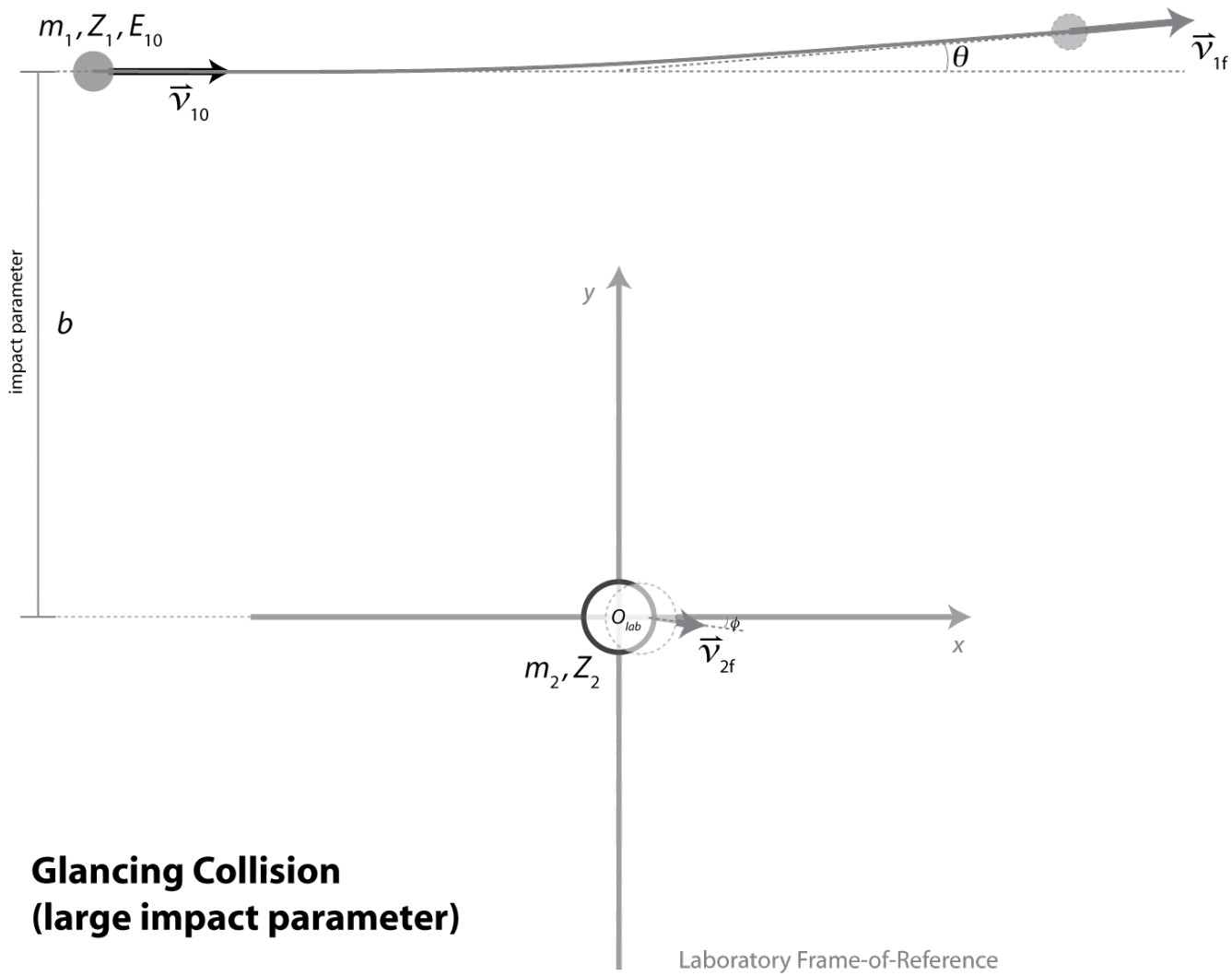

Glancing Collision
(large impact parameter)

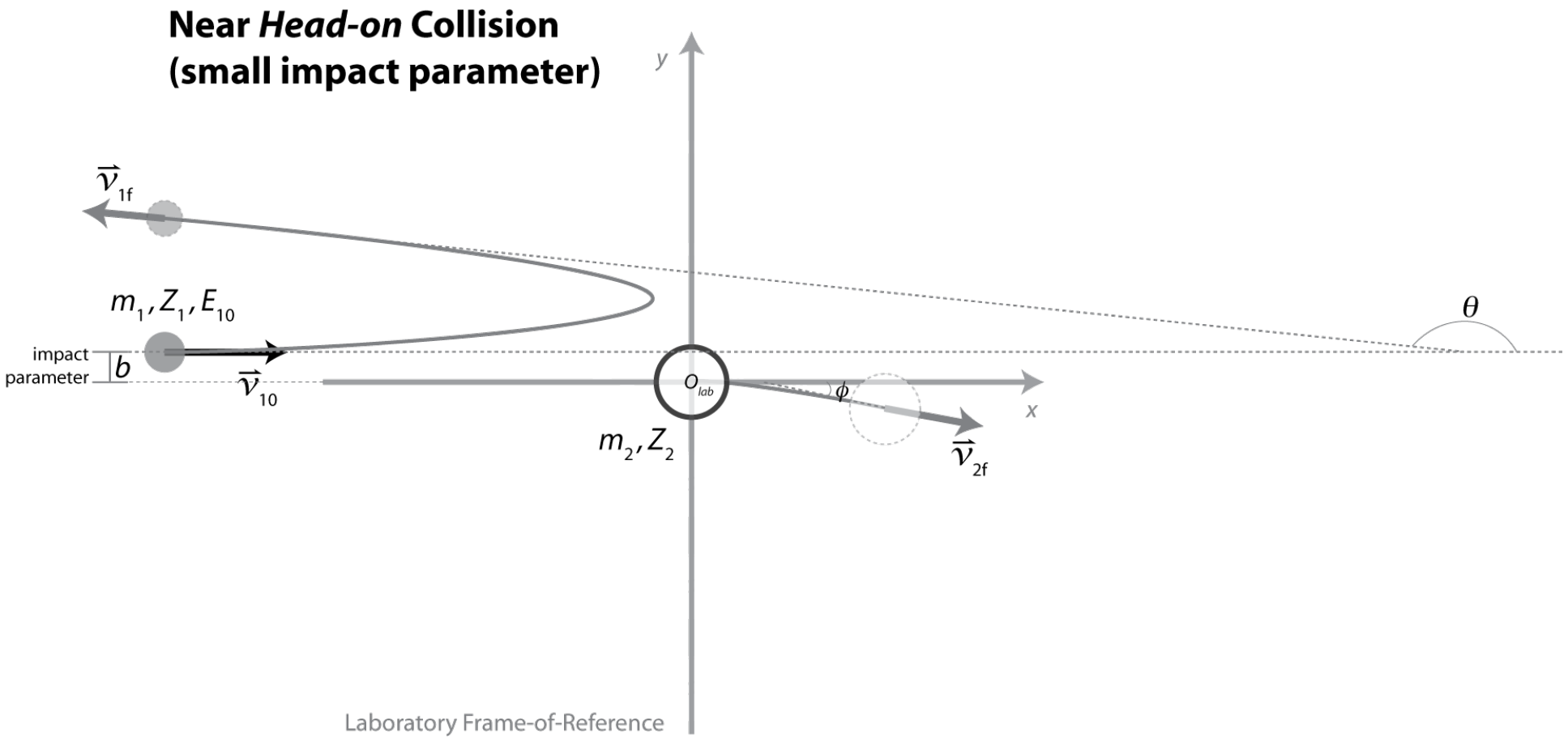
Near *Head-on* Collision
(small impact parameter)
y
$\vec{v}_{1f}$
m_1, Z_1, E_{10}
impact
parameter
b
$\vec{v}_{10}$
O_{lab}
ϕ
x
θ
m_2, Z_2
$\vec{v}_{2f}$
Laboratory Frame-of-Reference

Two-Body Collision
Energy transfer calculation

Ordinarily, in a first-year physics class, you would be asked to solve this problem using *Conservation of Energy* and *Conservation of Momentum* considerations.

This problem is algebraically intractable using these rules of conservation. However, the problem is solved elegantly using a transformation of coordinates to the Center-of-Mass (*CM*) Frame-of-Reference.

Identification of the Center-of-Mass (Two-Body System of Particles)

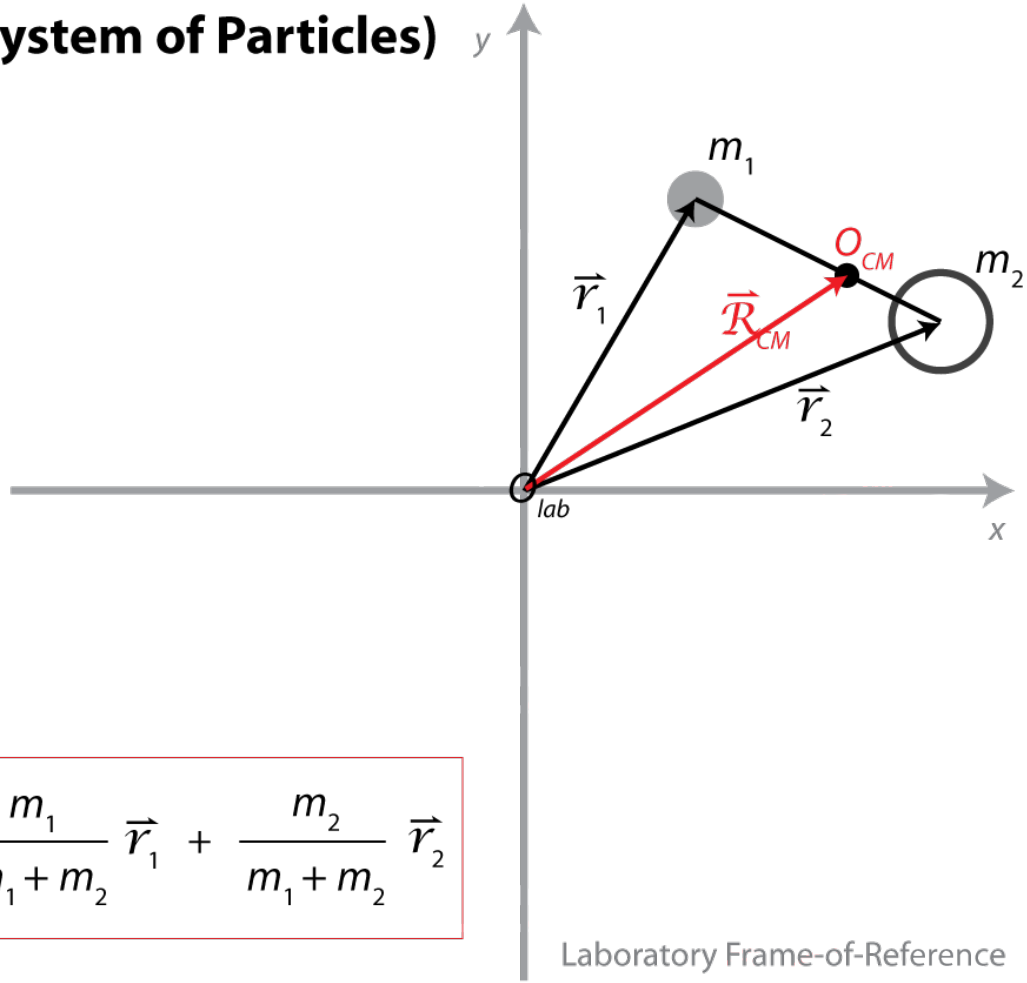

$$\vec{\mathcal{R}}_{CM} = \frac{m_1}{m_1 + m_2}\vec{r}_1 + \frac{m_2}{m_1 + m_2}\vec{r}_2$$

Laboratory Frame-of-Reference

The Velocity of the Center-of-Mass
(with respect to the Laboratory Frame-of-Reference)

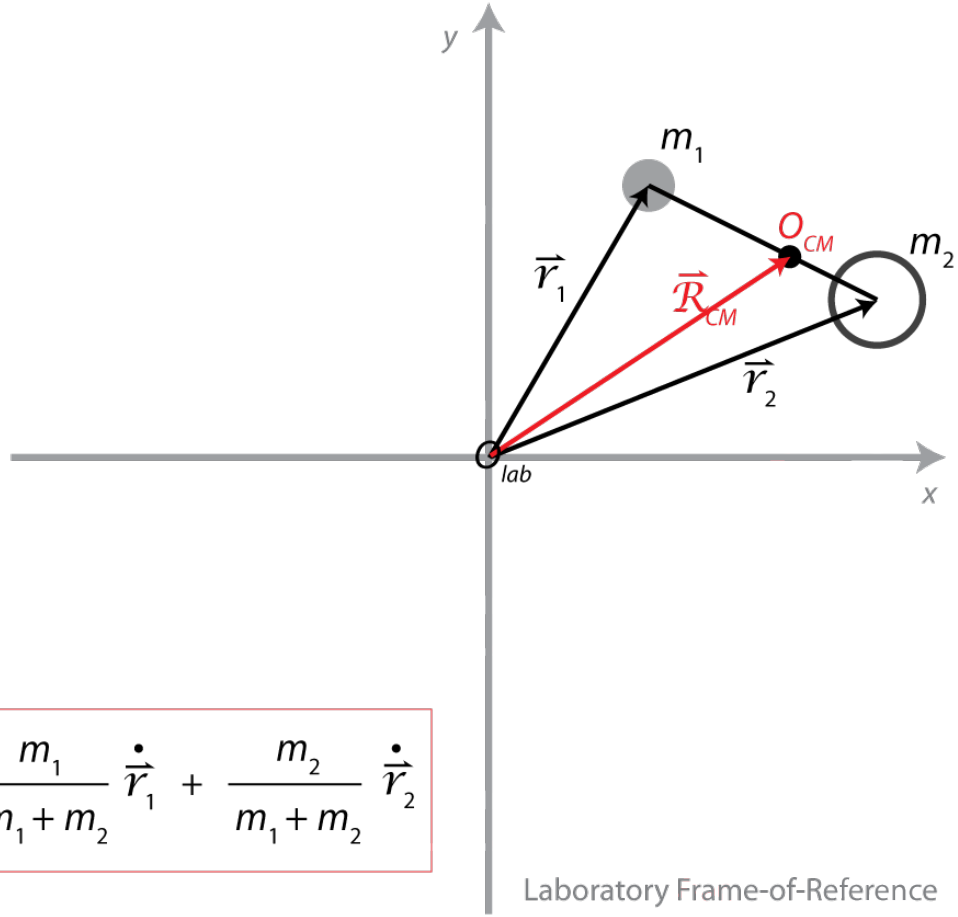

$$\vec{u} = \dot{\vec{\mathcal{R}}}_{CM} = \frac{m_1}{m_1 + m_2}\dot{\vec{r}}_1 + \frac{m_2}{m_1 + m_2}\dot{\vec{r}}_2$$

Laboratory Frame-of-Reference

The Velocity of the Center-of-Mass
(with respect to the Laboratory Frame-of-Reference)

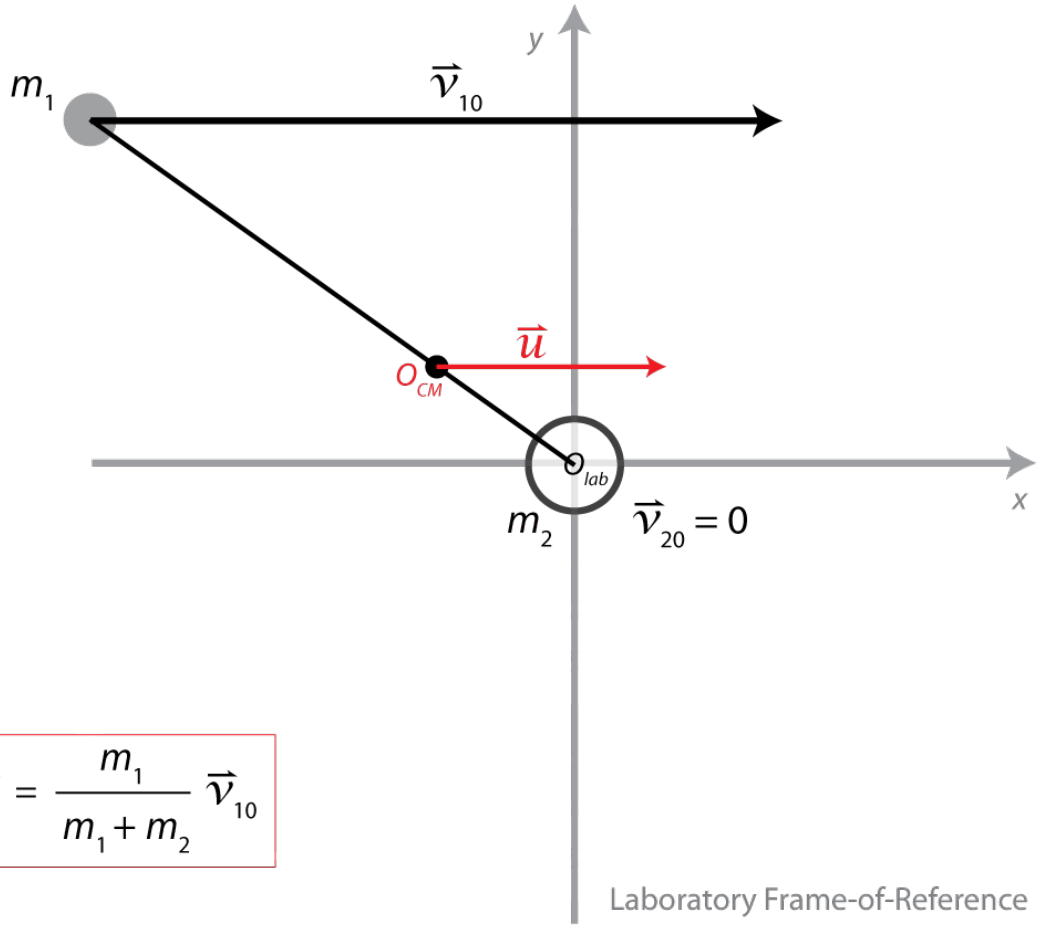

$$\vec{u} = \frac{m_1}{m_1 + m_2}\,\vec{v}_{10}$$

Proof that the net momentum in the Center-of-Mass (*CM*) coordinate system is *zero* - at all times.

$$\vec{R}_{CM} \equiv \frac{m_1}{m_1+m_2}\,\vec{r}_1 + \frac{m_2}{m_1+m_2}\,\vec{r}_2$$

$$\text{If} \quad \vec{r}_2 = 0, \quad \text{then} \quad \vec{R}_{CM} = \frac{m_1}{m_1+m_2}\,\vec{r}_1$$

$$\vec{r}_1 = \vec{R}_{CM} + \vec{r}_1^{\,*} \qquad \vec{r}_2 = \vec{R}_{CM} + \vec{r}_2^{\,*}$$

$$\vec{r}_1 = \frac{m_1}{m_1+m_2}\,\vec{r}_1 + \frac{m_2}{m_1+m_2}\,\vec{r}_2 + \vec{r}_1^{\,*} \qquad \vec{r}_2 = \frac{m_1}{m_1+m_2}\,\vec{r}_1 + \frac{m_2}{m_1+m_2}\,\vec{r}_2 + \vec{r}_2^{\,*}$$

$$\vec{r}_1^{\,*} = \left(1 - \frac{m_1}{m_1+m_2}\right)\vec{r}_1 - \frac{m_2}{m_1+m_2}\,\vec{r}_2 \qquad \vec{r}_2^{\,*} = \frac{-m_1}{m_1+m_2}\,\vec{r}_1 + \left(1 - \frac{m_2}{m_1+m_2}\right)\vec{r}_2$$

$$m_1\,\vec{r}_1^{\,*} = \left(m_1 - \frac{m_1^{\,2}}{m_1+m_2}\right)\vec{r}_1 - \frac{m_1 m_2}{m_1+m_2}\,\vec{r}_2 \qquad m_2\,\vec{r}_2^{\,*} = \frac{-m_1 m_2}{m_1+m_2}\,\vec{r}_1 + \left(m_2 - \frac{m_2^{\,2}}{m_1+m_2}\right)\vec{r}_2$$

$$m_1\,\dot{\vec{r}}_1^{\,*} = \left(m_1 - \frac{m_1^{\,2}}{m_1+m_2}\right)\dot{\vec{r}}_1 - \frac{m_1 m_2}{m_1+m_2}\,\dot{\vec{r}}_2 \qquad m_2\,\dot{\vec{r}}_2^{\,*} = \frac{-m_1 m_2}{m_1+m_2}\,\dot{\vec{r}}_1 + \left(m_2 - \frac{m_2^{\,2}}{m_1+m_2}\right)\dot{\vec{r}}_2$$

$$m_1\,\dot{\vec{r}}_1^{\,*} + m_2\,\dot{\vec{r}}_2^{\,*} = \left(\frac{m_1(m_1+m_2) - m_1^{\,2} - m_1 m_2}{m_1+m_2}\right)\dot{\vec{r}}_1 + \left(\frac{m_2(m_1+m_2) - m_1 m_2 - m_1^{\,2}}{m_1+m_2}\right)\dot{\vec{r}}_2 = 0$$

Two-Body Collision / Energy Transfer Calculation
Step 1.
Convert to Center-of-Mass Frame-of-Reference
(subtract $\vec{u}$ from velocities of m_1 and m_2)

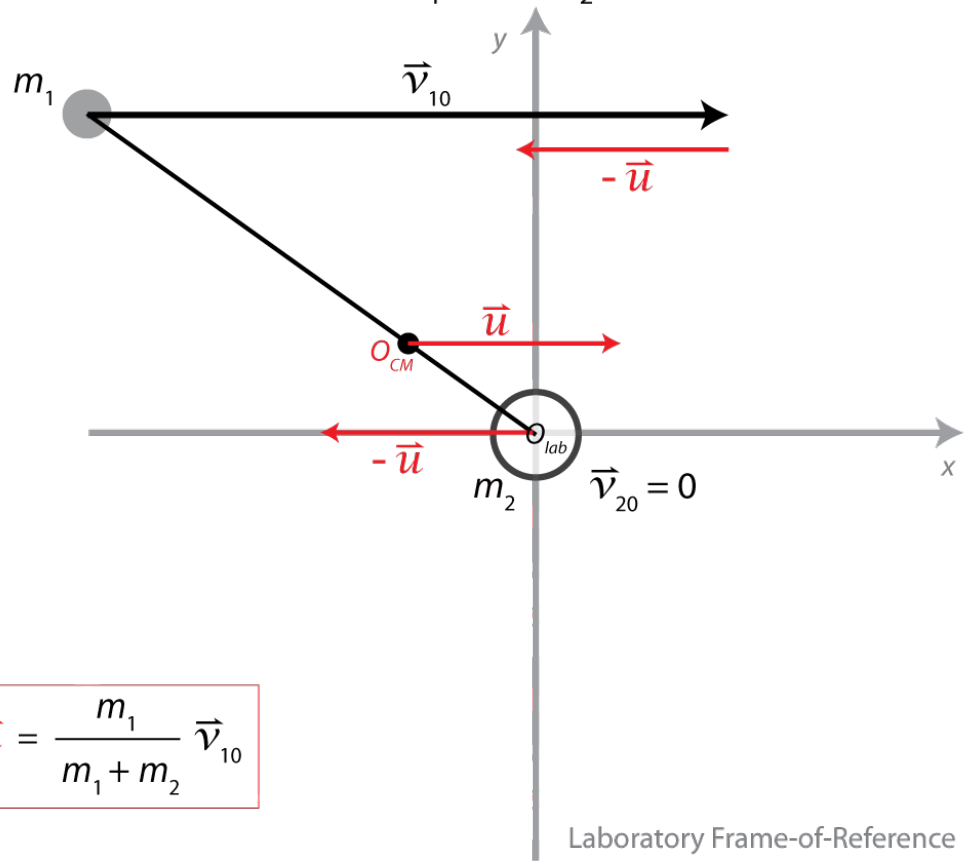

$$\vec{u} = \frac{m_1}{m_1 + m_2}\vec{v}_{10}$$

Calculate the energy transfer from projectile m_1 to target atom m_2.

Step 1. Transform from *laboratory* to *CM* coordinates.

$$\vec{R}_{CM} = \frac{m_1}{m_1+m_2}\vec{r}_1 \qquad \vec{u} = \dot{\vec{R}}_{CM} = \frac{m_1}{m_1+m_2}\dot{\vec{r}}_1 = \frac{m_1}{m_1+m_2}\vec{v}_{10} \qquad \left(\vec{v}_{20} = 0\right)$$

Subtract the velocity of the *CM* ($\vec{u}$) from the initial velocity of projectile m_1 ($\vec{v}_{10}$) and target atom m_2 ($\vec{v}_{20}$).

$$\begin{aligned}\vec{v}_{10}{}^{*} &= \vec{v}_{10} - \vec{u} \\ &= \vec{v}_{10} - \frac{m_1}{m_1+m_2}\vec{v}_{10} \\ &= \left(1 - \frac{m_1}{m_1+m_2}\right)\vec{v}_{10} \\ &= \left(\frac{m_1+m_2-m_1}{m_1+m_2}\right)\vec{v}_{10}\end{aligned}$$

$$\boxed{\vec{v}_{10}{}^{*} = \frac{m_2}{m_1+m_2}\vec{v}_{10}}$$

$$\begin{aligned}\vec{v}_{20}{}^{*} &= \vec{v}_{20} - \vec{u} \\ &= 0 - \vec{u}\end{aligned}$$

$$\boxed{\vec{v}_{20}{}^{*} = -\vec{u}}$$

Two-Body Collision / Energy Transfer Calculation
Step 1.
After Conversion to Center-of-Mass Frame-of-Reference

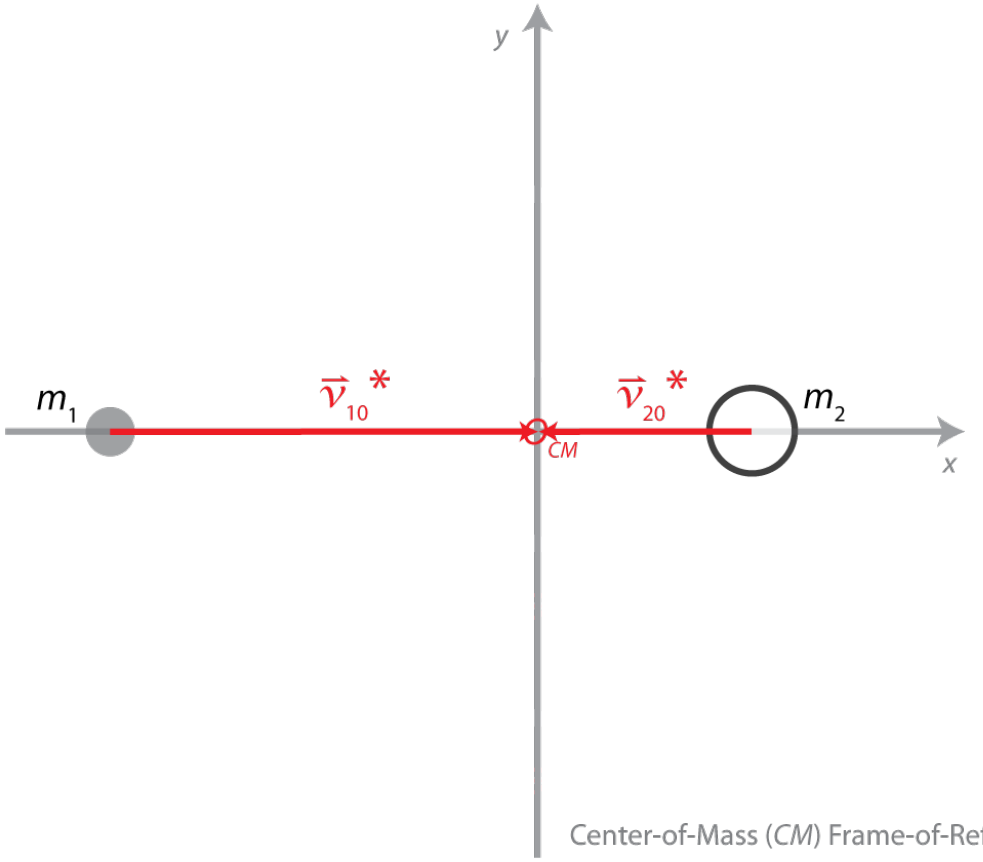

Calculate the energy transfer from projectile m_1 to target atom m_2.

Step 2. Perform the scattering interaction in *CM* coordinates.

Properties of the Center-of-Mass (*CM*) :

1. The net linear momentum in *CM* coordinates is *zero*.
2. In the absence of external forces (an inertial frame-of-reference), the velocity of the center of mass is *constant* (equal to $\vec{u}$).
3. In a two-body system, the center-of-mass must lie on the line adjoining the two particles at all times.
4. In a two-body system, the velocity vectors for the two particles in *CM* coordinates are *parallel* at all times.
5. In a two-body system, the magnitude of the velocity of each particle in *CM* coordinates is *unchanged* by the collision.

Two-Body Collision / Energy Transfer Calculation
Step 2.
After Scattering in the Center-of-Mass Frame-of-Reference

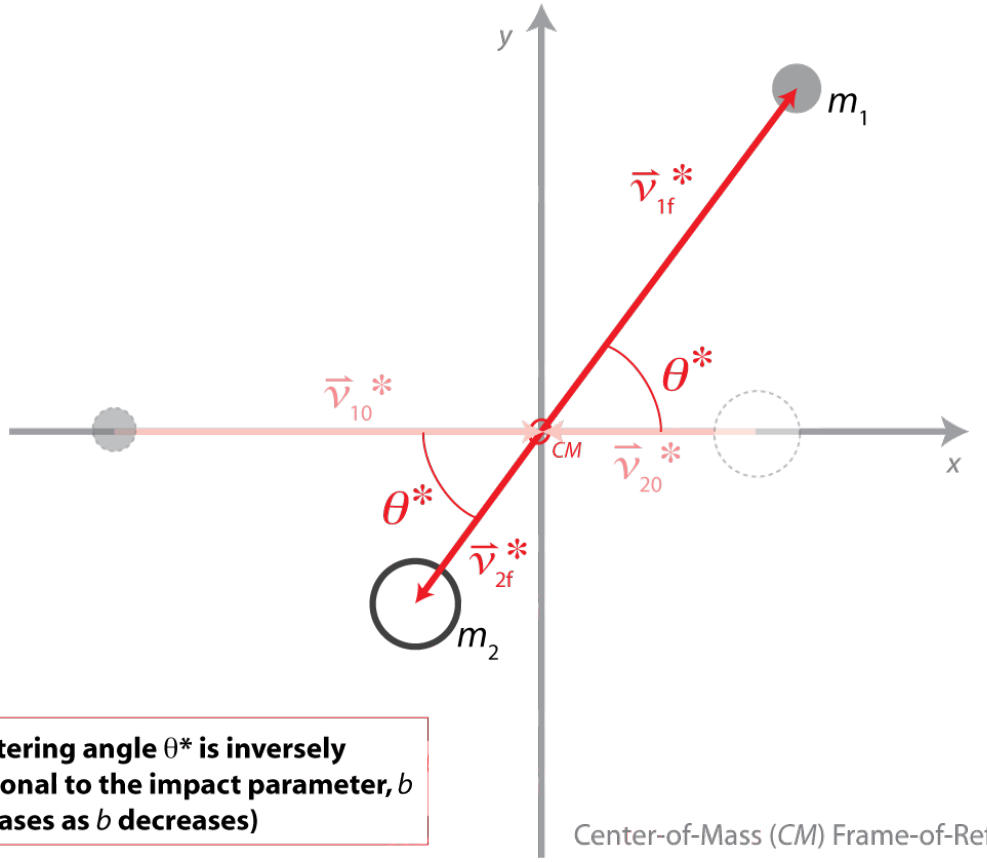

The scattering angle θ* is inversely proportional to the impact parameter, *b* (θ* increases as *b* decreases)

Center-of-Mass (*CM*) Frame-of-Reference

Two-Body Collision / Energy Transfer Calculation
Step 2.
After Scattering in the Center-of-Mass Frame-of-Reference

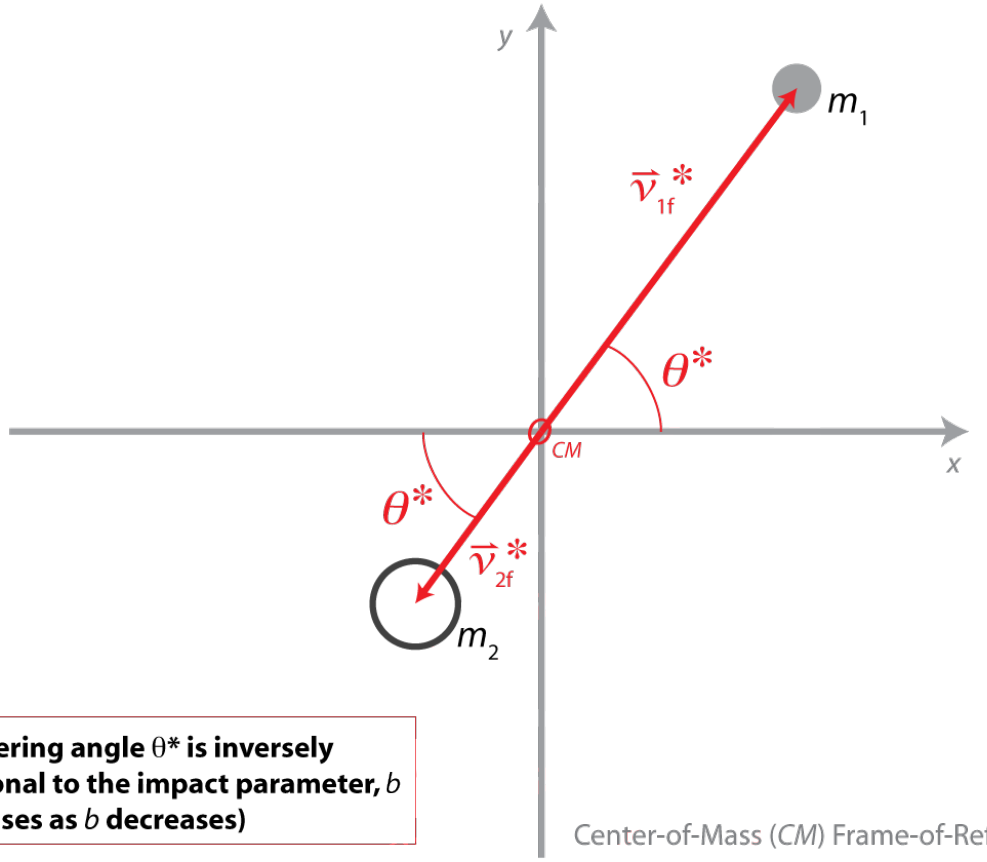

The scattering angle θ* is inversely proportional to the impact parameter, *b* (θ* increases as *b* decreases)

Center-of-Mass (*CM*) Frame-of-Reference

Calculate the energy transfer from projectile m_1 to target atom m_2.

Step 3. Transform from *CM* to *laboratory* coordinates.

Add the velocity of the *CM* ($\vec{u}$) to the final *CM* velocity of projectile m_1 ($\vec{v}_{1f}{}^{*}$) and target atom m_2 ($\vec{v}_{2f}{}^{*}$).

$$\vec{v}_{1f} = \vec{v}_{1f}{}^{*} + \vec{u} \qquad \vec{v}_{2f} = \vec{v}_{2f}{}^{*} + \vec{u}$$

Finally, solve for $\vec{v}_{2f}$ using trigonometry and convert to kinetic energy using:

$$\boxed{T_{2f} = \tfrac{1}{2}\, m_2\, v_{2f}{}^{2}}$$

Two-Body Collision / Energy Transfer Calculation
Step 3.
Convert back to Laboratory Frame-of-Reference
(add $\vec{u}$ to *CM* velocities of m_1 and m_2)

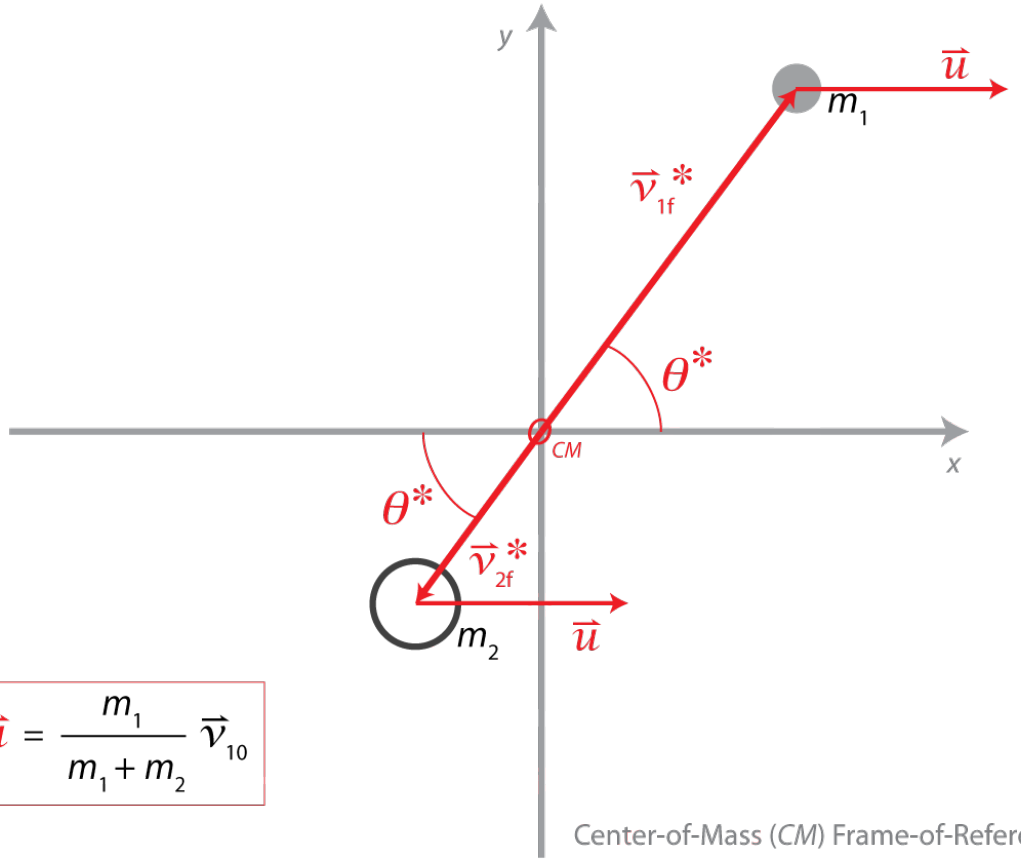

$$\vec{u} = \frac{m_1}{m_1 + m_2}\vec{v}_{10}$$

Center-of-Mass (*CM*) Frame-of-Reference

Two-Body Collision / Energy Transfer Calculation
Final geometry.
After converting back to Laboratory Frame-of-Reference

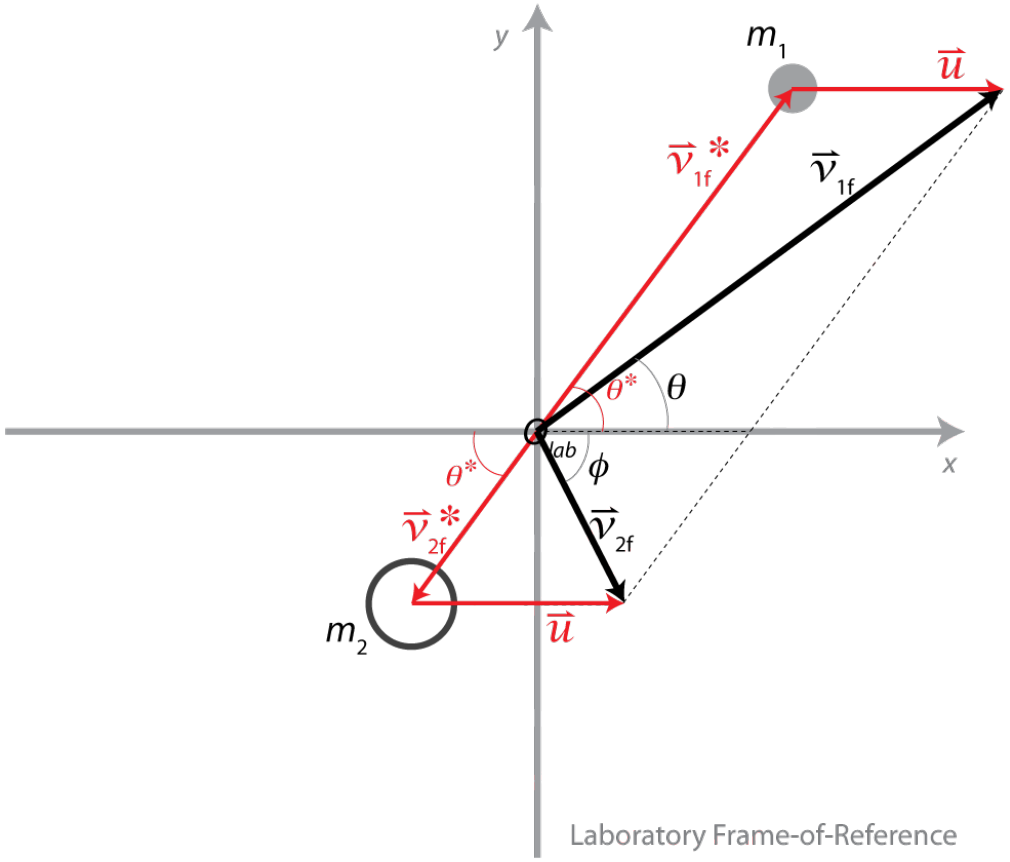

Two-Body Collision / Energy Transfer Calculation
Final geometry.
After converting back to Laboratory Frame-of-Reference

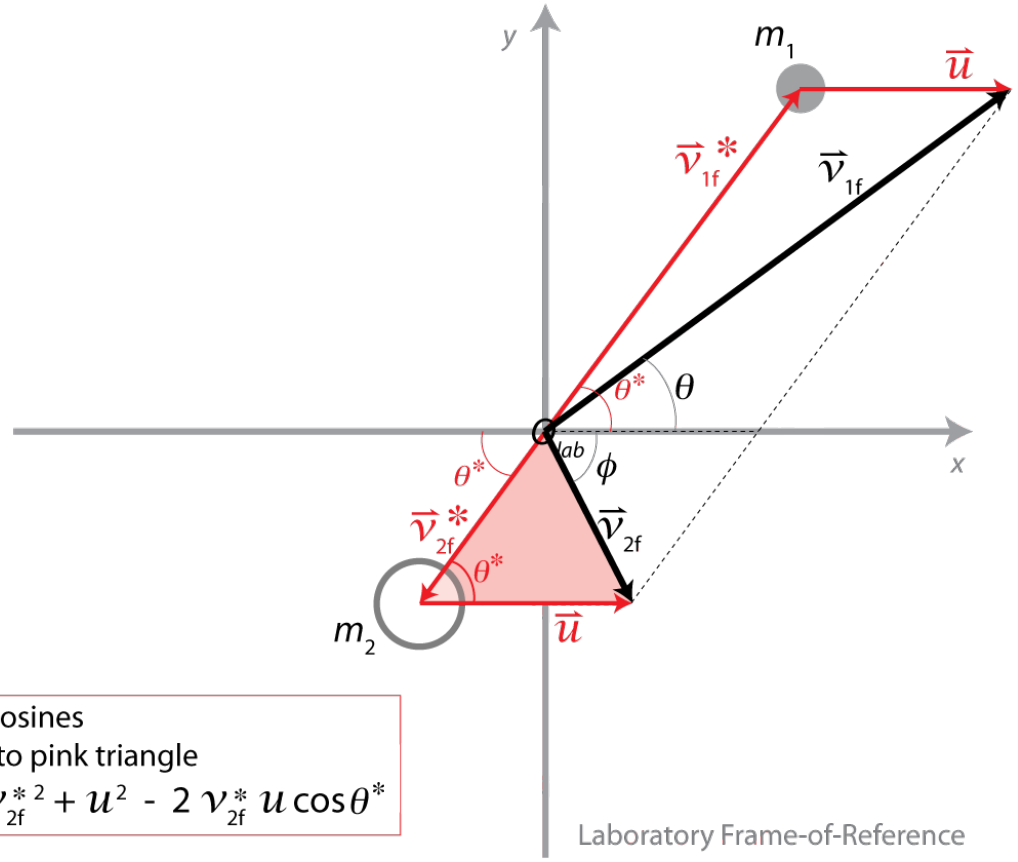

Law of Cosines
applied to pink triangle

$$v_{2f}^{\ 2} = v_{2f}^{*\,2} + u^2 \ - \ 2\, v_{2f}^{*}\, u \cos\theta^*$$

Trigonometry (Law of Cosines expression)

$$v_{2f}{}^2 = v_{2f}{}^{*2} + u^2 - 2\, v_{2f}{}^{*}\, u \cos\theta_{CM}$$

$$= u^2 + u^2 - 2\, u^2 \cos\theta_{CM}$$

$$= 2\, u^2 \left(1 - \cos\theta_{CM}\right)$$

Then: $\frac{1}{2}\, m_2\, v_{2f}{}^2 = \frac{1}{2}\, m_2\, 2\, u^2 \left(1 - \cos\theta_{CM}\right)$

$$\Rightarrow \quad T_{2f} = m_2 \left(\frac{m_1}{m_1 + m_2}\right)^2 v_{10}{}^2 \left(1 - \cos\theta_{CM}\right)$$

$$= \frac{m_1 m_2}{(m_1 + m_2)^2}\, m_1\, v_{10}{}^2 \left(1 - \cos\theta_{CM}\right)$$

$$= \frac{m_1 m_2}{\frac{1}{2}(m_1 + m_2)^2}\, \frac{1}{2}\, m_1\, v_{10}{}^2 \left(1 - \cos\theta_{CM}\right)$$

But: $E_{10} = \frac{1}{2}\, m_1\, v_{10}{}^2 \qquad \therefore \qquad \boxed{T_{2f} = \frac{2\, m_1 m_2}{(m_1 + m_2)^2}\, E_{10} \left(1 - \cos\theta_{CM}\right)}$

Maximum Kinetic Energy Transfer
Two-Body Collision

$$T_{2f} = \frac{2\,m_1 m_2}{(m_1+m_2)^2}\,E_{10}\left(1-\cos\theta_{CM}\right)$$

Head-on Collision: $\theta_{CM} = \pi$

$$\cos\pi = -1$$

$$\Rightarrow (1-\cos\theta_{CM}) = (1--1) = 2$$

$$\therefore \quad T_{2f}^{max} = \frac{4\,m_1 m_2}{(m_1+m_2)^2}\,E_{10}$$

$$\boxed{T_{2f}^{max} = \Lambda\,E_{10}}$$

$$\Lambda = \frac{4\,m_1 m_2}{(m_1+m_2)^2}$$

$\Lambda \equiv$ Kinetic Efficiency Factor

Kinetic Efficiency Factor, Λ

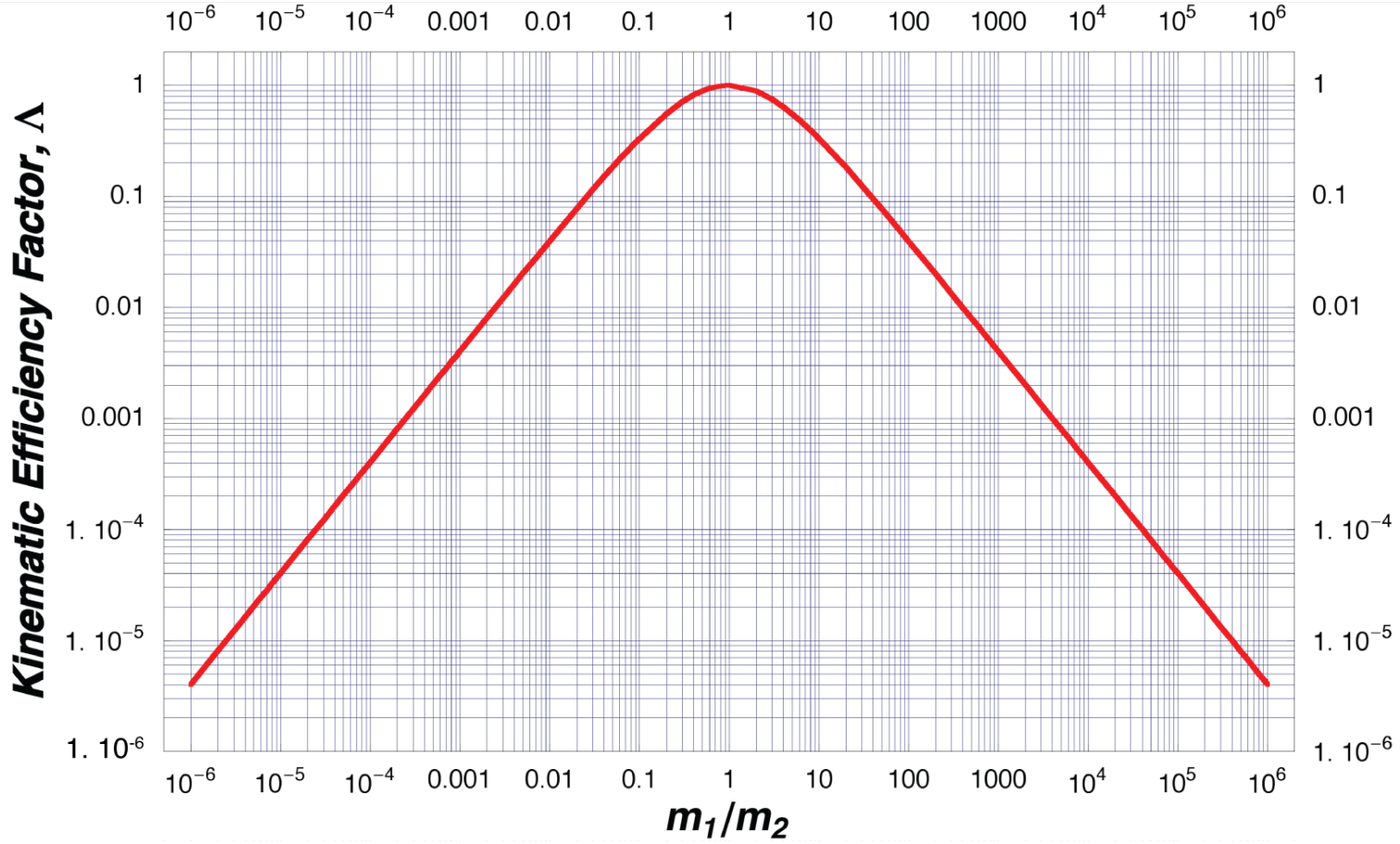

Kinetic Efficiency Factor
e^- / e^-, He, O, Cu, U

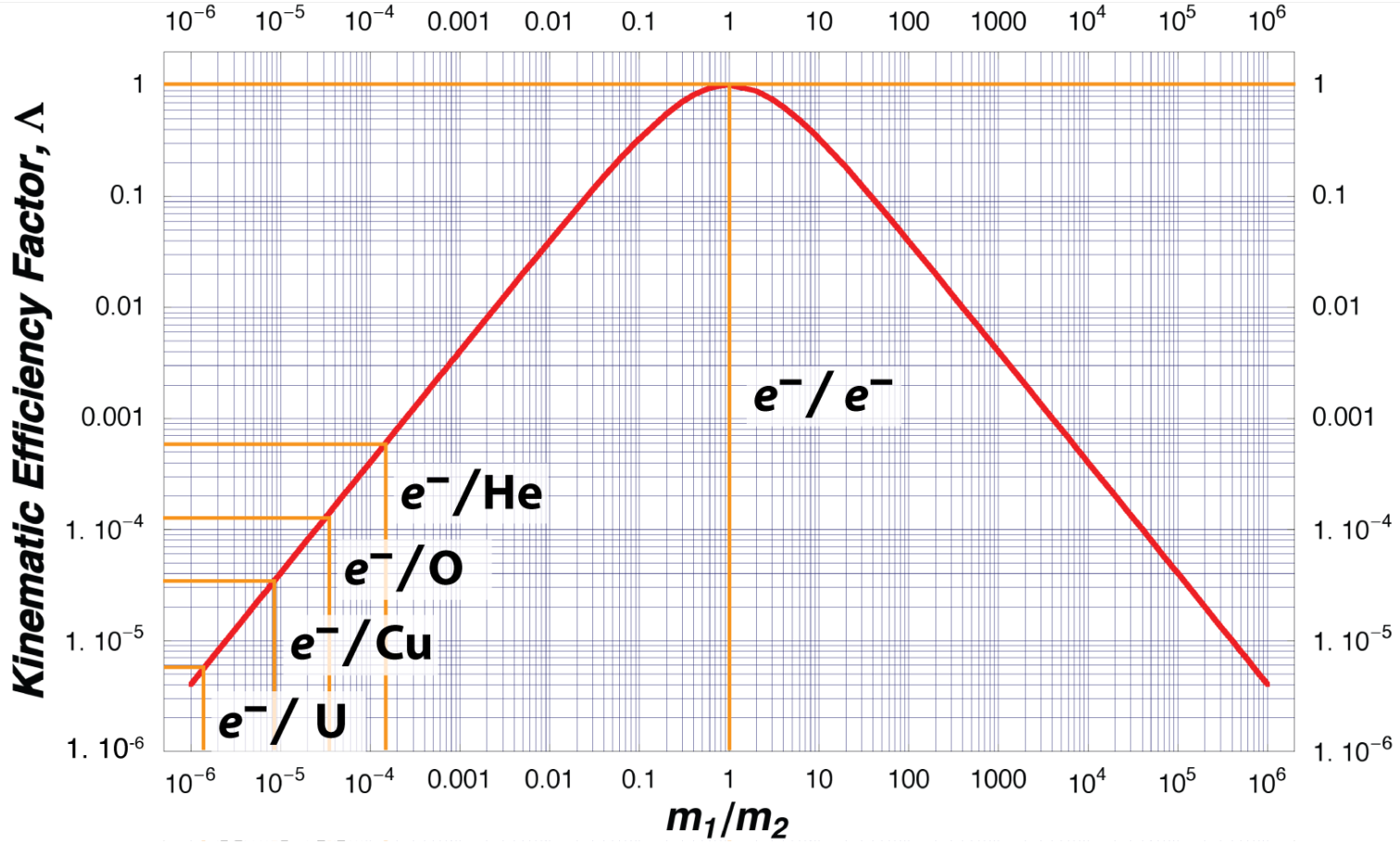

Kinetic Efficiency Factor
He / e^-, He, O, Cu, U

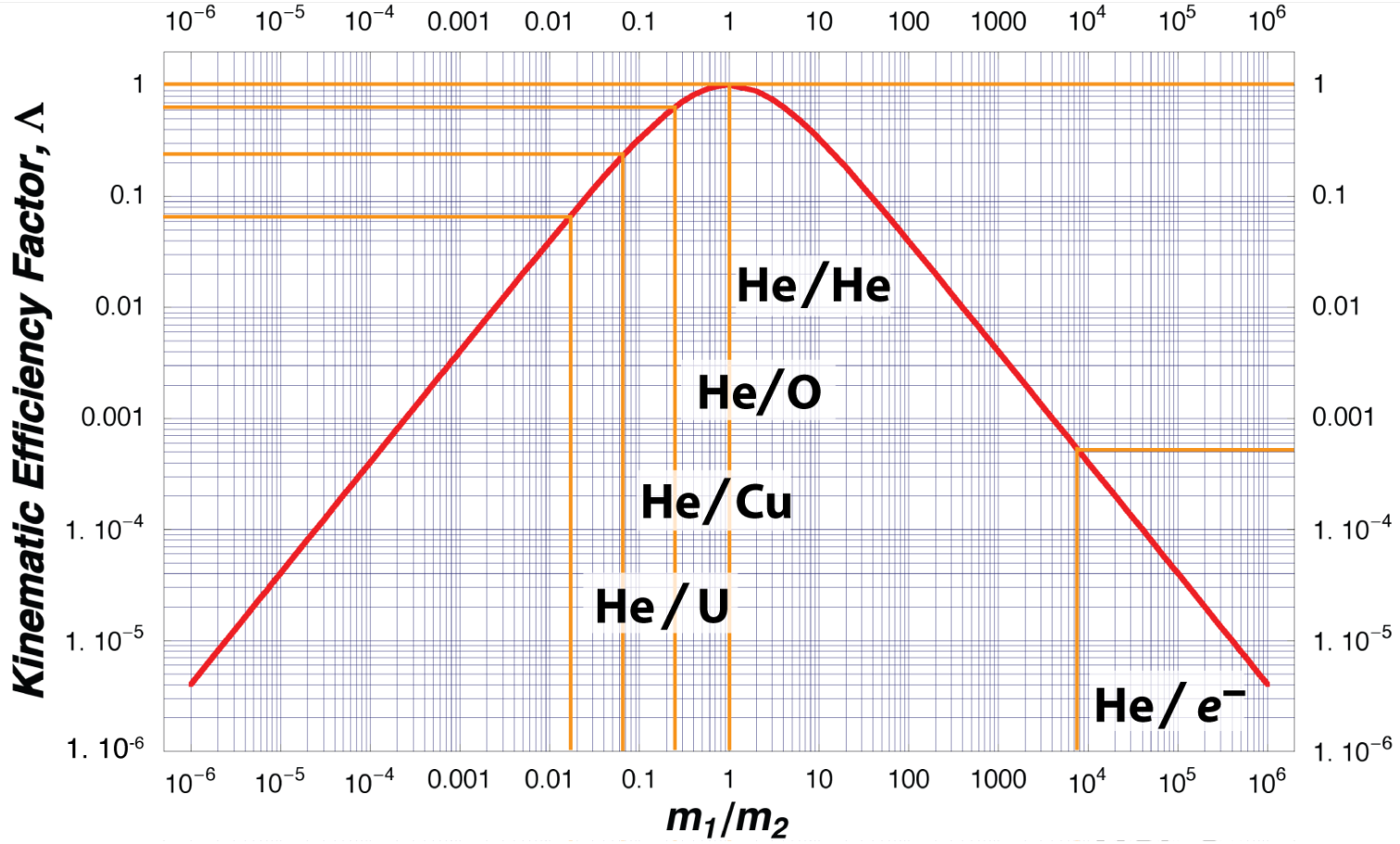

Kinetic Efficiency Factor
O / e^-, He, O, Cu, U

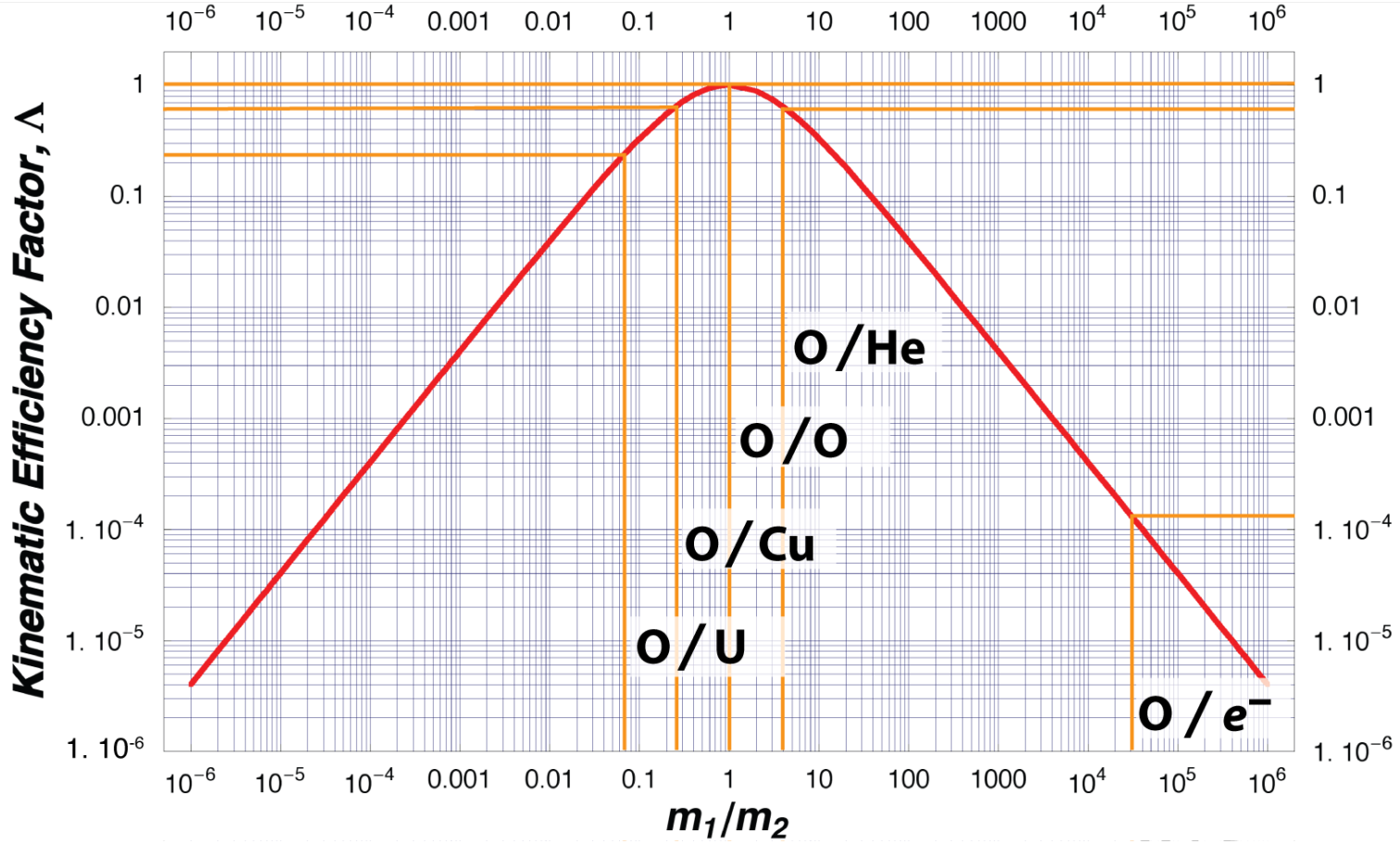

LSS Energy Partitioning Theory: Partitioning of PKA Energy Between Electronic and Nuclear Stopping

Lindhard, J. and M. Scharff (1961). "Energy Dissipation of Ions in the keV Region." Physical Review **124**(1): 128-130.

Lindhard, J., M. Scharff, and Schiøtt, H. E. (1963). "Range Concepts and Heavy Ion Ranges (Notes on Atomic Collisions, II)." Mat. Fys. Medd. Dan. Vid. Selsk. **33**(14): 1-42.

Lindhard, J., V. Nielsen, Scharff, M., and Thomsen, P. V. (1963). "Integral Equations Governing Radiation Effects (Notes on Atomic Collisions, III)." Mat. Fys. Medd. Dan. Vid. Selsk. **33**(10): 1-42.

Lindhard, J., V. Nielsen, and Scharff, M. (1968). "Approximation Method in Classical Scattering by Screened Coulomb Fields (Notes on Atomic Collisions, I)." Mat. Fys. Medd. Dan. Vid. Selsk. **36**(10): 1-32.

Winterbon, K. B., P. Sigmund, and Sanders, J. B. (1970). "Spatial Distribution of Energy Deposited by Atomic Particles in Elastic Collisions." Mat. Fys. Medd. Dan. Vid. Selsk. **37**(14): 1-73.

Derivation of the *LSS* integro-differential equation

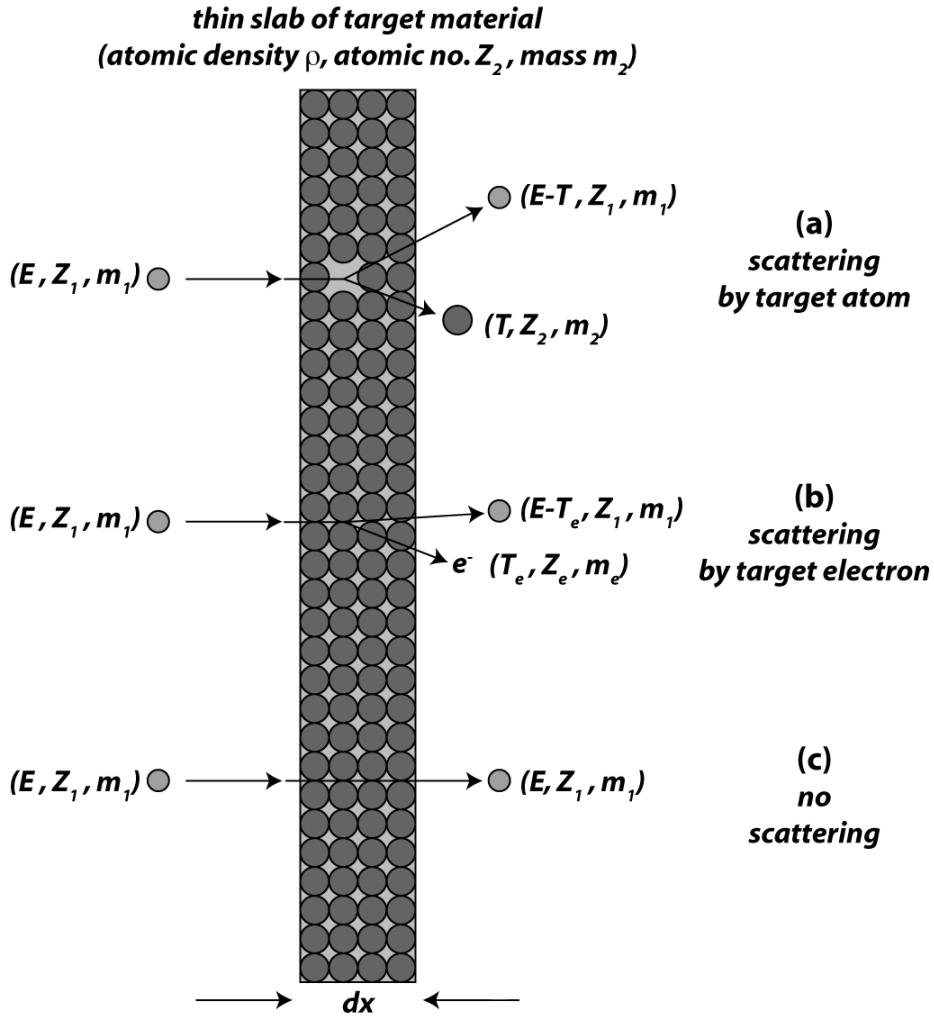

Shorthand notation

$$\sigma(E,T) = \frac{d\sigma(E,T)}{dT}$$ (differential nuclear scattering cross-section)

$$\sigma(E,T_e) = \frac{d\sigma(E,T_e)}{dT_e}$$ (differential electron scattering cross-section)

Differential Probabilities

We begin by writing the differential probabilities of nuclear, electronic, and no scattering in a target slab of thickness, dx:

$$P_n(T, T+dT) = (\rho\, dx)\ \ \sigma(E,T)\, dT \quad (2),$$

(differential probability of nuclear scattering in the energy range, $(T,\ T+dT)$.

$$P_e(T_e, T_e+dT_e) = (\rho\, dx)\ \ \sigma_e(E,T_e)\, dT_e \quad (3),$$

(differential probability of electron scattering in the energy range, $(T_e,\ T_e+dT_e)$.

$$P_0 = 1 - \int_0^E P_n\left(T, T+dT\right) - \int_0^{\Lambda_e E} P_e\left(T_e, T_e+dT_e\right) \quad (4).$$

(differential probability of no scattering in thickness, dx)

LSS integro-differential equation

$$\nu(E)+\frac{S_e(E)}{\sigma(E)}\nu' = \frac{1}{\sigma(E)}\int_0^E \Big[\nu(E-T)+\nu(T)\Big]\,\sigma(E,T)\,dT$$

$\nu(E)$ = number of displacements produced by the PKA

LSS, the hard-sphere potential, and the Kinchin-Pease formula

$$\frac{d\sigma(E,T)}{\sigma(E)} = \frac{dT}{\Lambda E}$$

LSS-Hard-sphere potential

$$\nu(2E_d < E < E_c) = \frac{E}{2E_d} \qquad (\text{for } m_1 = m_2, \Lambda = 1)$$

This is the famous Kinchin-Pease equation!

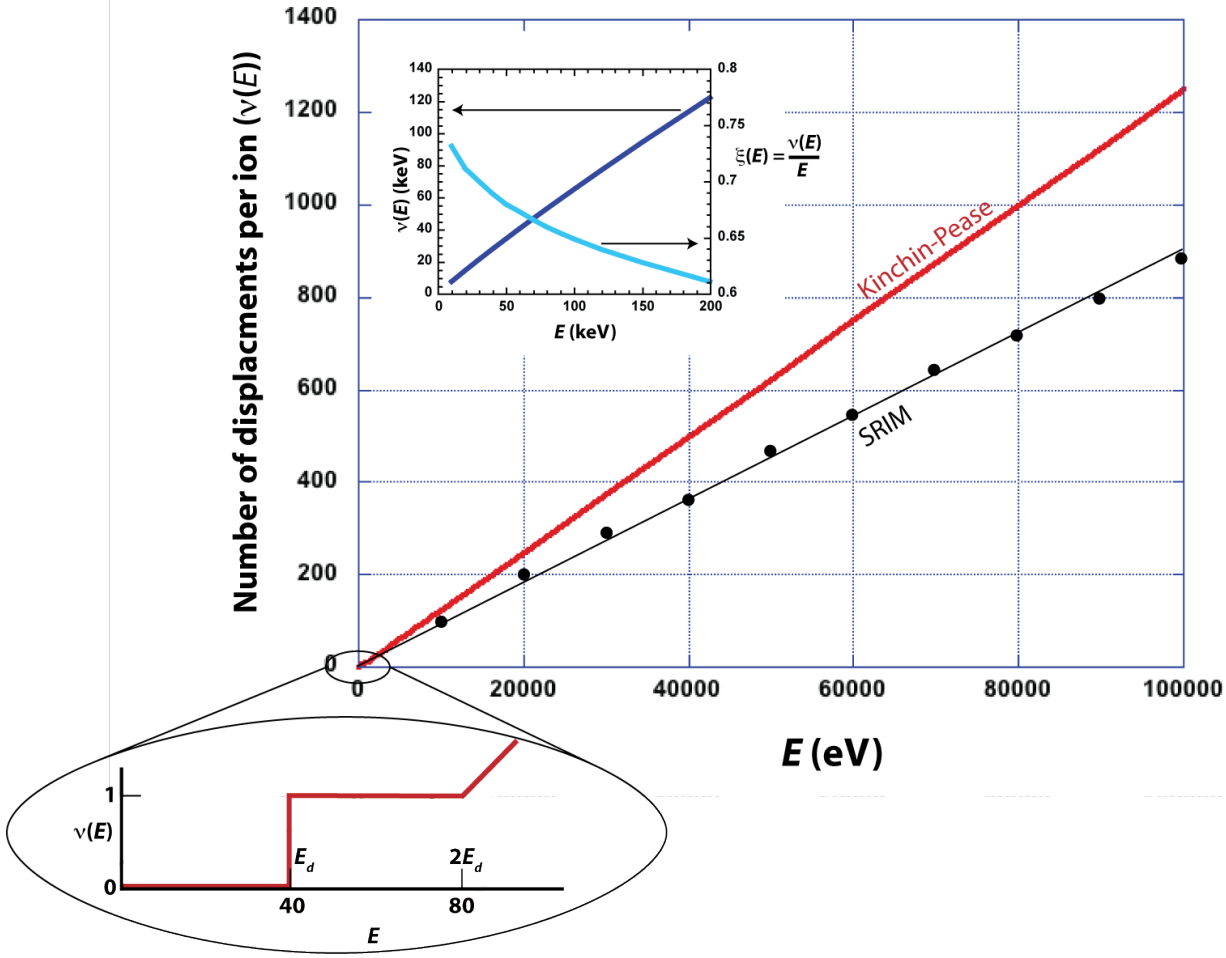
Number of displacments per ion (ν(E))
E (eV)
Kinchin-Pease
SRIM
ν(E) (keV)
E (keV)
ξ(E) = ν(E)/E
ν(E)
E_d
2E_d
E

LSS screened Coulomb nuclear stopping formula:

LSS universal differential cross-section

$$\frac{d\sigma}{dt} = \frac{\pi \hat{a}^2}{2} \frac{f\left(t^{1/2}\right)}{t^{3/2}}$$

LSS electronic and nuclear stopping formulas: (1) Electronic

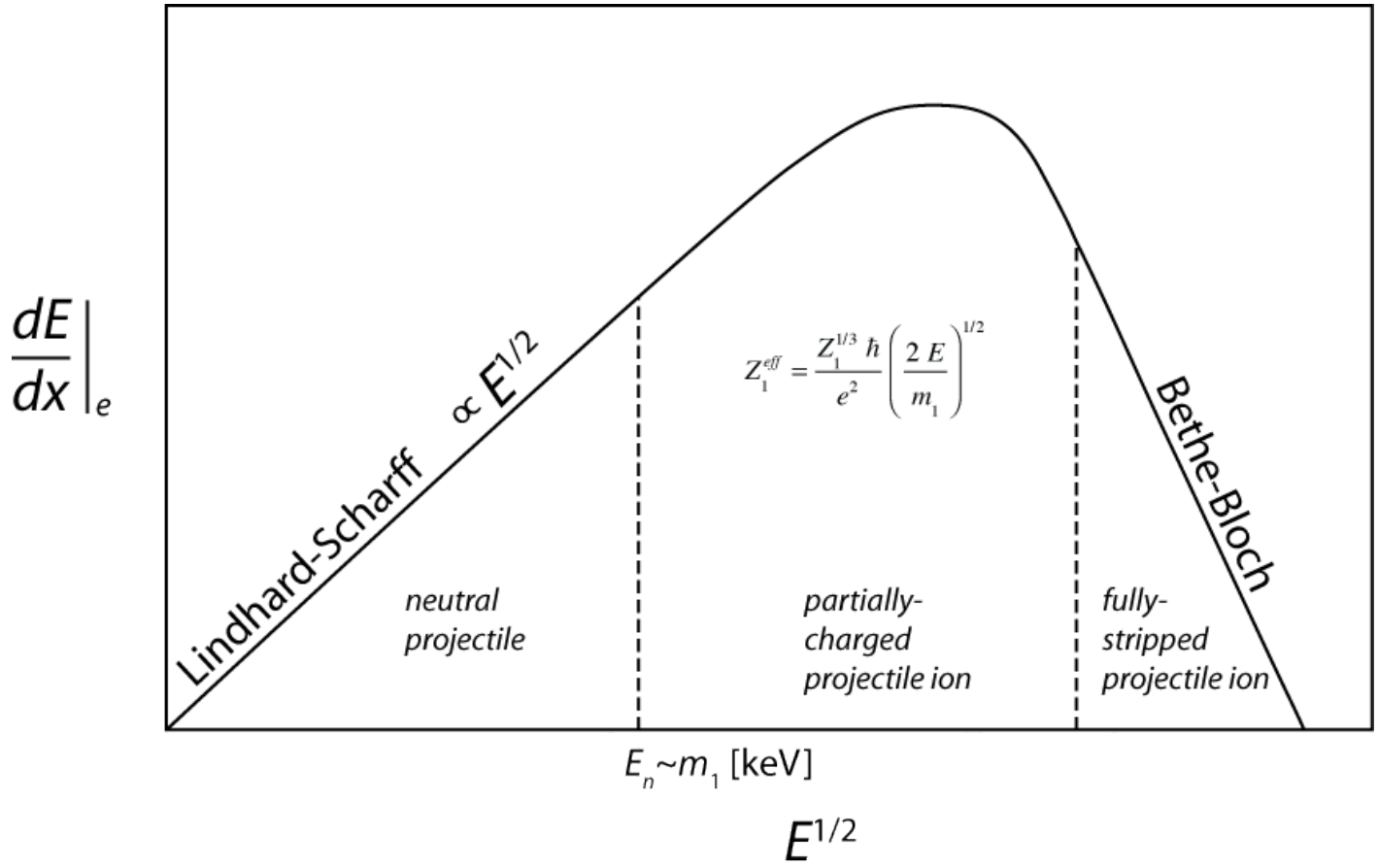

Low-*E* electronic stopping

$$S_e^{LSS}(E) = k\,E^{1/2}\left[eV \bullet \mathring{A}^2\right] \qquad (E \text{ in units of } [eV])$$

$$k = 1.216053\,\frac{Z_1^{7/6}\,Z_2}{\left(Z_1^{2/3}+Z_2^{2/3}\right)^{3/2}}\,\frac{1}{\sqrt{m_1\,[amu]}}$$

High-*E* electronic stopping

$$S_e^{BB}(E) = \frac{2\,\pi\,Z_1^2\,Z_2\,e^4\,(m_1/m_e)}{E}\ln\left(\frac{4\,E}{(m_1/m_e)\,Z_2\,I_0}\right)$$

$$= \frac{8\,\pi\,Z_1^2\,e^4}{I_0\,\varepsilon_B}\ln(\varepsilon_B) \qquad \text{where} \quad \varepsilon_B = \frac{2\,m_e\,v_1^2}{Z_2\,I_0}$$

Spline fit of Low-E High-E electronic stopping powers

$$S_e(E) = \left(\frac{1}{S_e^{LSS}(E)} + \frac{1}{S_e^{BB}(E)} \right)^{-1}$$

(Biersack and Haggmark 1980)

Multi-component solids

Use the *Principle of the Additivity of Stopping Powers* (also known as *Bragg's Rule*)

$$S(E) = \frac{1}{\rho} \sum_{i=1}^{c} \rho_i \, S_i(E)$$

Example calculations of electronic and nuclear energy partitioning: I^+ ions in spinel ($MgAl_2O_4$)

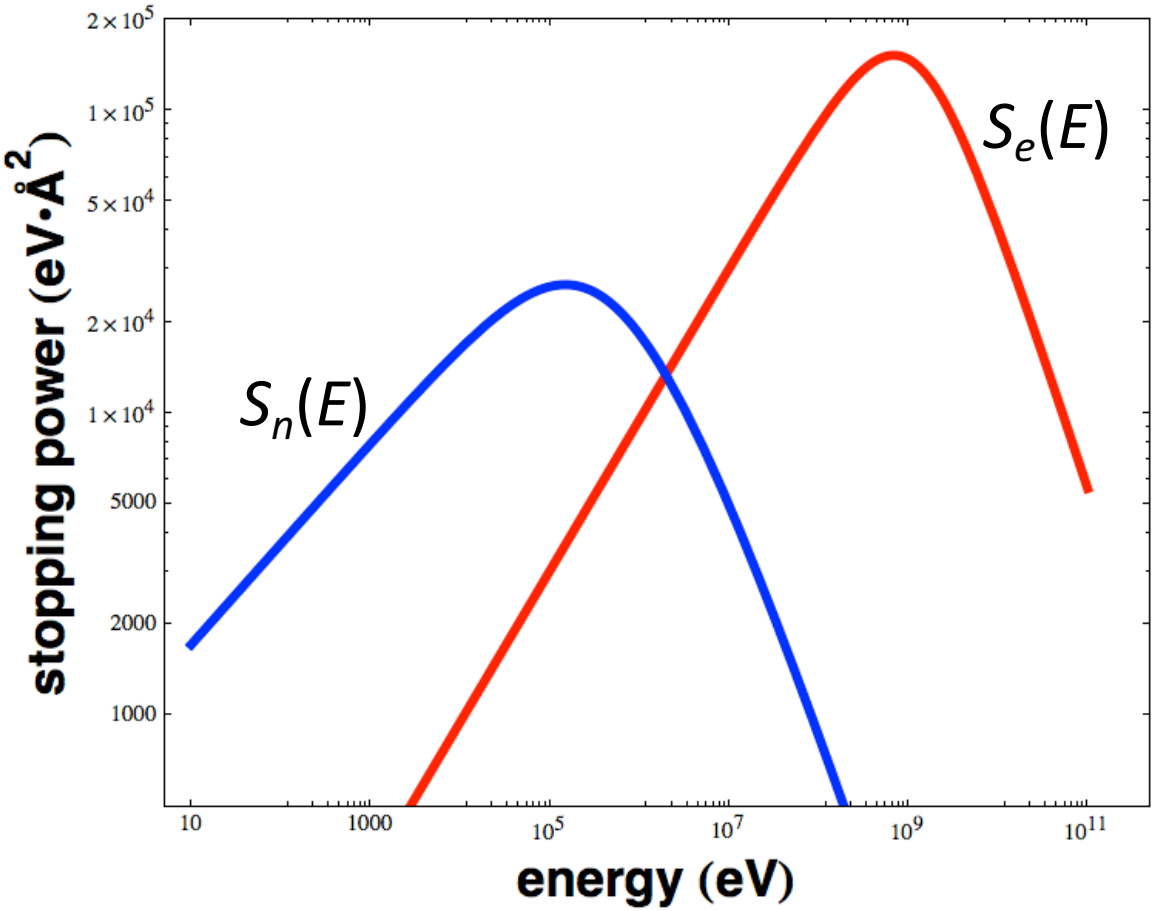

Stopping power versus linear energy loss rate

$$S(E) = \frac{1}{\rho}\left(\frac{dE}{dx}\right)$$

Example calculations of electronic and nuclear energy partitioning: I^+ ions in spinel ($MgAl_2O_4$)

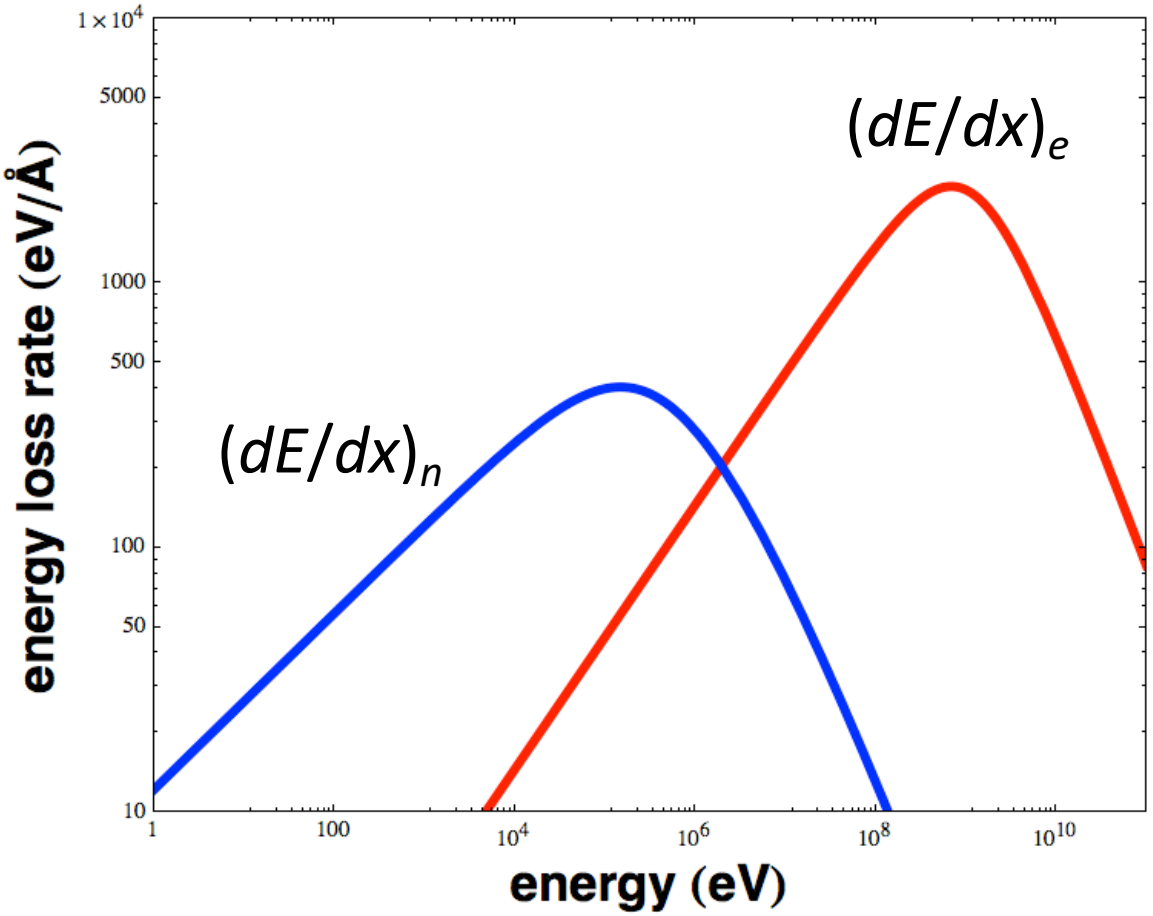

Example calculations of electronic and nuclear energy partitioning:
I^+ ions in spinel ($MgAl_2O_4$)

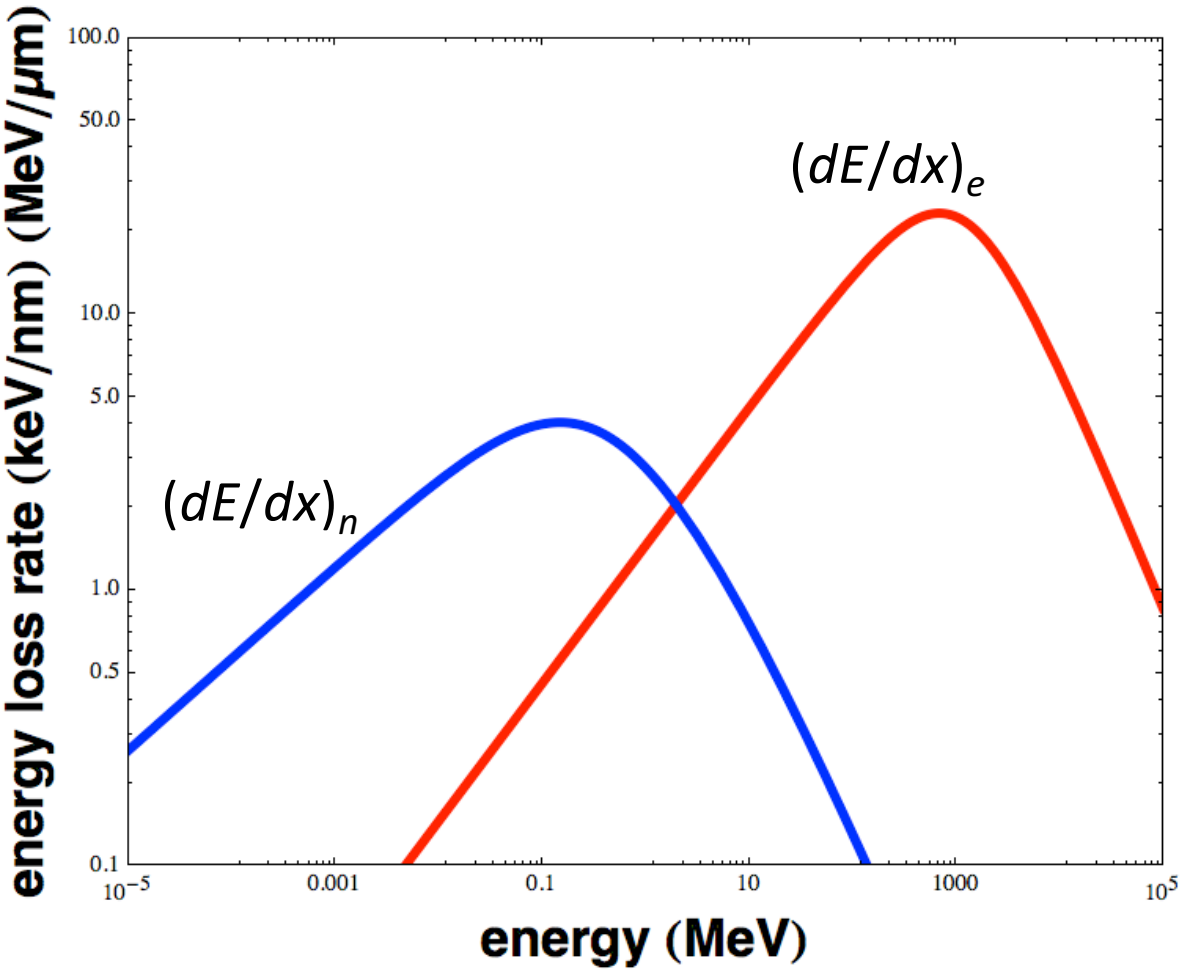

Example calculations of electronic and nuclear energy partitioning: I^+ ions in spinel ($MgAl_2O_4$)

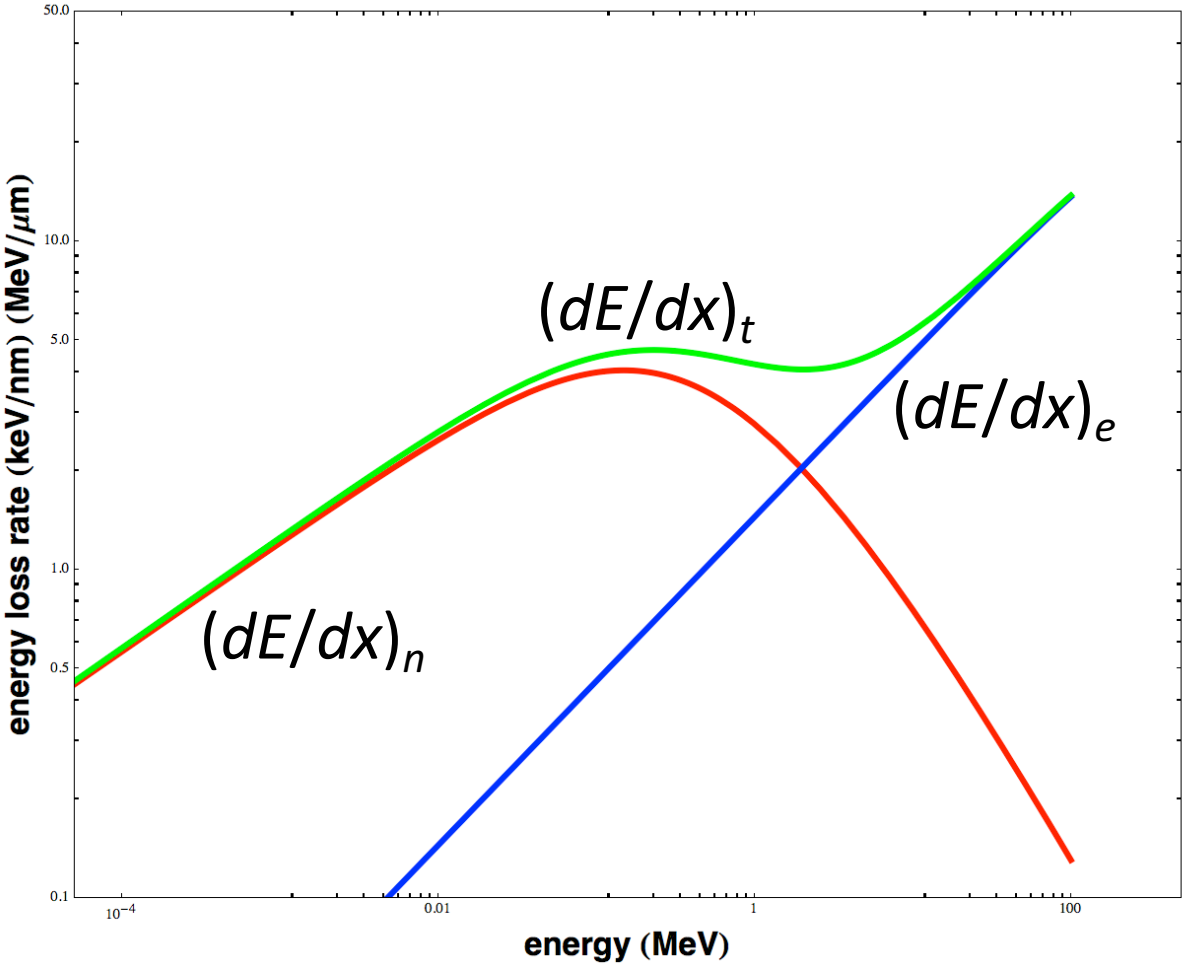

Example calculations of electronic and nuclear energy partitioning: I^+ ions in spinel ($MgAl_2O_4$)

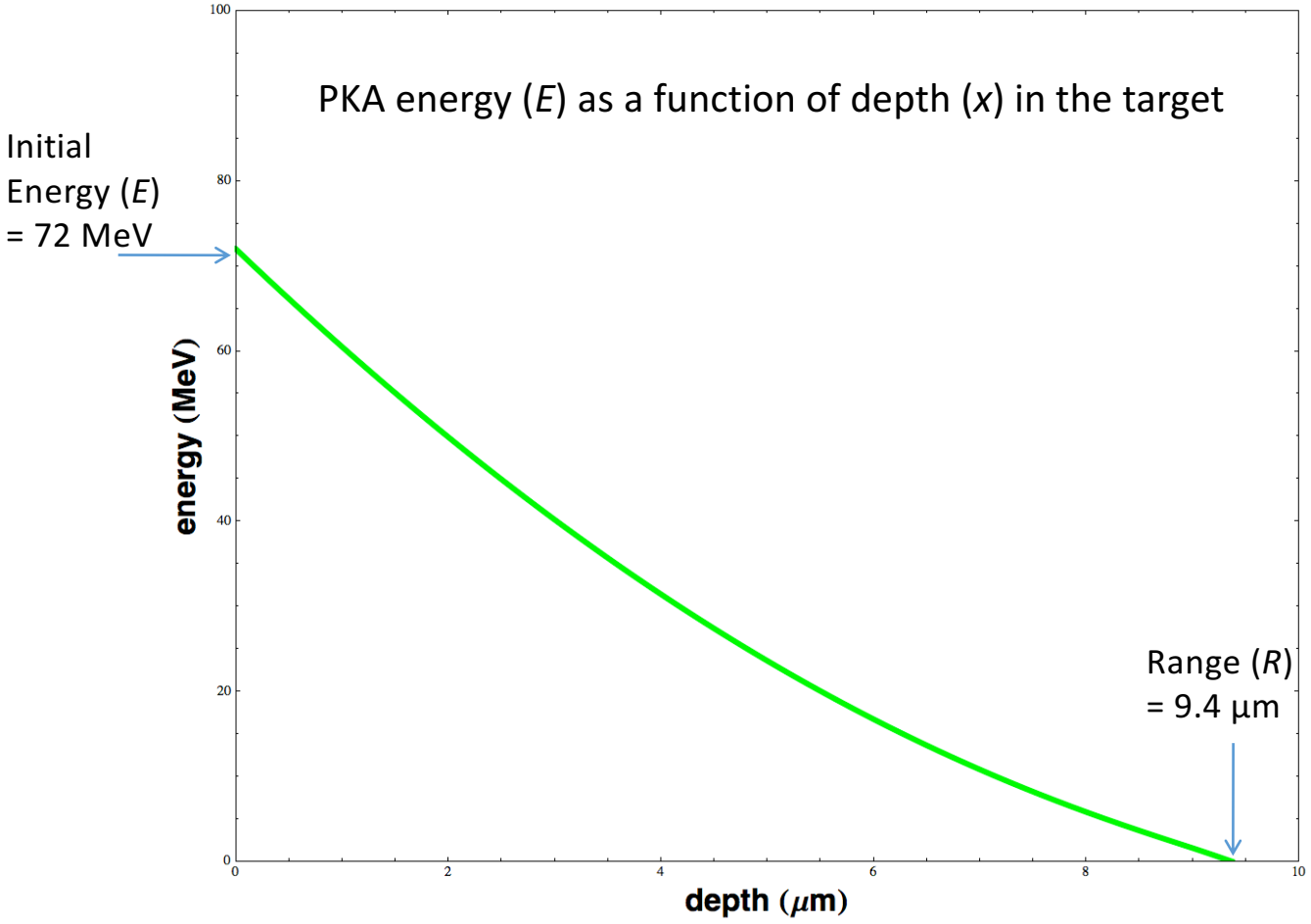

Example calculations of electronic and nuclear energy partitioning: I^+ ions in spinel ($MgAl_2O_4$)